Investigation of Formability of Material in Incremental Sheet Metal Forming Process

Hosein Khalatbari

Submitted to the
Institute of Graduate Studies and Research
in partial fulfillment of the requirements for the Degree of

Master of Science
in
Mechanical Engineering

Eastern Mediterranean University
September 2012
Gazimağusa, North Cyprus

Approval of the Institute of Graduate Studies and Research

Prof. Dr. Elvan Yılmaz
Director

I certify that this thesis satisfies the requirements as a thesis for the degree of Master of Science in Mechanical Engineering.

Assoc. Prof. Dr. Uğur Atikol
Chair, Department of Mechanical Engineering

We certify that we have read this thesis and that in our opinion it is fully adequate in scope and quality as a thesis for the degree of Master of Science in Mechanical Engineering.

Assoc. Prof. Dr. Fuat Egelioğlu
On behalf of Asst. Prof. Dr. Asif Iqbal
Supervisor

Examining Committee

1. Prof. Dr. Majid Hashemipour
2. Assoc. Prof. Dr. Fuat Egelioğlu
3. Asst. Prof. Dr. Neriman Özada

ABSTRACT

Currently, Incremental Sheet Forming (ISF) is known as a novel technology, which promises a higher flexibility in process, lower production price and lead time, in addition to improved formability of material compared to conventional forming processes. The beneficial aspects of ISF are mainly ascribed to the essence of this technique that is progression of forming process by propagation of localized plastic deformation. However, this special characteristic concurrently induces the major imperfection of the process that is long processing time. Furthermore, this attribute of ISF along with nonlinear behavior of material, lead to complexity in simulation of the process. Accordingly, to achieve better understanding of the process and to extend its application over different industrial fields, a great deal of efforts has been focused on experimental investigation of ISF during the last decade. However, a few number of research work are reported to aim at optimization of the process by consideration of process parameters. Moreover, the interaction effects of participating parameters are mostly neglected by these studies. This thesis, taking an experimental-statistical approach, attempted to investigate the individual and interactional effect of predictor parameters, namely tool and step size, feed rate, spindle speed and blank thickness upon formability of material in ISF. To do so, a set of screening trials of 16 runs conducted prior to the main experimental campaign of 72 runs in order to realize the reasonable levels of aforesaid participating factors. The preliminary and the main tests were designed and later analyzed according to Two-Factorial and Optimal Design of Experiment (DOE) by application of scholarly accredited commercial software, Design

Expert. For the sake of preciseness, a novel sensor system was developed and employed to detect the crack, once it appeared on the specimens. Based on the literature review and the knowledge of process acquired through this research, a new indicator proposed to effectively measure the formability of material in ISF. In addition, Individual and interactive effect of associated factors up on the new criterion were assessed by development of a quadratic and also modified cubic response surface models. More specifically, the positive effect of elevated spindle speed (2400 to 3000 rpm) on formability was highlighted in this study. However, feed rate (up to 5000 mm/min) was found to produce no significant effect, which means the process time can be remarkably reduced. Blank thickness was considered as a continuous numerical factor along with the rest of factors to provide an empirical model; hence it portrayed the greatest individual effect upon formability. Regarding the interaction effects, it was explored that the factors of spindle speed and blank thickness interdependently create the strongest effect on formability. At the next stage, interaction of the tool and step size was depicted to play a key role. Finally, the process was optimized in terms of maximum achievable formability, minimum processing time, and minimum sheet thickness. By optimized process parameters, it was demonstrated that approximately 96% of the maximum formability can be attained, using a moderate sheet thickness (1.26 mm), while the average forming time can be reduced to about 5.5 min. Maintaining the same criteria, but setting the spindle speed at zero, the most optimized situation revealed a reduction of about 29% in formability and an increase of about 62% in processing time.

Keywords: Incremental sheet forming, formability, design of experiments, process parameters, individual effects, interaction effects, optimization.

ÖZ

Şu anda, Artan Yaprak Şekillendirme (ISF), geleneksel kalıplama işlemleri ile karşılaştırıldığında malzeme Katlamaya ek olarak, bir süreç içinde daha yüksek bir esneklik, düşük üretim fiyat ve süreçte yeni bir teknoloji olarak bilinir. ISF ve yararlı yönlerini özellikle lokalize plastik deformasyonun yayılma sürecini oluşturan ilerlemesinde bu tekniğin özü atfediliyor. Bununla birlikte, bu özel karakteristik aynı uzun işlem zamanı işleminin büyük kusur indükler. Ayrıca, malzemenin doğrusal olmayan davranışı ile birlikte ISF bu niteliği, süreci simülasyon karmaşıklığı yol açar. Buna göre, sürecin daha iyi anlaşılmasını sağlamak ve farklı endüstriyel alanlar üzerinde uygulama genişletmek için, çabaları büyük bir anlaşma son on yılda ISF deneysel araştırma odaklı olmuştur. Ancak, araştırma çalışmalarının az sayıda proses parametrelerinin dikkate alarak süreç optimizasyonu yapılmıştır. Ayrıca, katılımcı parametrelerin etkileşim etkilerinin çoğunlukla bu çalışmalar tarafından ihmal edilmiştir. Bu tez, deneysel-istatistiksel bir yaklaşım alarak, ISF malzemenin şekillendirilebilirlik üzerine belirleyici parametreleri, yani uç ve adım büyüklüğü, besleme oranı, dingil hızı ve plaka kalınlığı bireysel ve etkileşimsel etkisini araştırmak için yapılmıştır. , Bu nedenle söz konusu katılımcı faktörlerin makul seviyelere gerçekleştirmek üzere 72 ana deneysel kampanyası öncesinde yapılan 16 pistlerinden tarama çalışmalarında bir set yapılmıştır. Ön ve ana testler tasarlanmış ve daha sonra bilimsel akredite ticari yazılım, “İki Faktöriyel” ve “Optimal Design of Experiment” (DOE)’e göre analiz edilmiştir. Bu numuneler üzerinde belirdi kez doğruluk uğruna, yeni bir sensör sistemi, geliştirilip çatlak tespiti yapmak için istihdam edildi. Literatür taraması ve araştırma yoluyla

edinilen sürecinin bilgiye dayanarak, yeni bir gösterge etkili ISF malzemenin şekillendirilebilirlik ölçmek için önerdi. Buna ek olarak, yeni ölçütler kadar ilişkili faktörlerin bireysel ve etkileşimli etkisi kuadratik ve ayrıca değiştirilmiş kübik yanıt yüzey modellerinin geliştirilmesi ile değerlendirildi. Daha spesifik olarak, şekillendirilebilirlik yükseltilmiş mili hızının pozitif etkisi (2400-3000 rpm) bu çalışmada vurgulanmıştır. Bununla birlikte, besleme hızı (5000 mm/dak) işlem süresi önemli ölçüde düşürüldüğünde hiçbir önemli etki ürettiğini tespit edilmemiştir. Plaka kalınlığı bir deneysel model sağlamak faktörlerin geri kalanı ile birlikte sürekli bir sayısal faktör olarak kabul edildi; dolayısıyla şekillendirilebilirlik üzerinde en büyük bireysel etki canlandırdı. Etkileşim etkileri ile ilgili olarak, dingil hızı ve plaka kalınlığı faktörlerin karşılıklı bir bağımlılık şekillendirilebilirlik üzerinde güçlü bir etki yaratmak olduğu araştırılmıştır. Bir sonraki aşamada, uç ve adım büyüklüğü etkileşimi önemli bir rol oynamak için tasvir edilmiştir. Son olarak, işlemi maksimum şekillendirilebilirlik, minimum işlem süresi ve minimum saç kalınlığı açısından optimize edilmiştir. Optimize edilen işlem parametreleri olarak, bu ortalama oluşturucu zaman yaklaşık 5.5 dk için azaltılmış olabilir iken maksimum şekillendirilebilirlik yaklaşık 96%, bir orta tabaka kalınlığı (1.26 mm) kullanılarak elde edilebilir olduğu bulunmuştur. Aynı kriterler bakımı, ama sıfır mili hızı ayarı, en optimum duruma şekillendirilebilirlikte yaklaşık 29% bir azalma ve işlem süresi yaklaşık 62% lik bir artış gösterdi.

Anahtar Kelimeler: Artımlı sac şekillendirme, şekillendirilebilirlik, deney tasarımı, proses parametreleri, bireysel etkileri, etkileşim etkisi, optimizasyon.

To My Family

ACKNOWLEDGMENT

I would like to express my sincere gratitude to my supervisor, Asst. Prof. Dr. Asif Iqbal for his continuous support and encouragement. I truly appreciate everything I have learned from him not only in his field of expertise, but also from his attitude and integrity.

I am deeply grateful to members of the examination comity, Prof. Dr. Majid Hashemipour, Assoc. Prof. Dr. Fuat Egelioğlu, Asst. Prof. Dr. Neriman Özada for their time and effort in reviewing of this thesis. Especially, I would like to thank Dr. Fuat Egelioğlu and Dr. Majid Hashemipour who advised me in absence of my supervisor.

I am greatly indebted to Prof. Dr. Lin Gao at Nanjing University of Aeronautics & Astronautics (NUAA), Jiangsu, China, who provided me with a research opportunity in his lab. My sincere thanks go to him for his full support, great kindness and tolerance.

I must also acknowledge Mr. Xiaofan Shi and Mr. Jiahui Xu for their intimate friendship and valuable assistance during my work at NUAA.

Last but not least, my deepest gratitude goes to my beloved parents and siblings for their endless love and encouragement. My appreciation also goes to Shahrbanoo Allameh for spiritually supporting me through the whole of my life.

TABLE OF CONTENTS

LIST OF TABLES

LIST OF FIGURES

Chapter 1

INTRODUCTION AND LITERATURE REVIEW

1.1. Introduction to Incremental Sheet Metal Forming

Incremental Sheet Metal Forming (ISF) is a latterly developed technology through which a simple tool (a rod of hemispherical tip or an equipped shaft by a rolling ball at the head) imposes localized plastic deformation on sheet metal along a previously adjusted path by a CNC (milling) machine. The naturally die-less ISF (single point ISF[1]) process demonstrates the ability of forming complex shapes of sheet metal, providing an increased level of formability in comparison to the conventional methods of forming. It is regarded as a low price flexible technology that is appropriate for rapid prototyping, customized and small-batch production of sheet metal components (Jeswiet et al., 2005).

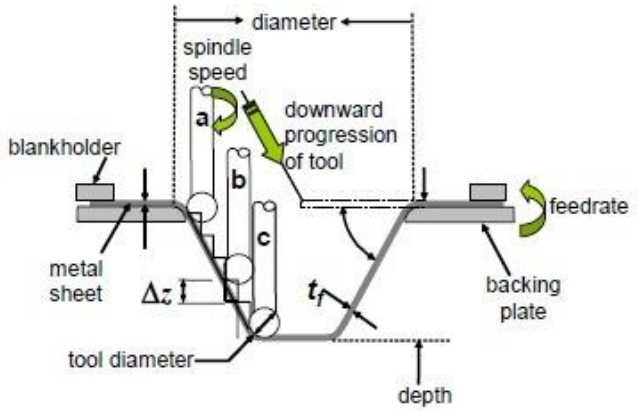

Figure 1.1 Schematic view of negative[2] ISF (M. Ham & Jeswiet, 2007)

[1] Or interchangeably "negative incremental forming"
[2] It refers to die-less or Single Point Incremental Forming

1.2. ISF applications

Since ISF is a novel technology which has been mostly developed through the last decade, it is not yet widely used for industrial applications or commercial production. However, ISF has been reported to be employed or to be capable of functioning in the following areas (Jeswiet et al., 2005):

- Customized medical products (e.g. ankle support, replacement for damaged bone in human skull, dental dentures etc.)
- Automobile body parts (e.g. car hoods)
- Architectural decorative parts
- Metallic and plastic prototypes
- Custom made house hold utensils
- Aircraft's body parts
- Ship hull parts
- Light weight and inexpensive dies (e.g. dies for casting of plastics)
- Post-forming or pre-forming followed or prior to other sheet forming processes
- Recycling of waste sheet metal
- Hybrid machining
- Forming of composite plates, sheets and sandwich panels

1.3. Competencies against imperfections

Single Point Incremental Forming (SPIF) by implementation of CNC technology, and also taking the advantage of a simple tool-clamping setup, avoids the need for expensive

punch-dies for sheet metal forming. Simultaneously, it represents a higher level of formability as compared to common forming technologies such as stamping. These characteristics that can be ascribed to propagation of localized plastic deformation by ISF, have introduced this process as to be capable of responding to the growing demand for customized manufacturing and products in small batch. Nevertheless, aforementioned simplicity may induce undesirable plastic deformation within unclamped forming area. Considering the elastic spring back effect as well, they result in dimensional deviation of finish part with respect to what is previously designed. For these reasons, considerable research effort has been concentrated on balancing positive and negative aspects of localized plastic deformation in ISF. However, much more is likely required to make the process entirely suitable for industrial applications. Table 1.1 briefly presents competencies of ISF process against its imperfections.

Table 1.1 Advantages and disadvantages of (single point) incremental forming process

Advantages	**Disadvantages**
Providing a higher level of formability compared to the conventional sheet metal forming technologies	Long forming (process) time
Low cost	Relatively low level of dimensional Accuracy
High flexibility	Restricted maximum thickness of blank to form
Simple tooling	High sensitiveness of process to elevated inclination angle of walls
There is generally no need for dies	
Short time from design to manufacturing	
Capability of producing complex sheet component	
It is almost noise less	

1.4. Formability of sheet material by ISF (literature review)

Among the advantages that ISF technology offers to the metal forming industries, improved level of material formability, has always attracted the interest of researchers in this field. To be able to estimate the formability, also known as spifability, of a material within a particular process, there is a need for an index that can be quantitatively measured and presented. In this regard, the Forming Limit Curve (FLC) or Forming Limit Diagram (FLD), as a record of amounts of strain experienced by a material through a particular forming process has been employed for over forty years to demonstrate the formability of sheet metal (Allwood & Shouler, 2009). In fact, Keeler and Backhofen (1963) are known as the first authors tried to develop the FLD to be capable of anticipation of sheet metal tearing resulted from the thinning phenomenon in forming processes. In addition to the work done by Keeler and Backhofen (1963), there are some other graphical demonstrations of sheet metals ability to stretch suggested thus far; e.g.:

- A diagram of major strain versus stress ratio, proposed by Swift (1952);
- A curve of effective strain versus stress rate ratio, which asserted by Ferron and contributors (1994) to be independent of strain paths;
- A diagram of plastic strain against stress ratio, plotted by Yoshida et al. (2007) in attribution to the one of Marin et al. (1953).

Thus, the graphical representation of sheet metals strain-ability is not limited to the FLD, but it is the most cited method of estimation of material formability in the

literature. In fact, traditional FLD is a diagram in which the vertical axis is taken for $\varepsilon_1$or ε_{major}, while the horizontal one is taken for ε_2 or ε_{minor}, considering that ε represents the triple principal strain components that $\varepsilon_1 > \varepsilon_2$ and $\varepsilon_3 = -\varepsilon_1 - \varepsilon_2$, according to the assumption of proportional loading and the rigid plastic deformation state. Figure 1.2 provides a conceptual illustration at which FLD is established. It has been shown by some research in ISF field (Filice, Fantini & Micari, 2002; Hirt et al., 2002; Fratini et al., 2004) that the conventional FLC which represents the formability of material in ISF process can be plotted as a descending straight line.

Since the strain track is adjacent to the major strain axis in FLD, FLD_0 which is the maximum amount of major strain while the minor one is equal to zero, is considered as a suitable indicator for formability of material in ISF process (Hussaina et al., 2009). FLD_0 can be expressed as a percentage or a positive real number.

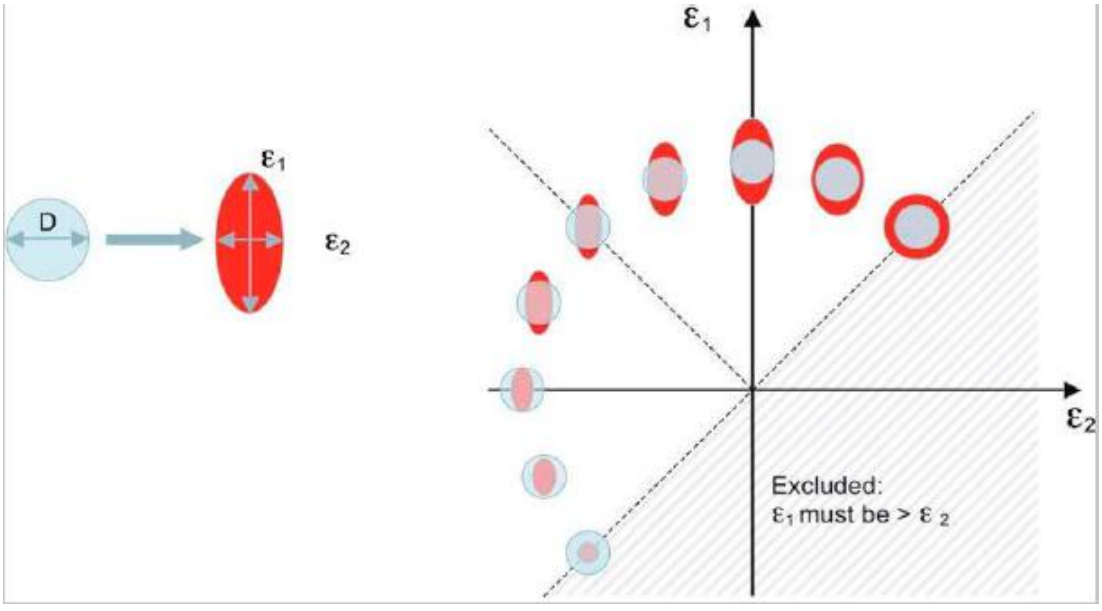

Figure 1.2 Conceptual illustration of FLD (Allwood & Shouler, 2009)

Furthermore, it is observed within a number of experimental investigations in ISF field that the increase in wall angle, φ, leads to decrease in wall thickness of component, considering the influence of 'thinning' phenomenon, it finally brings the sheet metal to rupture. Hence, the maximum wall angle (slop angle) of sheet metal component, φ_{max}, is suggested as an indicator of formability (Filice et al., 2002; Hirt et al. 2002; Jeswiet & Hagan, 2003; Hirt et al., 2003; Young & Jeswiet, 2005). Jeswiet et al. (2005) expressed that an ISF process designer using the φ_{max} criterion for a particular sheet metal of specific thickness in addition to the corresponding FLD_0, will be capable of deciding about the number of required passes (stages) to fabricate a desired component.

However, the main concern in this research area is how to provide a reliable FLD as it may be a preliminary step before some further analyzing and design procedures. There are two general approaches, adopted by researchers namely, analytical prediction and experimental determination of FLD.

Research work of the prior approach is classified by Yao and Cao (2002) into three categories, namely 'bifurcation analyses', 'local instability' at a defect and 'accumulation of damage'. Allwood and Shouler (2009) briefly reported some studies assigned to each category of the first approach. Among the mentioned research, they highlighted an analysis performed by Marciniak and Kuczynski (1967), well known as M-K model which has been widely employed to develop further analysis so far. In fact, the core of any analytical model of a particular forming process is the mechanism which is supposed to impel the process. Nevertheless, most of analytical modeling of sheet

metal forming processes is constructed on the assumption of pure in-plain stretching or plain-stress state of the problem.

In the case of ISF process, according to the visioplastic examination performed by Hirt, Junk & Witulski (2002), they stated that the deformation can be regarded as the state of plain strain, implying the occurrence of pure stretching within the forming zone (Micari & Ambrogio, 2004). On the other hand, Fratini et al. (2004), citing two investigations by Filice et al. (2002) and Ambrogio et al. (2003) argued that the discrepancy of what they said 'traditional FLD' with the experimental data is resulted from the different driving mechanism of deformation in ISF process. Moreover, an experimental investigation conducted by Allwood, Shouler and Tekkaya (2007), in which a sheet metal of inscribed pattern of lines on its both sides examined before and after an ISF process, indicated a considerable amount of 'through-thickness shear strain' in the blank.

Finally, Allwood and Shouler (2009) deduced that the discussed through-thickness shear strain is due to the incidence of normal and probably proportional loading in ISF process. Afterwards, they aimed to develop a 'General Forming Limit Diagram' (GFLD) based on M-K model, putting all six symmetric stress components into action. As a consequence of such an extension (excluding the effect of bending), predicted GFLD allows a higher level of formability that is practically shown to be accessible in ISF process compared to the conventional sheet forming technologies. In order that GFLD implies the same notion as conventional FLD, it is always possible to adjust Cartesian coordinate system in such directions that ε_{xx} and ε_{yy} $(\varepsilon_{xx} > \varepsilon_{yy})$ represent the principal surface strains, so $\varepsilon_{zz} = -\varepsilon_{xx} - \varepsilon_{yy}$. Considering the participation of the

above discussed shear strain in process it is proposed by Allwood and Shouler (2009) to allocate the third axes of introduced GFLD to ε_{tt} that $\varepsilon_{tt} = \sqrt{\varepsilon_{zy}^2 + \varepsilon_{zx}^2}$, ε_{zx} and ε_{zy} depict through-thickness shear strains.

Whatever deriving mechanism is deemed to provide an analytical model of an individual forming process, it is quite necessary to offer some experimental proofs, ensuring the reliability of such a modeling for any additional analytical, designing or optimizing procedures. The most referred trial technique of determination of FLC in conventional forming methods which best fits the ISF process conditions is based on the visual investigation of distortion of imprinted patterns on sheet surface due to the forming process. The procedure commences with inscribing, etching or imprinting a pattern of mutually tangential circles of identical diameters on blanks surface. As a result of plastic deformation of sheet metal by proceeding of ISF process, scribed circular shapes gradually transforms to appearance of ellipse (Figure 1.2). The length of major and minor axes of the ellipse which are visually measured is then employed to calculate the true principal strain components as following:

$$\varepsilon_{major} = ln \frac{length\ of\ major\ axis\ of ellipes}{diameter\ of\ original\ circle} \tag{1.1}$$

$$\varepsilon_{minor} = ln \frac{length\ of\ minor\ axis\ of ellipes}{diameter\ of\ original\ circle} \tag{1.2}$$

Thus, FLD_0 is equal to ε_{major}, when the length of minor axis of the corresponding ellipse equals to the diameter of the original circles. In order to experimentally produce

GFLD, the main issue is how to measure the through-thickness shear strains. There are at least two trail methods, recommended to perform such a measurement.

The first method involves the inscription of aforementioned circular pattern on both sides of sheet metal, in an adjusted way that each couple of corresponding circles form an imaginary cylinder through the thickness of the blank. Investigation of the shear in such hypothetical tubes makes it possible to calculate ε_{tt}. The difficulty of this technique, regardless of exact adjustment of corresponding circles after the accomplishment of process, is the survival of the imprinted pattern after being under a severe sliding contact with the forming tool.

The second technique uses small shallow holes, normally drilled on sheet surface instead of circles. The problem here is the consequential stress concentration that may induce a predate failure, even in case of filling holes with an appropriate material before the beginning of process. Based on the above mentioned experimental methods, some research has been done to investigate the influence of process as well as non-process parameters (such as mechanical property of material) that thought to be effective on formability of material in ISF process.

Shim and Park (2001) conducted a trial investigation as well as a Finite Element Method (FEM) aided analysis, measuring major and minor strains particularly closed to revealed tears in fully annealed aluminum A1050 sheet under ISF process to plot the pertinent FLC. They utilized a rolling tool of 9.575 mm diameter and three different lubricants to produce various shapes of sheet metal (with triangular, square, circular, etc. cross

section, all extruded along an almost perpendicular direction) by different scenario for vertical-horizontal step size. Consequently they found that FLC in ISF process appears as a descending straight line in positive region of major-minor axis, and it partially depends on the strain path. Considering the closed tool path of each pass, they explored that the deformation in corners can be regarded as equi-biaxial stretching, while almost a plain strain state in walls. Additionally, tearing was reported to happen mostly at corners. Finally, 'straight groove test'[3] was proposed in order to plot FLC of sheet metal through ISF process.

Kim and Park (2002) followed the same approach as Shim and Park (2001), to evaluate the influence of process parameters namely, tool type, tool size, pitch size (vertical step size), friction and plain anisotropy on formability of sheet metal in ISF process. To achieve this aim, they performed FEM analysis by PAM-STAMP commercial code as well as many experiments utilizing a ball-head tool and also a hemispherical tip tool of 5, 10 and 15 mm in diameter, pitch size of 0.1, 0.3 and 0.5 mm and three different lubricants to form a groove of about 40 mm in length along RD[4] direction and also TD[5] direction. In order to measure $(\varepsilon_{major} + \varepsilon_{minor})$ as the indicator of formability, they employed rectangular and circular (diameter of 2.54 mm) grids respectively inscribed and electrochemically etched on blanks' surface. Finally they briefly conclude that: ball-head tools induce enhanced formability compared to the hemispherical ones; a bit friction is required between tool and sheet to gain higher formability, however a large

[3] Generation of deformation in form of a wide-deep groove in sheet metal by forward-backward motion of ISF-tool with specified vertical and lateral step size at each course.
[4] Rolling Direction
[5] Transverse Direction

amount of friction will lead to more tool wearing, surface roughness and even happening of tearing; due to the plain anisotropy, formability alters as the trajectory of tool differs; formability rises as the pitch size reduces and the highest formability achieved by the tool of 10 mm in diameter under the arrangement of these experiments.

Filicel et al. (2002), performed a series of ISF tests on aluminum A1050-O sheet of 1 mm thickness (240×240 mm), using a rotating hemispherical tool of 12mm diameter to plot the pertinent FLD. They generated three different arrangements of tool path, trying to cover a range of strain from uniaxial to biaxial pure stretching through the experiments. The first arrangement was composed of a series of side by side square loops, constantly getting smaller by closing to the center while keeping the identical depth (step down) at a level. Any level is followed by another level of resembling pattern just after the same step down at the beginning in addition to constant steps along x-y directions to gradually form a pyramid shape in sheet metal. This configuration is asserted to lead to almost uniaxial stretching over the pyramid wall following the distortion of inscribed circular grids was investigated. It is also declared that the intensity of strain that may be implied by the ratio of major strain to minor strain, can be directly affected by the ratio of step-down size (along z axis) to step-in size (along x-y axes). The second arrangement of tool path was configured as two perpendicular line (x and y axes) to form a cross shape, keeping step-down size fixed in all passes along lines while imposing a constant step-in at the beginning of any pass along each line (in x or y direction). A state of near pure biaxial stretching at the central area of the cross was reported following the measurement of inscribed circular grids. The third configuration of tool path has been done in the form of a three dimensional spiral in order to cover a

range of strain from uniaxial to biaxial stretching. Hence, a steadily downward movement (along z axis) accompanied by a steadily inward radial movement to eventually create a cone shape of sheet metal. Following the assessment of inscribed circular grids in a number of experiments, it is concluded that the state of strain (e.g. uniaxial or biaxial) is affected by the ratio of the first round pass diameter to the tool head diameter. It is also reported that the ratio of pitch size to the radial displacement in two successive round passes directly affects the thinning phenomenon, as a result tearing of sheet metal. The above reported research may mostly be significant due to the consideration of the influence of tool path strategy on the mechanism of deformation, hence the formability of material.

The trial investigation that has been conducted by Fratini et al. (2004), attempts to present the impact of four mechanical properties of material, namely strain hardening exponent (n), percentage of elongation or area reduction (A%), ultimate tensile strength (UTS) and the strength coefficient (K) on the formability of material (FLD_0). FLD_0 is measured by performing many dome (bulge) tests as well as utilizing inscribed circular grids in different ISF experiments carried out, permitting a comparison between conventional FLD and FLD by ISF process. Blanks (240×240 mm) of six different materials namely, High Strength Steel (HSS), Deep Drawing Quality (DDQ) steel, Stainless Steel (SS) AA6114 T4, Copper, Brass and Aluminum AA 1050 O were used to form conic and pyramid shapes of different wall slop angle through ISF process. The other process and geometrical parameters (e.g. tool head diameter of 12 mm, step-down size of 1 mm and tool rotational speed of 600 rpm) kept fixed through all ISF trials. The first expected achievement of experiments was the illustration of higher formability of

material in ISF process compared to what is feasible by conventional forming processes, which is commonly determined by dome test. Furthermore, in furtherance of interpretation of tests' results, a statistical model of six dimension response hyper surface was proposed to evaluate how significantly FLD_0 is affected by each of four above cited mechanical properties of material. Aforementioned response surface that its fitness estimated as about 96% by 'residual statistical distribution analysis' represented that FLD_0 is mostly affected by strain hardening exponent (n), at the next level by the strength coefficient (K) and finally by the percentage of area reduction (A%). Figure 1.3 representing a simple flowchart, shows how the formability of material plays in ISF process (it can be regarded as a very brief summary of former section).

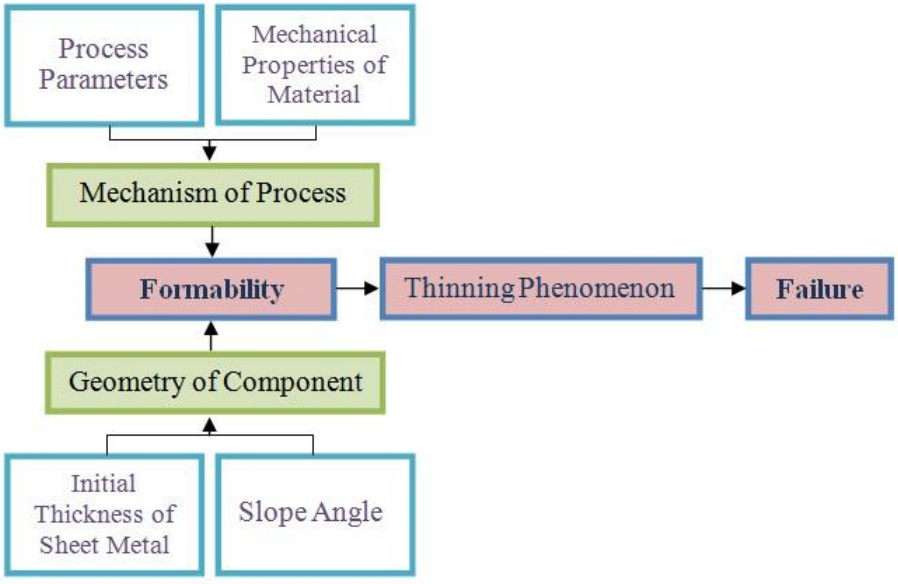

Figure 1.3 Formability of sheet material in ISF process

1.5. Statement of the problem

Recently emerging Incremental Sheet Metal Forming (ISF) process, in the same way as the many preceding forming technologies, involves various affecting input parameters

that cooperatively impress the characteristics of finish part. In pursuance of evolution of ISF forming technique to an industrially reliable and economically feasible technology, it is highly crucial to develop an appropriate process model. Such a model is required to be capable of anticipation of output parameters' value based on the distinct input process parameters. Considering a number of research attempting at analytical modeling or empirical investigation of ISF process, input-output parameters of the process have been organized in Table 1.2.

Table 1.2 Predictor and response parameters in ISF

Predictor (Input) Parameters	Response (Output) Parameters
Mechanical properties of material[6]	Formability
Part's Dimensions + Part's profile	Force
Tool head diameter	Surface quality (roughness)
Tool pitch, vertical step size or step down	Dimensional accuracy-Spring back
Spindle speed	Forming time (process time)
Feed rate (forming speed)	
Sheet metal initial (flange) thickness	
Method of tool pass generation	
Lubricant	
Temperature of blank (e.g. in hot forming)	

The main issue in the modeling of such a process of a relatively large number of involving parameters is limited ability of the developed model to deal with the diversity of process arrangements according to the different design necessities. Generally, the

[6] Ultimate tensile strength (UTS), yield strength (YS), strain hardening exponent (n), percentage of area reduction (A%), strength coefficient (K).

most modeling approaches, no matter analytical or empirical one, have considered a limited number of varying input parameters to investigate the formability of material under a limiting assumptions or special arrangement of the experiments. Furthermore, preceding research (Micari, 2004; Hirt, Junk & Witulski, 2002; Bambach, Hirt & Junk, 2003) concerning the effect of predictor parameters upon formability of sheet material by ISF, mainly have not taken into account the interactional effects of parameters.

1.6. Purpose of the study and the achievements

Being aware of how profoundly interactive effect of process parameters might impress the formability by ISF, an effective experimental-statistical approach aimed to be taken through this thesis to investigate theses effects along with the individuals. I other words, the reaction of the process (in terms of formability) to different combinations of process parameters is intended to be studied by making use of suitable "Design of Experiment" methods in this research. More specifically, predictor parameters namely tool and step size, feed rate and spindle speed in addition to blank thickness are the matter of concern, while considering the material's[7] mechanical properties. By varying parameters over reasonably wide ranges, detailed statistical analyses on the individual and interactive effect of parameters upon the formability have been reported in this dissertation. Furthermore, a novel effective measure of formability has been proposed. Finally, this research work accomplished by optimization of the process to achieve the maximum formability, while the minimum process time and minimum required amount of material.

[7] Aluminum alloy AA-3003 has been used for this experimental study.

1.7. Significance of the study

The outcomes of this research provide designer engineers with a predictive-optimizing tool, as well as better understanding of the process mechanism. By the empirical model reported here, given the value of some restrictive predefined process parameters, it is possible the adjustment of the remaining parameters as they best fit to the desired value of response parameters such as maximum formability or minimum lead time.

Generally, hereby presented research involves well arranged empirical efforts, in achievement to promote the promising innovative Incremental Sheet Metal Forming technique to a mature and industrially reliable technology.

Chapter 2

EXPERIMENTAL METHODOLOGY AND SET UP

2.1. Introduction to experimental methodology

As it is reported in the first chapter, the better formability of material by ISF process in comparison to conventional forming technologies is frequently highlighted in the literature. This beneficial characteristic of the process can be ascribed to the localization of plastic deformation in ISF. However, forming by propagation of localized plastic deformation reveals the higher time-cost as an imperfection of the process, which indeed restricts the industrial application of ISF. On the other hand, aforementioned attribute of the process, induces strong nonlinearity in material behavior, hence considerable complexity of any analytical explanation for the process. For this reason, the mechanism of ISF process is not yet entirely realized.

During the last decade, a great deal of efforts has been focused on experimental examination of ISF in order to get a better understanding of the process. Despite such noteworthy attempts, researchers have devoted a little attention to application of advanced statistical methods for design of experiments, and later to analyze acquired data. This dissertation represents one of a few studies, in which “Design of Experiment” (DOE) has been exploited to attain new findings about individual and interactional effects of design parameters on formability in ISF. Such an insight definitely aids any

further analytical-numerical investigations, in turn optimization of the process and extension of its industrial application.

To quantitatively describe the formability, the maximum slope angle of incrementally formed parts and also the "Forming Limit Curve", are commonly employed by researchers in this field. Moreover, distribution of sheet thickness along the depth of the parts has been taken into account in some cases (the relevant details are provided in the chapter of introduction). However, it has been discerned in previous studies that they partly suffer from some deficiencies by application of each above mentioned criterion. Take for instance, insufficient accuracy, disability to adequately represent different expected mechanism involving in the process, being highly dependent on specimens' profile, being dependent on rarely available instruments and being time consuming.

To address these problems, this study has benefited from the previously introduced measures to propose a new benchmark for formability of material in ISF. Furthermore, considering that formability can be evaluated just after the onset of crack on the part, it intimates the importance of prevention of crack from great expansion. Accordingly, a novel electronic system has been developed for the first time in this research, to detect the crack at its very earlier stages and alert the operator to stop the forming process.

To discuss the methodology of this dissertation in detail, this chapter has been managed in seven sections as following: Introduction to experimental methodology; statistical DOE rather than traditional OFAT; RSM and optimization; Optimal design and

practical-theoretical justification; determination of factors' levels; material, tools and equipments; and the manufacturing of part and measurement.

2.1.1. Statistical DOE rather than traditional OFAT

"Industrial physicists no longer can afford to experiment in a trial-and-error manner, changing one factor at a time, the way Edison did in developing the light bulb" (Anderson & Whitcomb, 1974). The "One factor at a time" (OFAT) is an experimental approach in which each Design or Process Factor[8] will be examined in discrete values within a predefined range, while all other relevant factors are fixed at a particular point. The resultant scatter diagrams of Response Data[9] versus each factor will be considered later to inspect the individual influence of each factor on response variable.

However, taking this approach, many probable Interaction Effects of factors will be neglected. By interaction effect, it is supposed that the relationship between any especial factor and response significantly changes if other factors set into different values. Furthermore, in contrast to limitation of time and resources for industrial or scientific researches, by application of OFAT, there would be a large number of runs required to acquire enough information about the mechanism of the investigated process. Moreover, this method is barely capable of making contribution to a reliable optimization of the process. For these reasons and taking the complicated nature of ISF in to account, it was decided to make use of DOE herein.

[8] Input parameter for trials. It has been briefly referred to as Factor in the literature.
[9] Output parameter for trials. It has been briefly referred to as Response in the literature.

By deployment of suitable DOE, it is intended to design an experiment with the minimum number of runs, in the same time, providing unbiased data to analyze desired individual and interaction effects that are not confounded together[10]. In other words, by careful utilization of DOE, it is possible to portray a system or process by consideration of all associated factors together as it practically works in real world, which is hardly feasible by application of traditional OFAT. However, there are several methods for experimental design, reported in standard text books (Anderson & Whitcomb, 1974; Anderson & Whitcomb, 2005; Box & Draper, 1987; Box, Hunter, & Hunter, 2005; Mason, Gunst, & Hess, 1989; Montgomery, 2008; Ryan, 2011; Taguchi, Tung, & Clausing, 1987). Therefore it is of high importance to choose the most efficient and suitable design.

Two-Factorial-Design (TFD) can be regarded as the simplest among all the DOE techniques to fulfill aforementioned desires by setting each factor in two levels, concluding in 2^k trials[11], which k is the number of desired factors. Nevertheless, the main flaw of TFD is the implicit assumption of linear relation between factors and responses. In addition, interaction effects of higher order (larger than two) will be disregarded (Hill & Lewicki, 2006). Thus, if a curvilinear relationship is presumed according to the preceding empirical evidence or due to the awareness of process nature and especially for control or optimization proposes, as in the case of this study, so application of Response Surface Methods (RSM) is recommended. Alternatively, TFD

[10] It depends on the Resolution of the design, the number of runs and the model that is adjusted for Response Surface. For further details, anyone can refer to Hill and Lewicki (2006), and StatSoft, Inc. Electronic Statistics Textbook. Tulsa, OK: StatSoft. (2012)
[11] It is indeed full factorial design in two levels.

and particularly Fractional TFD[12], is still useful for "Screening Design", which provides preliminary information for factor's main effects[13] as well as some hints about interaction effects (Montgomery, 2008). As it is reported in following sections, a set of screening experiments was performed in this research to inspire the adjustment of factors' levels for the main DOE.

2.1.2. Model fitting by regression

Normally, the relationship between response[14] and factors[15] of a process can be demonstrated by a mathematical function, which is identified as "response model"[16]. For instance, let y and $x_1, x_2, \dots, x_k$ respectively represent response and factors, so the basic form of response model can be easily derived as $y = \varphi(x_1, x_2, \dots, x_k)$. In more details, general "multiple linear regression model" can be established through the following equation (Montgomery, 2008):

$$y_i = \beta_0 + \sum_{j=1}^{k} \beta_j x_{ij} + \epsilon_i \quad i = 1, 2, 3, \dots, n \tag{2.1}$$

Where, k represents the number of factors, n stands for the number of runs[17], ϵ_i[18] is

[12] Half fractional TFD that provides half number of runs compared to full TFD ($\frac{1}{2} \times 2^k$) can be regarded.
[13] "Main effect" is interchangeably used for "individual effect".
[14] "Response" which is frequently used as in DOE terminology can be interchangeably replaced by "Dependent variable".
[15] "Factor" which is frequently used as in DOE terminology can be interchangeably replaced by "Independent variable", "predictor" or "repressor", however there is a slight difference.
[16] "Response model" which is frequently used as in DOE terminology can be interchangeably replaced by "empirical model".
[17] Each experimental campaign is composed of specific number of runs, trials or observations in DOE. However, sometimes in statistics, observation is regarded to a sample of data points that is resulted from measurement of a response for the same combination of factors in different times.
[18] It represents the "uncontrolled error variable". Variance of these terms provides the standard deviation for the whole observations.

regarded as the noise factor, β_0[19] is a constant value, and β_j is called "regression coefficient". In particular, considering any observation, β_1 indicates the amplitude of variation of response parameter for the unit variation of x_1, while all other factors of x_j ($j \neq 1$) are fixed. Although, equation 2.1 resembles to a first order polynomial, but any higher order of single factors or their interactions can be taken into account by this equation. For example, to develop a quadratic model of two factors, the following equation is first assumed:

$$y = \beta_1 x_1 + \beta_2 x_2 + \beta_{11} x_1^2 + \beta_{22} x_2^2 + \beta_{12} x_1 x_2 \tag{2.2}$$

However, If say $x_1^2 = x_3;\ \beta_{11} = \beta_3;\ x_2^2 = x_4;\ \beta_{22} = \beta_4;\ x_1 x_2 = x_5$ and $\beta_{12} = \beta_5$, the new equation will be such as following:

$$y = \beta_1 x_1 + \beta_2 x_2 + \beta_3 x_3 + \beta_4 x_4 + \beta_5 x_5 \tag{2.3}$$

In fact, equation 2.1 is referred to as "multiple linear regression" (MLR) equation as it is linear in terms of regression coefficients (β), however it is capable of creation of response surfaces of any shape, considering varying number of factors. Anyway, utility of higher order equation of regression, specifically near to the minimum, maximum or saddle points of response surface might be advantageous. In order to create corresponding response surface to the data points resulted from observations (experiments), proper values of regression coefficients can be calculated by application of "least square method", which minimizes the sum of the square of error factors, (ϵ_i). For further details anyone can refer to Montgomery (2008) and Myers (1990). Broadly speaking, regression is applicable wherever quantitative explanation of DOE's outcomes

[19] β_0 implies the intercept of the response surface in *k* dimensional space.

is necessary, as in the case of Factorial Design or particularly if highly efficient optimizing RSM based solution such as CCD is required.

2.2. RSM and optimization

In fact, Factorial Design of multiple factors in three levels is the most straightforward discipline which provides the capability of covering nonlinear relationship of factor-response. However, it significantly reduces efficiency of experimentation as far as required number of runs is concerned (e.g. 243 runs are required in an experimentation of 5 factors). Instead, extended TFD are strongly recommended, when it is appended by center and additionally by axial points.

Center point is a data point pertaining to a trial in which all factors are set at the middle of their upper-lower levels (in TFD). This unit of experimentation should be entirely repeated for a specific number of times through the whole experiments. In most of the cases, three to five center points are adequate however; in some cases increased number of center points can improve the accuracy of design. Axial points or star points[20] are data points corresponding to experimental attacks in which, all factors are set at the average of their upper and lower levels, but one factor have a distinct distance (α) from its upper-lover levels' midpoint. Axial distance (α) can be calculated based on assumption of standard criteria for the design matrix[21] (rotatable[22], spherical[23], etc.).

[20] Number of star points usually equals twice the number of factors (k).

[21] Each row in design matrix contains factors' levels (coded such as -1, 0, 1, which respectively correspond to high, mid and low levels). Hence, total number of rows in matrix, represent the number of runs in experiments.

[22] It means that the variance of predicted response for all the data points in equal distance from the center point should remain constant. Thus, to augment the full factorial design of k factors, axial distance can be calculated as following: $\alpha = 2^{k/4}$ (Box & Hunter, 1957).

Figure 2.1 schematically represents a Central Composite Design (CCD) that is made by a TFD (eight black points located at the cube's corners) which is augmented by center point (red circle at the center) and star points (black stars located on the axes).

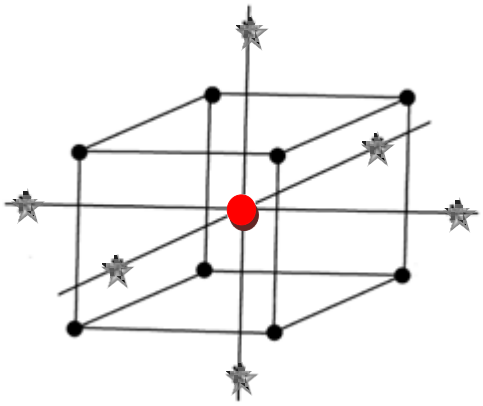

Figure 2.1 Schematic representation of three-factor TFD, augmented by center and axial points

Additionally, a spherical model proposed by Box and Behnken (1960), is available with the lower number of needed trials, due to the exclusion of cubic corner points (higher-lower levels). This model (Figure 2.2.a) provides the possibility of considering categorical factors (factors which can be qualitatively described rather than numerically measured), while in the most cases it represents lessened precision compared to CCD. Another possibility is adaption of CCD to create a new design in which each factor is arranged in three levels by placement of star points on faces of an imaginary cube or $\alpha = 1$ (Figure 2.2.a). This method is especially suitable for the case of cubic region of experimental interest (rather than spherical), also when there is a situation that limits the maximum available number of levels to three. As it is evident, this design is not

[23] In this way, the design points including axial and factorial points will be located in the same distance from the center point. The radios of such a sphere is denoted by $\alpha = \sqrt{k}$.

rotatable; however it can produce acceptable distribution of response variance within the cubic design space.

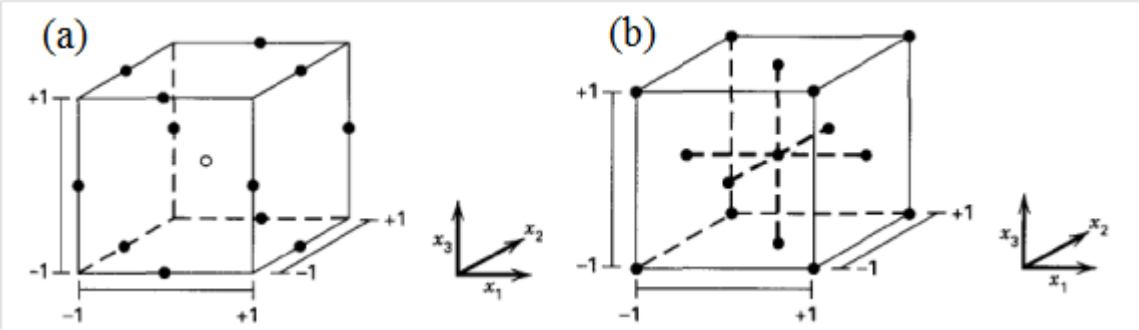

Figure 2.2 (a) Box-Behnken design and (b) face centered CCD design for three factors (Montgomery, 2008)

It should be noted here that whatever design is adopted for an experimental campaign; currently, application of DOE whether in academy or industry is hardly imaginable without making use of the relevant software. Hence, many commercial computer utilities are reported to be utilized in scholar or industrial research namely, SPSS, Design Expert and MINITAB to mention a few. This research, has taken the advantage of Design Expert, due to a considerable number of scholars that referred to this software and also because of its advanced technical capabilities and its user friendly design as well.

2.3. Optimal design and practical-theoretical justification

In particular, under the condition that some practical-technical limitations constrict applicable range of factors, so that the problem no longer matches any spherical or cubic design solution (e.g. CCD), then utilization of computer aided DOE should be considered. This situation might be exemplified in five different cases. First, whenever

the maximum number of obtainable factors' levels is lower than the requisite for standard experimental designs (e.g. CCD). Second, whenever a particular factor (or more) cannot be regarded as continuous numerical variable, so that it should be considered as a nonnumeric categorical or discrete numerical factor. Next, when there may be a certain practical-technical limitation for individual factors or their interaction. For example, $C_1 \leq \alpha_1 x_1 + \alpha_2 x_2 \leq C_2$, which $C_1, C_2, \alpha_1, \alpha_2$ are constant coefficients and x_1, x_2 represent factors. Additionally, if the surface model[24] is preferred not to be a common linear or quadratic one, then it would be another case of the above mentioned situation. For instance, in the case that a reduced quadratic or cubic practical model is expected to better fit the data. Lastly, when there would be a limitation that reduces the total number of affordable runs with respect to what is needed for a standard design. In the case of herby reported research, considering the participated factors in the study, a probable DOE should remedy some of the above mentioned situations.

As it is given an account in the chapter of introduction, current dissertation experimentally explores the way that five participating factors in ISF, namely tool and step size, feed rate, spindle speed and blank thickness affect the formability of material. Indeed, all the mentioned parameters can be regarded as continuous numerical factors which will be later adjusted at appropriate levels according to preliminary knowledge of the process and the one that is acquired by screening trials. Usually, there are common limitations in practically attainable levels of the last factor, blank thickness. The first problem is that it was difficult to find suitable sheet metal of five different thicknesses in the local market, and then it is almost impossible to meet the levels that are proposed by

[24] Practical model

a standard design such as CCD. Considering the limitation of maximum-minimum feasible levels of blank thickness according to screening trials, there will be some more restrictions. Moreover, consideration of each additional thickness impels some extra expenses, as the sheet metal is normally sold in full size blank in the market (e.g. $2 \times 1\ m^2$) that is much more than what is required for experiments.

For these reasons, despite its acknowledged importance, blank thickness has not been taken into account in DOE by some previous studies that attempted to experimentally investigate the formability of material in ISF (Hussain et al., 2010). In another case (Ham & Jeswiet, 2007), it is reflected as a categorical factor, divided in three qualitative levels, namely thin, medium and thick through a standard design, Box-Behnken. Such a qualitative arrangement is insufficient to give quantitative information on mid level thicknesses and interaction effects of blank thickness, which are absolutely necessary for further optimization procedures. The same authors have reported similar study (Ham & Jeswiet, 2006) in which they used a three-level-factorial design for two factors including blank thickness, which is multiplied by another factor in two levels. In this paper they provided some graphs of linear individual effects; additionally they claimed a significant interaction effect of blank thickness and step size. Nonetheless, apart from inefficiency of their experimental design for a larger number of participating factors, it was neglected to render diagnostic criteria to prove design's qualification.

As it is briefly reviewed above, although some similar studies have been carried out to date, considering the application of DOE; however they have failed to properly treat the factor of blank thickness by their experimental designs. Therefore, it was decided to make use of a robust efficient computer-developed DOE, clearly "Optimal Design", to

address the aforesaid situations in this study. The core idea of optimal design (it is mainly based on the work done by Kiefer (1961), is to seek for the best design in respect of certain criterion and existing restrictions. More specifically, given the being studied factors and their practical-technical boundaries in addition to the total number of affordable runs as well as a preliminarily desired model, a computer program searches for the most optimal design by consideration of specific principles.

Among different criteria for optimal design, namely D, A and IV, the first one is probably the most commonly employed. By D-criterion it is intended to maximize the order of orthogonality of design matrix (X)[25]. Recalling the basic equation of regression model (2.1) in matrix form, $y = X\beta + \epsilon$, it reveals underlying logic for D-criterion that is the higher independency in design matrix hints the further available information from the design space. In other words, correlated components of design matrix (X), provide the same value for different regression coefficients, which it means that there is no way to distinguish the individual or interaction effect of corresponding terms to theses coefficients. According to matrix algebra, dot product of two orthogonal vectors (each pair of columns in a matrix)[26] equals to zero, which implies the independency of two vectors' components with respect together. In the same way, by D-criterion for a design matrix (X), the purpose is assessment of $|X'X|$[27], so as the maximum possible measure calls for the maximum optimality (Hill & Lewicki, 2006). To compare the efficiency of

[25] Design matrix (X), includes all the factors' levels of a specific design, in which each component of x_{ij} represents the coded (e.g. $-1,0,1$) level of the j^{th} factor for the i^{th} observation.
[26] Each particular column in design matrix represents all applicable levels of the pertinent factor for all the runs in the whole experiment.
[27] It is the determinant of the design matrix that is multiplied (cross product) by its transposed matrix (X').

two consequent designs for the same situation by D-criterion, equation 2.4 is applicable (Montgomery, 2008):

$$D_e = \left(\left| \frac{(X_2' X_2)^{-1}}{(X_1' X_1)^{-1}} \right| \right)^{1/p} \tag{2.4}$$

Where p stands for the number of terms in response model, and X_1, X_2 represent design matrices. However Hill and Lewicki (2006) proposed another equation containing the same essence:

$$D_e = 100 \times \left(\frac{(|X'X|)^{1/p}}{N} \right) \tag{2.5}$$

Where N is the number of total observations.

A-criterion attempts to maximize the sum of the orthogonal components (trace) of the $X'X$ matrix, which in turn leads to reduction of the average variance in regression coefficients vector. The associated efficiency can be calculated by equation 2.6 (Hill & Lewicki, 2006).

$$A_e = 100 \times \left(\frac{P}{trace[N \times (X'X)^{-1}]} \right) \tag{2.6}$$

By IV-criterion it is meant to decrease the prediction variance to the least possible value. Notably, it is underlined in Design-Expert User's Guide (Stat-Ease, 2011) that the software recommends IV-criterion in the case that accurate response surface is desired for prediction and optimization purposes. They also have referenced to the work done by Piepel (1988) for further information about the relevant algorithm that is named as "convert algorithm". However, it is highlighted there and then by Anderson and Whitcomb (2005) that D-criterion is probably the best choice in the case that fractional factorial design (e.g. for screening design) is in demand. Moreover, Hill and Lewicki

(2006) stated that D-criterion is faster than A-criterion as far as computational speed concerned. They also added that the former criterion is generally privileged compared to the later, except in case of complicated design space in terms of boundaries and restrictions, that it would be more wisely if other criterion were examined likewise.

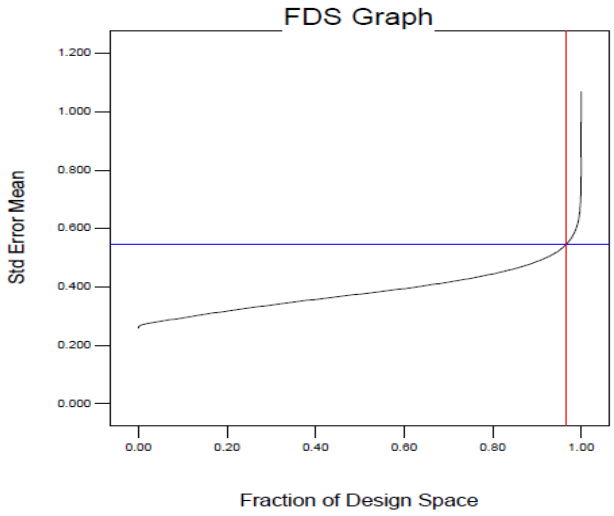

Figure 2.3 FDS graph for a specific IV-Optimal design (FDS=97%; Std error mean=0.54; d=1; s=1; a= 0.05, No. of runs=72)[28]

For this study, both D and IV optimal criterion adopted to verify the best resulted design. It subsequently observed that the later criterion provides a slightly better design regarding convenient applicable factors' levels that it rendered; and also by consideration of Fraction of Design Space (FDS) plot. Figure 2.3 reflects the FDS graph for IV-Optimal design of five factors in seventy two runs by employment of a quadratic model that is augmented with interaction of three factors.

Previously given a specific model, FDS is a graph that illustrates the percentage of

[28] "a" is the standard significance or confidence level. The ratio of sigma (s) to delta (d) gives an estimation for design accuracy, so that the higher ratio ($\frac{s}{d}$) leads to the higher accuracy and the lessend FLD.

design space that provides lower or equal prediction error with respect to an already specified expectable error (Anderson & Whitcomb, 2005). Generally, a smother FDS curve that is located in lower place in coordinate system is desired as it infers that a lower prediction error is uniformly distributed through the design space. It is recommended as the most important measure for prior evaluation of an Optimal Design by Design-Expert User's Guide (Stat-Ease, 2011). However, an optimal design cannot be successfully accomplished except by exact determination of factors' levels, probably as a consequence of a suitable screening design.

2.4. Determination of factors' levels

Coleman and Montgomery (1993) recommended that "Prior to conducting the experiment a few trial runs or pilot runs are often helpful". Normally screening experiments (trial or pilot runs) are executed for two major purposes, namely detection of characterizing factors[29] in being studied process and also realization of the appropriate levels[30] of such factors. Nevertheless, in this research the first objective is already achieved by the process knowledge arisen from the previous research works. As it is discussed before in the chapter one, five major predictor parameters, namely tool and step size, feed rate, spindle speed and blank thickness are designated to be examined as for their individual or interaction effect on material formability in ISF process. Typically as in the case of this study, screening experiments commence with arrangement of factors in two wide-range levels, and sequentially progresses by the

[29] Individually significant factors

[30] Appropriate levels translate the number of the levels as well as their ranges, which are in close correlation with adoption of the proper experimental design.

knowledge acquired from each run to finally narrow the range of levels to reasonable applicable measures.

In pursuance of aforementioned objective, in this research a half fractional two-level factorial design of resolution V was adopted by combination of five relevant factors in sixteen trials. The Introductory factors' levels are listed in Table 2.1. General description of examination process was given in the first chapter and the detailed explanation is provided through the next sections.

Table 2.1 Introductory factors' levels for screening experiments

Factor	Name	Units	Lower level	Upper level	Mean	Std. Dev.
A	Tool Tip Diameter	mm	4	10	7	3
B	Step Size	mm	0.05	1.2	0.63	0.57
C	Feed Rate	mm/min	400	6000	3200	2800
D	Spindle Speed	rpm	0	4000	2000	2000
E	Blank Thickness	mm	0.87	2.23	1.55	0.68

However, it should be briefly noted here that through screening trials, frustum conic parts[31] of specific profile was formed until occurrence of the crack on the part. Afterwards, the depth of the part at which crack had taken place was considered as the numerical measure of formability with regards to each combination of factors' levels. More importantly, the appearance of formed part, including its surface quality, was taken in to account as a qualitative measure of process feasibility, because it reveals practically valuable information about workability of factors' levels. Additionally, processing time was considered for each run, as it plays a key role in case of industrial application of ISF process. The results of such experimentation are managed to be described with regards to each factor in the following.

[31] The material used is aluminum alloy sheet AA 3003. Detailed properties of material are provided in the next section.

Through the screening trials, the major problem appeared as a considerable removal of sheet material by tool when the upper level of blank thickness (2.23 mm) employed (Figure 2.4). The situation deteriorated especially by involvement of the lower level of tool tip diameter in trials. More observations imparted that higher level of step size and spindle speed can significantly intensify this phenomenon. However the impact of high feed rate found as to be regarded in the second place, compared to the rest of factors.

Figure 2.4 Two parts formed by identical process parameters and different thickness.

This phenomenon can be realized due to accumulation of different causes, which can be explained with the aid of the model proposed by Silva et al. (2008), for the mechanism of ISF (Figure 2.5).

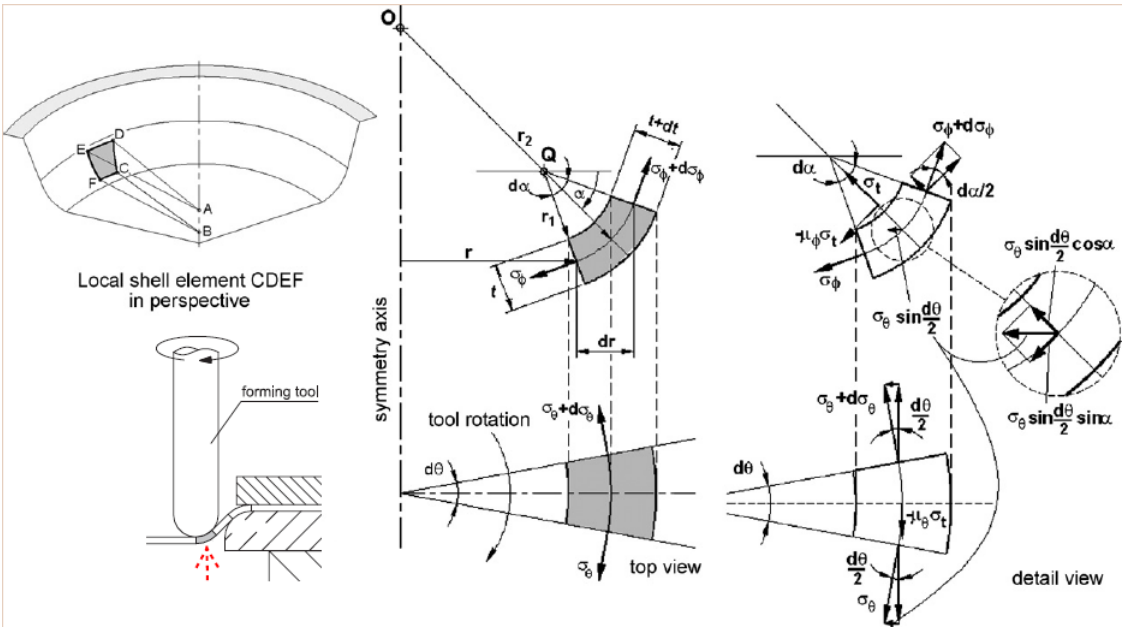

Figure 2.5 Schematic drawing for membrane analysis of contact zone in ISF (Martins et al., 2008)

Indeed, assuming the portion of the sheet adjacent to the moving tool as a curved shell element subjected to frictional contact forces, and excluding the minor effect of bending and shear forces, they concluded the strain state as to be plain strain. This conclusion is in consistence with those of the experimental investigations reported by Filice et al. (2002), Jeswiet and Young (2005). Nevertheless, it is in contrast with the outcome of empirical and also analytical studies performed by Allwood et al. (2007), Jackson and Allwood (2009). By later studies, authors inferred that the shear strain along the inclination direction of part wall in meridional intersectional plane can be regarded as the mainspring in ISF mechanism. Even so, it seems that the model proposed by Silva et al. (2008), despite the widely used simplifications, well serves in characterizing the above mentioned phenomenon. They eventually derived the normal stress along sheet thickness (σ_t) to be as following:

$$\sigma_t = -\frac{t\sigma_Y}{r_{tool} + t} \tag{2.6}$$

Where, t represents the sheet thickness; r_{tool} stands for the tool radius, and σ_Y denotes flow stress (yield stress) of the sheet.

For instant, considering the tool tip diameter of 4 mm, the thickness of 1.69 mm and the yield stress of 107.99 MPa[32] for AA 3003 aluminum alloy sheet utilized in this experiment, the magnitude of normal stress along thickness will be equal to 32.07 MPa. Keeping the tool size identical to the former case, but decreasing the sheet thickness to 0.87 mm, so that σ_Y will be 118.99 MPa, hence $|\sigma_t|$ reduces to 21.26 MPa that is about 66% of the previous value. By increasing the tool size to 6 mm, the corresponding stress will be 15.07 MPa that is less than 50% of the first measure, given as another example. As it is obviously evident from above reported evaluations, application of the higher sheet thickness translates to the higher stress (load) in thickness direction, which will be increasingly heightened by implementation of tiny tool tip.

More specifically, increase in thickness not only affects the through thickness normal stress by itself, but also calls for alternation in sheet material yield stress (in n and k[33] values as well), and then the rate of aforesaid stress. Moreover, it has been demonstrated by several studies (Hosford, 2005; Meyers & Chawla, 1999) that the relationship

[32] According to the result of tensile test reported in Table 2.4.

[33] n is strain hardening exponent; and k is the strength coefficient in power low ($\sigma = k\varepsilon^n$). Both of these measures can be attained as a result of tensile test and they are normally used to describe plastic behavior of material.

between hardness[34] as a measure of material resistance to penetration, and the yield stress is direct and linear[35]. This means that by consideration of the pure effect of sheet thickness as well as the consequential change in mechanical properties of material, increase in sheet thickness generally leads to increase in through thickness normal stress, while decrease in surface resistance of sheet material to penetration.

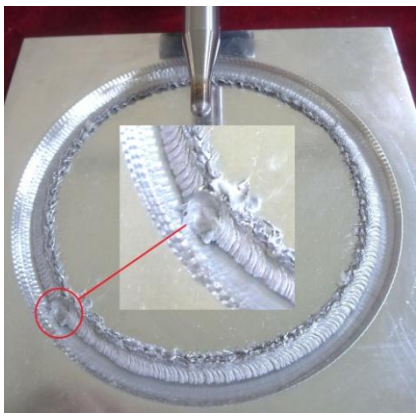

Figure 2.6 Remarkable penetration of tool to sheet material

For these reasons, tool tip remarkably penetrates the thick sheet (Figure 2.6); in the same time the higher through thickness normal stress motivates magnified frictional stress (load) in both the axial and circumferential directions of tool movement. Such a stress can be clearly intensified by application of smaller tool tip and the larger step-down size as well. This excessive frictional force (stress) compels adherence of sheet material to tool's tip (Figure 2.7) that in turn results in removal of sheet material as tool proceeds.

[34] Although it is not an independent mechanical property of material such as yield stress, but it provides the most convenient guide to plastic behavior of material.

[35] According to Hosford (2005), for Brinell, Vickers, and Knoop hardness in the case of plain strain state, the relationship after unit conversion can be concluded as $hardness \approx 3\sigma_y$. Meyers and Chawla (1999) suggested that, for work hardening material, the flow stress at the strain of 0.375 should be replaced by simple yield stress (σ_Y).

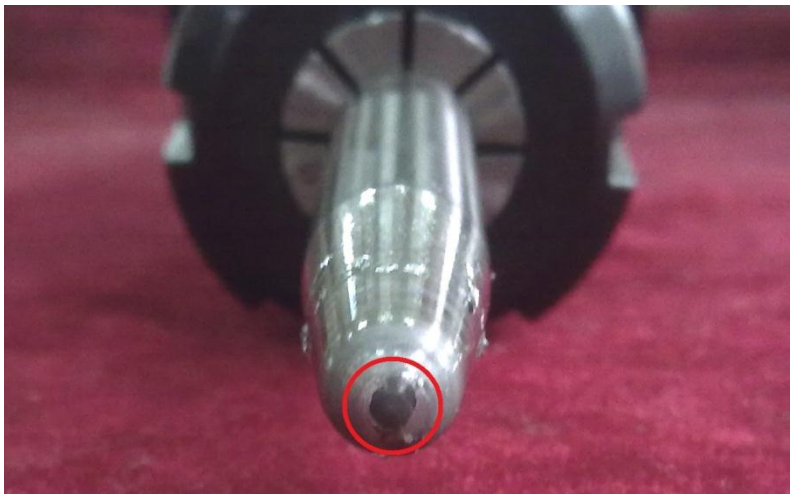

Figure 2.7 Adherence of sheet material to tool tip

Additionally, by setting the spindle speed at the upper level, it obviously induced to a higher level of sliding friction. It consequently generates extra heat, thus the lessened yield stress and hardness of sheet material (Davis, 1993; Kaufman, 1999), which accumulatively contributes to further removal of material. It is notable that the, the yield stress of work hardened AA 3003 sheet may reduces to almost the half amount by increase of its temperature from $25^{\circ}c$ to about $175^{\circ}c$[36]. It is also observed during the screening trials, the bubbling, burning and evaporation of the lubricant (oil) in such elevated temperatures by greatly boosted spindle speed. Even in case of moderate temperature of tool-sheet, resultant kinetic energy from highly elevated spindle speed makes lubricant to scatter from the tool-sheet contact zone. Therefore, deployment of excessive spindle speed, indirectly amplifies the removal of sheet material by reducing the effectiveness of lubrication, thereby aggregation of frictional stresses. This last statement implies that application of more efficient method of lubrication may alleviate the problems arisen from high spindle speeds, so that better putting advantageous

[36] This temperature is not perceivable by naked eyes through the ISF process, as aluminum alloys do not blush due to the elevated temperature, and it is not enough exalted temperature to redden the high speed steel tool.

attributes of rotating spindle into effect. Figure 2.8 represents a kind of wrinkle effect on back side of a specimen, owing to excessive frictional stresses arisen from concurrently application of very high spindle speed (4000 rpm) and a thick blank (2.23 mm).

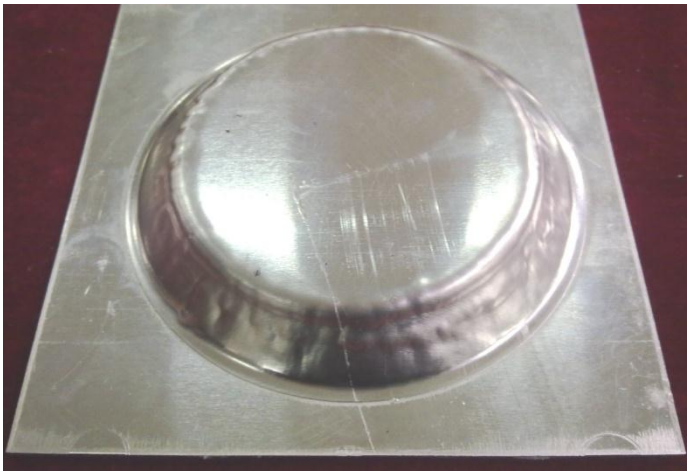

Figure 2.8 The effect of excessive frictional stress at the back side of specimen

Lastly, the lower level of spindle speed was set at zero for the main experimental campaign, as the comparative study of sheet material formability owing to rotating and also fixed spindle (tool) was desired. The lower level of sheet thickness (0.87 mm), resulted in no problem during pre-experimentation, hence it was fixed for the main trials. As for detection of suitable levels of step size, by actuation of upper level of this factor in preliminary experimentation, deep penetration of tool to sheet material experienced that made severe damage to material by progression of forming process.

Apart from technical aspects, from efficiency point of view application of very small pitch size (0.05 mm) suggests a huge amount of time required for accomplishment of process that is unacceptable in industrial applications. In order to obtain a very close approximation of process time, in addition to step size, the value of feed rate and the

profile of specimen are necessary to be predetermined. For the sake of compromising between time efficiency and experimental adequacy, the lower level of step size was decided to be 0.1 mm, and the lower level of feed rate was set at 800 mm/min for the main experimental campaign. By simultaneously application of the lower levels of step size and feed rate, processing time[37] was calculated about 140 min that is considerably higher than that of normally required by conventional sheet forming process[38]. Although feed rate has not been beheld as a driving factor in failure[39] of forming process by itself, however the interaction effect of this factor by spindle speed, step size and sheet thickness should be carefully looked out. Figure 2.8 illustrates a normal groove made by ISF at spindle speed of 1000 rpm, feed rate of 1500 mm/min in portion (a), and then appearance of a kind of wearing effect by increasing the spindle speed to 1500 rpm and feed rate to 5000 mm/min, in portion (b).

[37] It is for a standard depth of a particular specimen. It is discussed further in the following sections.
[38] It is shown in the following chapter that the processing time can be reduced to about 5 min through a reasonable combination of factors levels and compromise between acceptable formability and time efficiency.
[39] By failure it is meant unacceptable removal of sheet material in the way that progression of process is not any longer tolerable (it is unsafe or harmful for tool or machine) or the quality of formed part is so poor (Figure 2.4 and Figure 2.8).

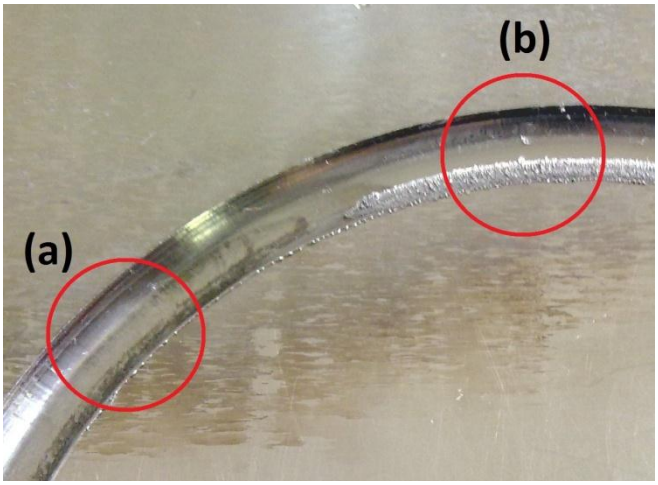

Figure 2.9 (a) Appearance of the normal ISF-made grove by application of low spindle speed and feed rate; (b) the effect of higher frictional stress by giving a rise to spindle speed and feed rate

To guaranty the workability of sheet material, eventually it was found that it is much more convenient if the commencement of process happens with the lower levels of spindle speed and feed rate. Afterwards, it should proceed by gradually rising of the measures up to the predefined levels, through the first two rounds of forming process. Such an enhancement is very likely due more to the strain hardening effect during the initial rounds of forming, and before the appearance of excessive frictional stresses and the consequent heat. It should be underlined here that alternation of theses factor at the beginning of forming process, have no effect on expected results from the previously determined level of factors for each trial.

AS it mentioned before, simultaneous application of the faster spindle speed, thicker blank and-or smaller tool tip by the larger pitch size, significantly intensify the removal of sheet material. In addition to aforesaid points to avoid the damage to material, the stiffness of incremental forming machine's part should be taken into account to prevent harm to machine. To deal with this last requisite aspect, approximate evaluation of involved loads (such as equation 2.6) should be taken into consideration along with

information about the maximum safely tolerable loads and effective power produced by machine. More importantly, the appearance and surface quality of forming parts including the shape, size and quantity of chips (removed material), can provide a good guide about how the process harshly proceeds. Eventually keeping all these points in mind, and performing iterative follow up screening trials, experimentally enough broad and synchronously practicable upper-lower levels of participating factors was achieved. Reorganized factors' levels followed by screening experimentation are managed in Table 2.2.

Table 2.2 Finalized factors' levels for the main experimental campaign acquired by screening experiments

Factor	Name	Units	Lower level	Upper level	Mean	Std. Dev.
A	Tool Tip Diameter	mm	6	12	9	3.00
B	Step Size	mm	0.10	0.88	0.49	0.39
C	Feed Rate	mm/min	800	5000	2900	2100
D	Spindle Speed	rpm	0	3000	1500	1500
E	Blank Thickness	mm	0.87	1.69	1.28	0.41

Eventually, these extreme levels for the first four continuous numerical factors and the last discrete numerical factor (blank thickness) inserted into the software (Design Expert). The IV Optimal design was selected for 72 trials, including 62 model points, 5 center points, and 5 replications for detection of lack of fit. It is notable that the number of model points suggested by Design Expert was 31, nonetheless, the efficiency of design compromised for its high accuracy and robustness, so this number multiplied by two. For the reasons that thoroughly discussed before, and also taking into account the results of screening experiments, the factor of blank thickness was already arranged in three levels, namely 0.86, 1.3 and 1.75 mm. The last step before creation of design was managed by initially consideration of five response factors, including four criteria for formability of sheet material, in addition to process time as a measure for efficiency of

ISF process. Further explanations regarding response factors are provided in the section of trials and measurements. Finally continuous numerical factors, given the extreme levels, arranged by Design Expert in five levels (see Table 2.3).

Table 2.3 Final levels of factors for the main Optimal design of experiment

Factor	Name	Units	Levels				
A	Tool Tip Diameter	mm	6	8	9	10	12
B	Step Size	mm	0.1	0.36	0.49	0.62	0.88
C	Feed Rate	mm/min	800	2200	2900	3600	5000
D	Spindle Speed	rpm	0	1000	1500	2000	3000
E	Blank Thickness	mm	0.87		1.3		1.69

2.5. Material, tools and equipments

Explanation regarding the sheet material, forming tool, clamping device, ISF machine, lubrication and part profile is given through upcoming sections.

2.5.1. Sheet metal

Aluminum alloy sheet AA3003-H12 was utilized in this study, due to its wide industrial application and also availability in local market. The mechanical properties of the sheet material acquired by performance of sixty tensile tests for blanks of five different thicknesses in both Rolling and Transverse directions (RD and TD). Figure 2.10 shows some specimens examined by tensile test.

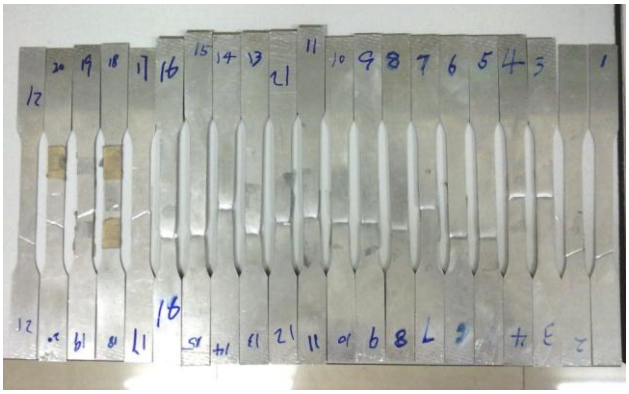

Figure 2.10 Some of examined specimens in tensile test

The resultant mechanical properties for applicable blanks of 0.87, 1.3 and 1.69 mm in thickness, according to Table 2.3, are tabulated in Table 2.4. In this regard, further details are provided in appendix A. Blanks were cut to the size of 140×140 mm^2 to fit the clamping device.

Table 2.4 Mechanical properties of utilized aluminum AA3003-H12 sheet material

Thickness (mm)	**RD**			**TD**		
	UTS (MPa)	**YS** (MPa)	**%E**	**UTS** (MPa)	**YS** (MPa)	**%E**
0.87	126.57	118.99	1.38	137.97	135.47	0.55
1.3	117.26	111.16	4.92	126.68	123.62	1.06
1.69	114.02	107.99	6.38	122.45	119.90	2.07

2.5.2. Forming tool

Forming tools of hemispherical tip were made out of High Strength Steel (HSS)[40] bars by application of turning and grinding machines in different steps. To attain the better stiffness and strength, tools of lower tip size were tapered by inclining angle of 6 degree before forming the hemispherical portion. Figure 2.11 presents the forming tools that are manufactured in six various sizes from 4 to 12 mm in diameter.

[40] Hardness of HSS material was in the range of 60 to 65 HCR.

Figure 2.11 Forming tools in six various tip size

Considering the application of high spindle speed in specified DOE for this study, it highlights the importance of dimensional accuracy in manufacturing of forming tool. Even a minor distortion of tool tip or indiscernible deviation between symmetric axis of tool shank and perpendicular direction, will produce a kind of jumping or hammering effect on sheet surface as it is being formed (see Figure 2.12).

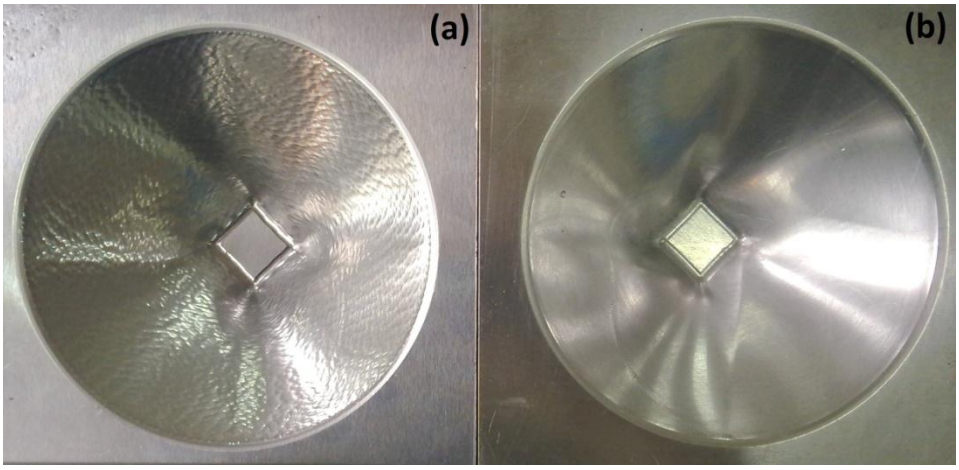

Figure 2.12 (a) Part formed by an inaccurately made tool and spindle speed (SS) of 500 rpm; (b) part formed by the same tool that is fully constrained from rotation (SS=0).

Such an effect, apart from reduction of surface quality, produces an uncontrolled error factor in experiments that prevents accurate assessment of underlying process factors. Taking into account that the forming tool must be made out of a hard to form material

(HSS), it suggests careful selection of the cutting tool. In this regard, CBN[41] cutting tools are commonly recommended; however a kind of cemented carbide[42] cutting tool was used herein to make incremental forming tool, owing to its acceptable functionality and also because of its availability in local market.

To avoid the negative effect of sheet material adhered to tool on formability and surface quality of parts, visual inspection and then in case of necessity, polishing of the tool tip should be considered from each trial to the next. This procedure followed by initially application of relatively rough sand papers by abrasive particle size of 30, 25 or 15 μm and then continued by making use of diamond paste of 10, 5, 3.5 and 1 μm in abrasive particle size (see Figure 2.13).

Figure 2.13 Diamond paste of different abrasive particle size, used for polishing of tool tip

2.5.3. Fixture and clamping device

Figure 2.14 represents the clamping device, which is constituted from back holding plate and upper blank holder plate that can be fastened on a mounting frame by six screws. The mounting frame can be fixed on the machine table by using fixtures. The back

[41] Cubic boron nitride

[42] Resulted from sintering the crystals of tungsten carbide (WC), titanium carbide (TiC), and tantalum carbide (TaC) in a cobalt matrix.

holding plate was designated to minimize the amount of bending and spring back side effect, especially during the initial rounds of forming. All the clamping system's parts had been made out of steel.

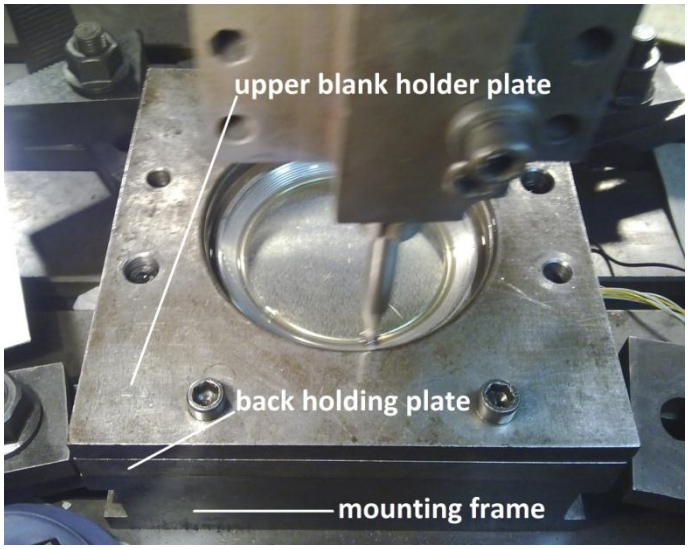

Figure 2.14 Clamping device

2.5.4. Incremental forming machine

Generally, it is possible to make use of CNC milling machines for ISF process. In this study, we have used two CNC milling machines (Figure 2.15); the first one for trials of non-rotational spindle (spindle speed=0) and the other for trials of spinning tool (spindle speed≠0). The reason behind such an approach was inability of the second machine to keep the tool fixed (constrained to rotation); however thanks to its mechanical system of spindle, it was capable of providing enough power for the purpose of experiments. On the other hand, the spindle of the first machine was directly driven by a high speed electric motor; hence the generated power as well as the maximum tolerable load was expected to be not adequate for ISF application. To remedy the situation, an especial

installation, which had been mounted on working arm of the machine, was employed to firmly hold the tool (See Figure 2.14).

Figure 2.15 Machine with the fixed tool holder (a); machine with the rotating spindle (b)

General specifications of the first CNC milling machines (a) are provided in Table 2.5.

Table 2.5 Specification of CNC milling machines employed for ISF process

Name	NH-SK1060			
No. of Axis	4			
Range of Axis (mm)	X: 1000	Y: 600	Z: 550	A: 400
Total Power (KW)	17			
Spindle Power (KW)	7.3			
Maximum Spindle Speed (rpm)	18000			

2.5.5. Lubrication

By lubrication not only improvement in surface quality of part and reduction in tool wearing is desired, but properly managed lubrication can bring the beneficial aspects of friction into play. As it is briefly discussed in section 2.4, the presence of sufficient

friction can lead to better formability of material in different ways. Such an enhancement can be explained by augmentation of shear stress-strain along the thickness, and also by elevation of temperature in the restricted contact area between tool and sheet[43].

Considering the literature, Carrino et al., (2006) and also Leach, Green, and Bramley (2001) claimed no significant effect of lubrication method on accomplishment of ISF process. Skjødt et al. (2007) reported profound influence of lubrication on surface quality of incrementally formed part. However, with regards to sheet material formability, Silva et al. (2008) maintained that the effect of lubrication is insignificant. As it is reported in the section of 2.4, the former authors in contrast to the finding of Allwood et al. (2007) and also Jackson and Allwood (2009), disregarded the participation of shear strain-stress (through thickness) in the mechanism of ISF. In order to incrementally form titanium sheet (CP Ti)[44], Hussain et al. (2008) examined different lubricants namely mineral and machine oil, graphite, molybdenum disulfide and brome nitride[45] by application of different methods. Taking into account the amount of sheet material adhered to the tool tip[46] as well as surface roughness of finish part, they made judgment about the effectiveness of each method. Finally, they found that a mixture of molybdenum disulfide powder and an especial jelly when it is rubbed on the coated[47] Ti CP sheet, better serves to accomplishment of process.

---

[43] However adherence of sheet metal to tool tip should be carefully avoided.
[44]It is a good example of hard-to-form material by which, excessive frictional stresses are expected through ISF process.
[45] Graphite, molybdenum disulfide and brome nitride are solid lubricants.
[46] Visual observation made along with inspection by the aid of Energy dispersive spectroscopy (EDS) and Scanning Electron Microscope (SEM).
[47]Coating occurred by means of micro-arc oxidation, to create a layer of titanium oxide with specific thickness and porous size.

Eventually, it can be concluded that for efficient lubrication it is necessary contemplating the factors involved in determination of loads and also the sheet material alloy utilized in ISF trials. Subsequently the viscosity of lubricant[48], physical and chemical reaction of lubricant with tool-sheet material in elevated temperature and the method of lubrication should be taken into consideration. For this study, considering the results of screening experiments, machine oil was exploited for lubrication, which is in accordance with the works presented by Aerens et al. (2010) and also Hussain et al. (2009).

2.5.6. Part profile and CAD-CAM process

In order to investigate the ISF process, especially the formability of material by ISF, truncated conic or pyramidal parts were normally shaped by researchers in this field. Particularly, it is reported in several studies, making use of the former specimen in pursuance of this purpose (e.g. Dejardin et al., 2010; Duflou & D'hondt, 2011; Duflou et al., 2008; Martins et al., 2008; Takano, Kitazawa, & Goto, 2008; Ziran et al. (2010)). This is probably due to the simplicity and axi-symmetry of conic shapes that facilitate the forming process, in turn acquisition of the useful information.

According to descriptions provided in preceding sections and also during the first chapter, the maximum inclination angle of successfully formable part can be regarded as a criterion for formability of material in ISF process (Filice et al., 2002; Hirt et al., 2002; Hirt, et al., 2003; Jeswiet & Hagan, 2003; Jeswiet et al., 2005). However, application of

[48] In solid lubrication the size of particles and in the case of using coating film on the sheet surface the size of porous might be considered instead.

specimens with constant inclination angle of sides implies many trials to be required for assessment of maximum achievable slop angle. For this reasons, Hussain and Gao (2007) and also Hussain, Gao, and Dar (2007) proposed truncated conic parts with varying wall angle along the symmetry axis, as a new benchmark for examination of material formability in ISF process. Subsequently, forming parts with circular, parabolic, exponential and elliptical curvature of profile[49], they explored the height (depth) along the symmetry axis of part, at which fracture occurred. Using this value along with the equation of each curvature, they rendered the relevant maximum attainable slop angle. Ultimately, they declared that the maximum wall angle for parts of curved profile depends on the characteristics of each profile (e.g. the radius of the circular curvature, or generally the rate of increase in angle). Additionally, they demonstrated that the maximum wall angle corresponding to the part of constant slop angle is lower compared to that of all parts with varying wall angle (for the curved walls of given specifications).

To provide the most comparable condition to the standard method[50] of formability assessment in ISF, and also to compensate the likely effect of altering rate of rising slop angle, a new profile was introduced in this study. By this profile (Figure 2.16), inclination angle of wall increases uniformly along the symmetry axis of part (e.g. conic or pyramidal part). In other words, similar to the standard method, the rate of slop angle increment is constant (e.g. one) by the later design, however, it is zero in the former case.

[49] They noted corresponding measures to each profile curvature (e.g. the radius of the circular curvature)
[50] By this method, different conical parts of constant slop angle will be successively formed by increasing the wall angle, until the maximum feasible slop angle achieved.

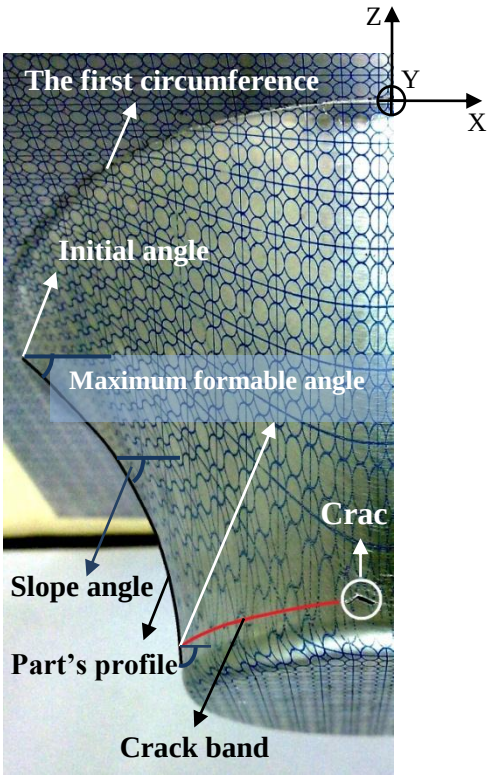

Figure 2.16 Illustration of part's profile and the coordinate system

Assuming the rate of slop angle (θ) increment along[51] the symmetry axis of part (z) to be constant ($\frac{d\theta}{dz} = a$; that a is a constant value); the relation between θ and z can be simply derived as following:

$$\theta = az + b \tag{2.7}$$

Considering $\tan(\theta) = \frac{dz}{dx}$, so that $\tan(az + b) = \frac{dz}{dx}$; and then:

$$\int dx = \int cot(az + b)\, dz \tag{2.8}$$

Resolving the integral in equation 2.8, the general equation of the profile with constant rate of increasing slop angle (CRISA) along symmetry axis (z) of part can be derived as following:

[51] Here, by the slop angle, the angle between flat portion of the blank and inclined wall of conic part is intended.

$$x = \frac{1}{a} ln[sin(az + b)] + c \quad (2.9)$$

Where a, b and c are constant values that can be determined by consideration of boundary conditions of the problem, namely the radius of the first circumference[52], the initial angle[53] and the maximum depth[54] (along z direction), which is corresponding to $\theta = 90^{\circ}$. Solving the system of equations for boundary conditions, the profile with CRISA for the condition of this experimentation, can be obtained as:

$$x = -85.470\, ln[sin(-0.012z + 0.750)] + 23.790 \quad (2.9)$$

In the same way, by substitution of values of a and b resulted from boundaries conditions in equation 2.7:

$$\theta = 0.67h + 43 \quad (2.10)$$

Where θ represents the slope angle in degree (see Figure 2.16), and h (mm) stands for the vertical height (depth) of the part along negative portion of z axis, but in absolute measure ($h \geq 0$). Finally, equations 2.9 and 2.10 were adapted to produce CAD model of the truncated conical part with CRISA[55] (Figure 2.16) in commercial software, UG NX-3 (Figure 2.17).

[52] It specifically depends on the internal size (radius) of back holding plate in clamping device along with the tolerance appointed for the safety.
[53] It is the inclination angle of profile at the any point lactated on the first circumference ($z = 0$). For the main experimental campaign performed for the current study, it is equal to 43°.
[54] It usually depends on the thickness of the back holding plate added to height of the mounting frame.
[55] Constant rate of increasing slope angle

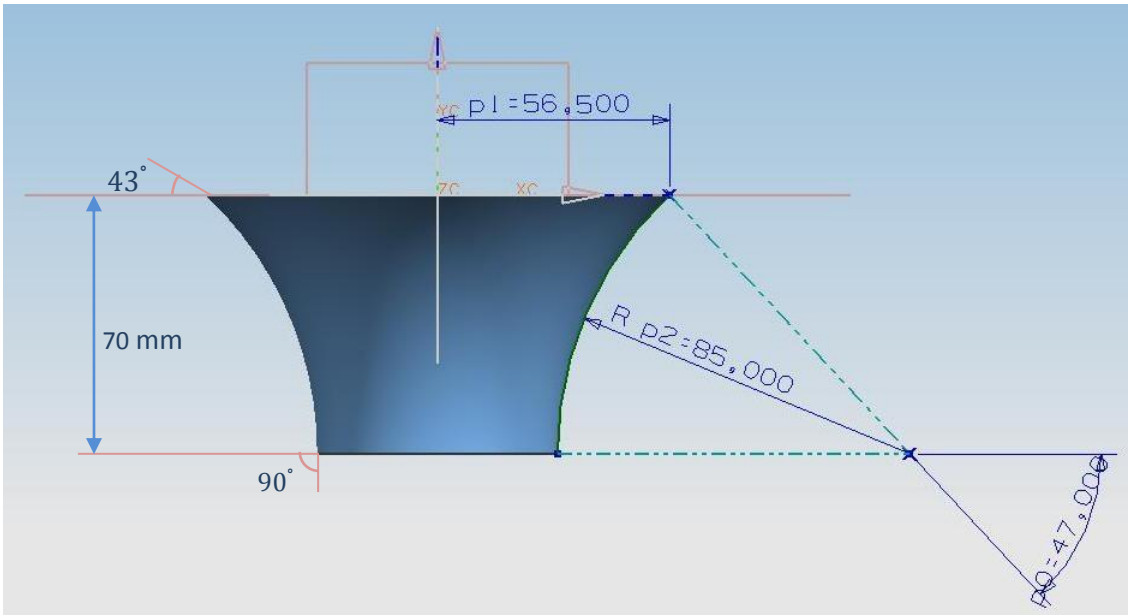

Figure 2.17 Schematic representation of CRISA specimen modeled in UG NX-3

Afterwards G-codes were generated for each specimen by the same software, then inserted to the CNC milling machine to eventually form the parts. For this purpose, considering the increasing inclination angle of parts, and also to investigate the effect of forming pitch size on formability of material, tool path was created by successive and equal stepping down[56] of forming tool along part's profile, passing each round. However, the main defect by this approach is a deep trace that tool leaves behind as it stepped down. In the case that the end of each contour and the beginning of the next one, continually take place in the same locus, tool's footmark effect becomes deeper and stronger by each step, leading to premature fracture. To diminish this defect, linear locus of tool's downward movement can be replaced by the spiral trend. Figure 2.18, shows the implemented trajectory of forming tool from different points of view.

[56] Trying some commercial CAD-CAM software for creation of tool trajectory, it was deemed to be impossible forming of parts with varying inclination angle of walls by application of spiral tool path, while setting pitch size to a constant value.

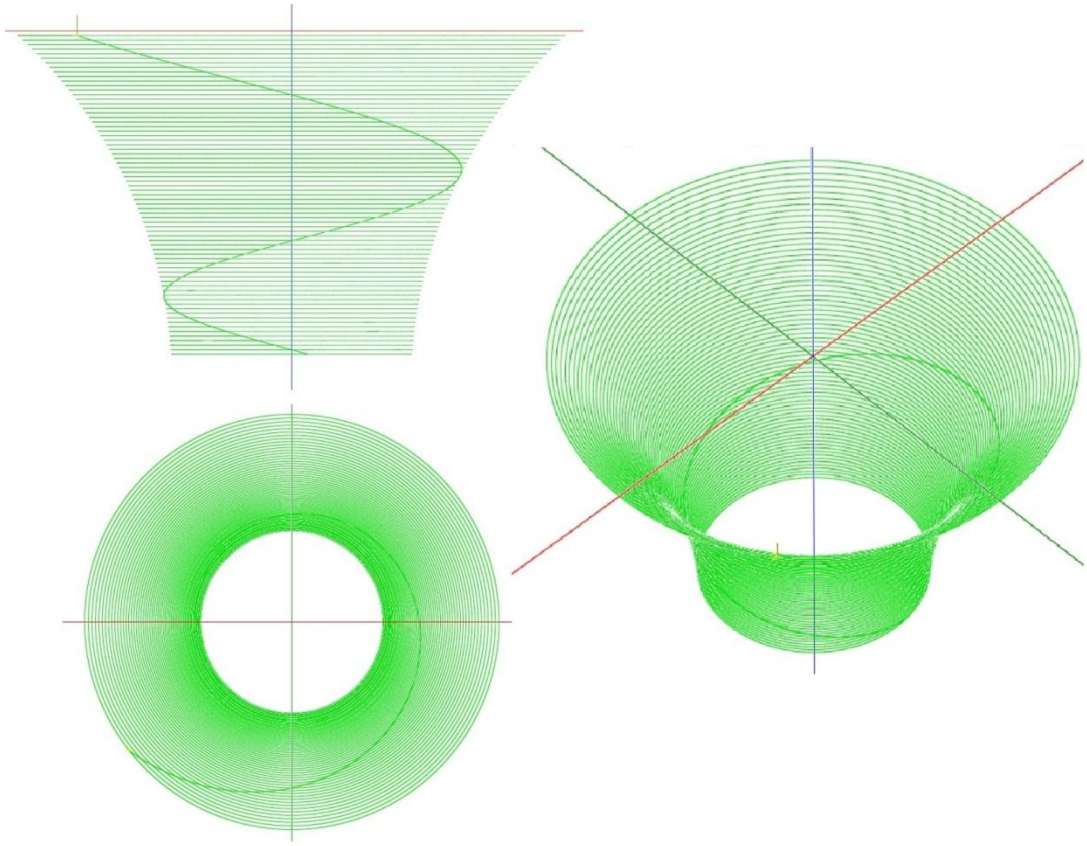

Figure 2.18 Tool path represented from different point of view

By application of proposed profile, the higher efficiency will be achievable as far as the number of required trials is concerned. Moreover, by deployment of a new formability criterion which is discussed through the following section, the maximum draw angle of the above mentioned profile can be utilized to predict the same factor for the parts of different profiles.

2.6. Measurements

After accomplishment of all trials, measurement of specimens should be carried out to specify the formability of material due to the relevant combination of contributing factors. In order to quantify the formability, two main methods are extensively adapted by scholars, namely assessment of planar and through thickness strains and

determination of the maximum attainable forming angle. To do so, it is necessary to form the parts until appearance of crack, and then immediately stop forming to investigate the part, especially around the fracture area. Pertinent clarifications on the mentioned subjects are managed in subsequent sections.

2.6.1. Detection of the crack

The relative position of the moving tool, clamping device and operator, in addition to the presence of oil and material chips or particles; particularly in the condition of high speed forming, make it difficult to detect the crack then stop the machine at once. Such a delay between the beginning and discovering of the crack can lead to rapid propagation of the crack, therefore reduction of accuracy in measurements. To properly address the problem, an optical sensor system was designed to detect the crack, for the first time according to author's knowledge. Figure 2.19 depicts different stages of preparation and application of the sensor system.

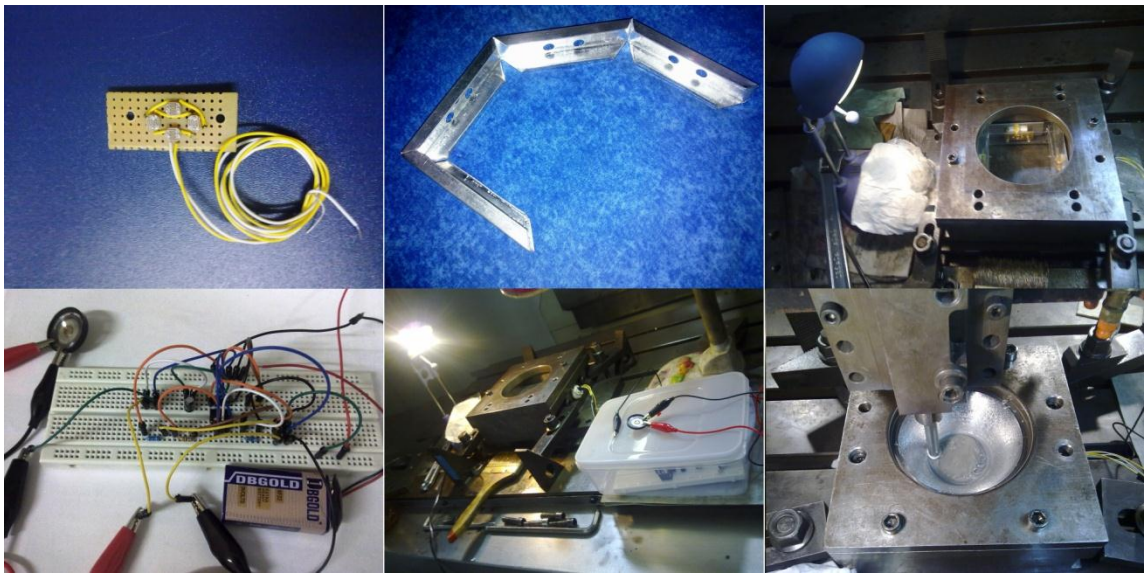

Figure 2.19 Different stages of preparation and application of the sensor system

This system, by implementation of Photo Conductive Light Sensors (PCLS), benefits from a simple bright idea that is the darkness in internal space of the clamp in which part is being formed. Special type of PCLS, Light Dependent Resistor (LDR) is made out of semiconductor material which reacts to specific spectrum of light, by altering its electrical resistance. More specifically, putting LDRs in complete darkness, they provide electrical resistance in the order of mega ohms, which means they pass no electrical current in circuit. However, putting them under elimination, their resistance suddenly reduces to magnitude of hundreds ohms, thus passing the current in circuit. Therefore, LDR can be used as a light switch in circuits. To increase sensitivity of the system to light radiation, especial combination of LDRs was designed to be mounted on a frame. This frame of adjusted dimensions, was positioned at the bottom of the clamping device in the way that the head of being formed part, at any expected height (depth) of fracture will be surrounded by the frame's eyes. Once the crack on the part's apex, grew to some extent that could pass a slight light beam, the sensor reacts by passing the current to the connected circuit, hence making alarm by a buzzer as well as a LED[57]. This system was utilized through the whole experimental campaign (72 runs), so that a significant improvement was observed in limitation of crack size, compared to the situation of screening experiments without use of the system. Figure 2.20 allows comparison between the sizes of cracks limited by implementation of the system, and the ones widened in absence of the system. It is notable that due to the nature of the system that is light dependent, Illumination plays a key role in efficiency of the system.

[57] Light Emitting Diode

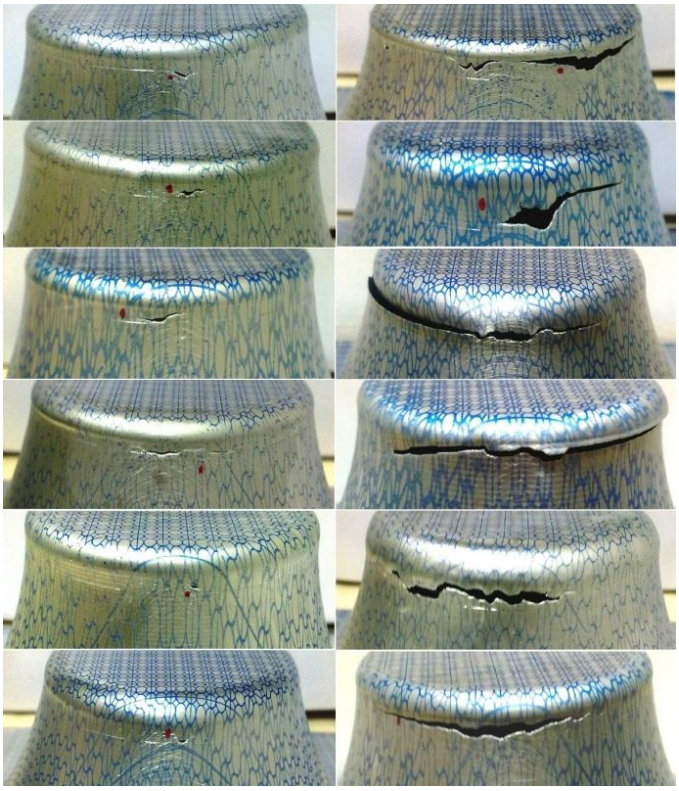

Figure 2.20 Cracks limited with the aid of sensors (left side); cracks controlled by visual observation (right side)

2.6.2. Forming limit diagram (FLD) and forming limit curve (FLC)

These two terms, FLD and FLC almost refer to the similar concept that is already explained in the first chapter. To make a quick review, FLD is a diagram of major strain (ε_1) along perpendicular axis versus the horizontal axis that represents minor strain (ε_2). By initially inscription of circular grids on the blank, circles transform to elliptical shapes due to the different strain in latitudinal (radial) and longitudinal (meridional) directions in forming area. The ratio of transverse and conjugate diameters of each ellipse to the diameter of the initial circles respectively can be translated to the major and minor strain corresponding to that particular elliptical portion in FLD (Filice et al., 2002; Shim & Park, 2001). Measuring elliptical shapes in and around the fracture area, it will be possible drawing FLC by resulted points, which divides the major-minor strain

space into safely formable, and failure regions (Hussain et al., 2010). To render a singular value as an indicator of formability, the maximum ratio of major to minor strain ($\frac{\varepsilon_1}{\varepsilon_2}$) or the intercept of FLC in FLD that is the amount of ε_1 while ε_2 equals to zero (FLD_0) has been utilized by researchers (Fratini, Ambrogio, Di Lorenzo, Filice, & Micari, 2004). For the same purpose, the maximum sum of major and minor strains ($\varepsilon_1 + \varepsilon_2$) is reported as well. It is notable that the shape and intercept of FLC varies depending on each contributor mechanism to ISF (stretching, shear and bending) to what extend participates in the process. This is in turn under the influence of mechanical properties of material, geometrical considerations (part's profile, diameter of the first contour, initial slop angle, etc.) and the process parameters' value.

For this study in which the last aspect is the matter of interest, initial attempt at application of FLD_0 made by printing circular pattern of radius 2 mm, using silk screening method. The next step was taken by practice of a visual inspection system[58] composed of a CCD camera and the related software, by which it was expected to measure the ellipses' axes in an effective and efficient manner. However, due to the malfunction of the system, the results found to be considerably inaccurate. To remedy the situation, a traveling microscope that was available in the same lab, was tried. The accuracy of adjusting screws was at the range of 0.01 mm, and a tolerance of $\mp$3% was supposed by the embedded lenses. Figure 2.21 presents the microscope and the adjusted set up.

[58] Similar to all other facilities have been reported in this dissertation to be used, this system was made available by the sheet metal forming lab, Department of Mechanical and Electrical Engineering at Nanjing University of Aeronautics & Astronautics, Nanjing, Jiangsu, China.

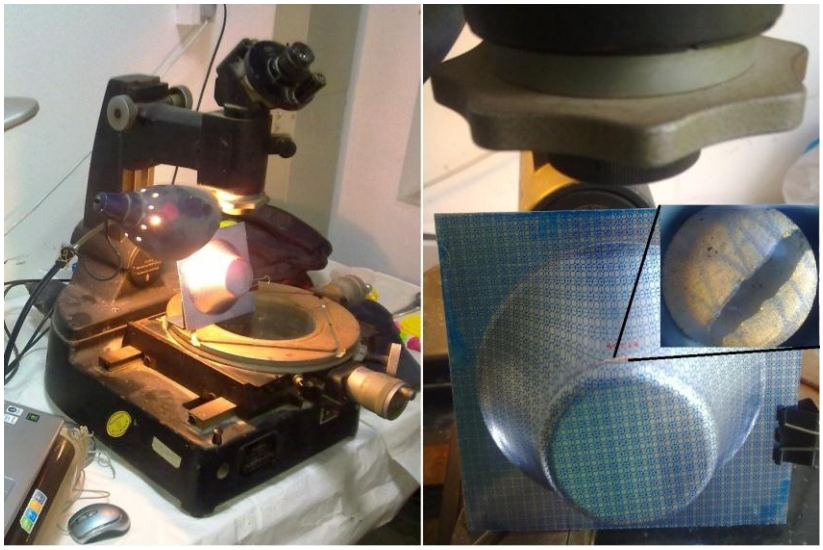

Figure 2.21 Application of Mylar microscope for measurement of minor-major strains

Nevertheless, by assessment of a limited number of specimens, and at the same time, considering other indications for formability, it was realized that the resultant measures of FLD_0 is not adequately reliable for the purpose of the study. To mention some of the reasons, old design of microscope, curved profile of parts in radial and meridional directions, relatively large longitudinal strain as well as the twisting phenomenon (Duflou et al., 2010) that induced to distortion of the ellipses and the shape of the cracks. Therefore, other criterion of formability, namely the depth of part at which crack occurs (h_f), in turn the maximum attainable slop angle and also the average thickness of the sheet at h_f, so that the average trough-thickness normal strain at this height were taken into account.

2.6.3. Measurement of h_f

To measure the height (depth) of the part, at which crack occurs (h_f), a height meter of 0.01 mm precision was employed. Figure 2.22 demonstrates the instrument.

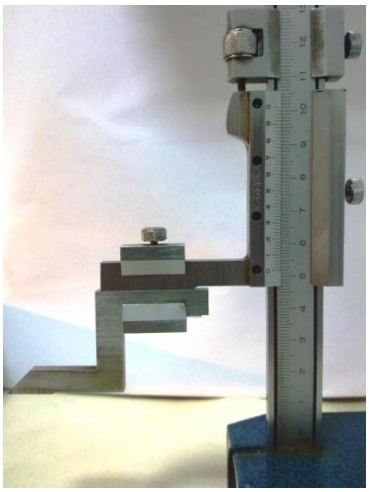

Figure 2.22 Employed height gauge in this experimental research

2.6.4. Measurement of the sheet thickness at h_f

To measure the sheet thickness at the same depth as the crack, first a guide line was gently inscribed around the part's head at h_f. Afterwards, sheet thickness was measured in 14 points of equal distances along inscribed line, using a micrometer of 0.001 mm accuracy which had been already adapted by author for this application (Figure 2.23). Finally, the average value of 14 measurements was appointed as the sheet thickness at fracture point, t_f.

Figure 2.23 Point micrometer adapted for assessment of sheet thickness at h_f

2.6.5. Calculation of the maximum draw angle

To determine the maximum achievable slop angle (θ_{max}), acquired values of h_f from previous stages were adapted in Equation 2.10. Considering axi-symmetry and constant rate of increasing inclination angle of part's profile as well as part's size[59], dimensional deviation between actually formed part and CAD profile is not deemed to be significant. Therefore, calculated measures of θ_{max} were estimated to be adequately reliable to be used in analysis of experiments. It should be mentioned here that Hussain et al. (2007) and also Silva, Alves, and Martins (2010) have used the same method to specify θ_{max}.

2.7. Introduction of a new criterion for formability

To produce absolutely meaningful indicator of formability by t_f , it is possible calculation of the true and engineering normal (average) strain along the normal vector of sheet surface (through thickness), as following:

$$\varepsilon_f = ln\frac{t_f}{t_0} \tag{2.11}$$

$$e_f = \frac{t_f}{t_0} - 1 \tag{2.12}$$

That t_0 is the initial thickness of the blank. ε_f and e_f, respectively represent true and engineering normal (average) strain which can be regarded as the main strain along perpendicular direction to part's surface (ε_3 versus ε_1 and ε_2). In the case that the plain strain condition to be considered as driving mechanism of the process, ε_f or e_f, should provide the same value as the corresponding measures of FLD_0. Owing to the method of measurement, by ε_f or e_f and h_f it is possible to more precisely gauge the formability

[59] In addition to the sheet material, the relative size of the tool, the first circumference radius, and constant step size for each trial that are reported to be affecting in dimensional accuracy of part.

compared to the situation of using θ_{max} individually. However, correlation of material formability and drawing angle of specimens is frequently highlighted by scholars. For these reasons and in pursuance of a reliable indicator of sheet formability in ISF, a compound criterion of formability (CCF) has been proposed in this study. The new criterion can be developed as following[60]:

$$CCF = \varepsilon_f \int_{t_0}^{h_f} \theta_{(z)}\, dz \tag{2.13}$$

That $\theta_{(z)}$ represents the relationship between slope angle and depth (height) of each point on part's profile. Considering the part with constant rate of increasing angle that previously proposed herein (Equation 2.9 and 2.10[61]), pertinent compound criterion of formability can be derived as following[62]:

$$CCF = (5.85 \times 10^{-3})\varepsilon_f(h_f - t_0)(h_f + t_0 + 128.30) \tag{2.14}$$

It should be underlined here, that CCF provides the possibility to acknowledge the influence of different rate of varying inclination angle along part's profile, thus better comparison between different profiles in terms of attained formability. The four above cited variables, namely h_f, θ_{max}, ε_f or e_f and the CCF were specified for each trial and inserted to the software, Design Expert, to be investigated as the criteria for formability of sheet material in ISF trials.

[60] e_f is also applicable instead of ε_f.

[61] θ in Equation 2.10 should be multiplied by $\frac{\pi}{180}$ to produce suitable value (in Radian rather than degree) for integration.

[62] e_f is also applicable instead of ε_f.

Chapter 3

RESULTS AND DISCUSSION

As it has been previously mentioned, by this research it is intended to investigate individual and interaction effect of five participating factors[63] on formability of sheet material in ISF. In pursuance of this goal, the suitable DoE was discussed to be Optimal Design, and the proper factors' levels for such a design specified through a series of preliminary experiments. Afterwards, the main experimental campaign of 72 trials, accomplished by forming of truncated conic parts of especial profile, until appearance of crack. By assessment of four criteria of formability[64] for each part, and also calculation of process time corresponding to the average height of fracture ($h_{f_{avg}}$), the process of data collection was ended. To precede data analysis, level of factors for each trial along with the acquired measures for response parameters, namely formability and process time were carefully inserted to the software, Design Expert 8.

This chapter, using Design Expert, begins by selection of response surface model, then performing Analysis of Variance, ANOVA, to realize which individual or interaction effects are significant in terms of each criterion of formability. By the followed sections, based on a privileged model, these individual effects, one by one, and interaction effects,

[63] Namely, diameter of hemispherical tool, pitch or step down size, rotational spindle speed, feed rate or tolls transitive speed and initial blank thickness.
[64] h_f, θ_{max}, ε_f or e_f and CCF.

two by two, are scrutinized. At the end, by consideration of the process time, CCF, t_0, and an especial terms for prediction error (POE) in different levels of superiority, the process has been optimized.

3.1. Selection of response surface model (fitness analysis)

The first step in analysis of acquired data should be taken by assignment of a response surface model for regression. Following to statistical evaluation of predicted response values versus the actual ones, it will be realized that to what extent a particular appointed model fits to real response data. To do so, four basic polynomial models, namely linear, interactions of two factors (2FI), quadratic and cubic model were considered. By each model, software did F-Test to investigate whether any significant improvement (small P value) happens by addition of higher order terms to the lower order model. For example by 2FI, significant improvement due to inclusion of interactions of two factors (e.g. AB) to the linear model (composed from A or B, etc.) will be examined. Finally three statistics[65], namely p-values, lack of fit (LF) and R-squared (adjusted and predicted) were provided by the software (Table 3.1) to aid selection of the best model (normally the model of highest order with no alias).

Table 3.1 Results of fitness analysis

	Improvement	**Lack of Fit**		**R-Squared**		
Model	**P value**	**P value**	**F value**	**Adjusted**	**Pridected**	**Aliased**
Linear	< 0.0001	0.0003	9.76	0.5778	0.5364	No
2FI	0.1206	0.0004	9.15	0.6148	0.4850	No
Quadratic	< 0.0001	0.0051	4.94	0.7914	0.6835	No
Cubic	0.0146	0.0459	3.23	0.9040	-0.9784	Yes

[65] Statistical functions used in statistical analysis.

Generally the small P value, lower lack of fit (smaller F value) and more reasonably comparable values of adjusted and predicted R-square are desired. Results of fitness analysis[66] presented in Table 3.1, reveals that the best model is quadratic or a modified cubic model in which some terms of higher orders are neglected (to remedy the problem of aliased terms).

3.2. ANOVA

ANOVA can be described as "a statistical technique which subdivides the total variation of a set of data into component parts associated with specific sources of variation for the purpose of testing a hypothesis on the parameters of a model" (Montgomery, 2008). In the case of appointing a response surface model (RSM), by ANOVA it is especially intended to distinguish factors of significant effect on a particular response factor, among all contributing factors in the process. Table 3.2 represents the results of ANOVA corresponding to a quadratic RSM for each of five criteria of formability.

Table 3.2 Summary of results of ANOVA corresponding to a quadratic RSM

Response Factor	Significant Factors	LF	Chance of LF due to noise	R^2	R^2_{adj}	R^2_{pre}	Adeq Precision[67]
$\boldsymbol{\varepsilon_f}$	A-B-D-E-BE-CD-DE-D^2-E^2	4.94	0.51%	85 %	79 %	68 %	16.25
$\boldsymbol{\theta_{max}}$	A-D-E-AB-DE-A^2-D^2-E^2	7.16	0.11%	79 %	70 %	52 %	11.20
$\boldsymbol{\int \theta_{(z)} dz}$	A-D-E-AB-DE-A^2-D^2-E^2	6.50	0.16%	78 %	70 %	51 %	11.10
$\boldsymbol{h_f - t_0}$	A-D-E-AB-DE-A^2-D^2-E^2	7.19	0.11%	77 %	68 %	48 %	10.52
$\boldsymbol{CCF}$	A-B-D-E-AB-CD-DE-D^2-E^2	4.30	1.13	83 %	77 %	64 %	14.88

A: Tool Tip Diameter | **B**: Step Size | **C**: Feed Rate | **D**: Spindle Speed | **E**: Blank Thickness

[66] This analysis performed considering ε_f as response factor.
[67] It is a measure of signal to noise ratio (values greater than 4 are recommended by the software).

From table 3.2 it can be seen that factor C (feed rate) has been realized as insignificant factor by any criteria of formability. It means that increase of feed rate even up to its upper level (5000 rpm) has no significant effect as formability is concerned. However such a degree of ascent can lead to a great improvement in terms of time efficiency of process, which is highly desired. On the other hand, Table 3.2 shows a difference as for significant factors in the case of distinctive categories of criteria is taken into account. First category is composed of ε_f and CCF, by which the normal strain through thickness, is the main matter of concern. The second category includes the three rests of formability criteria, by them the height of specimens at crack point, so that the strain along longitudinal direction can be implied. According to table 3.2, factor B (step size) provides significant effect when the through thickness strain is principally regarded as the criterion for formability. Nevertheless, by consideration of the criteria primarily attributed to the meridional strain, step size renders no significant effect. This fact suggests that a particular criterion may not represent all the different mechanism involved in the process, hence emphasizing the importance of defining a proper gauge for formability. However, different gauges can provide suitable indications for different mechanism; thereby better understanding of the process. In the former case, by merely consideration of the second category, for instance θ_{max}, as the gauge of formability, step size can be freely increased up to its upper size, 0.88 mm to considerably reduce the process time, while no harm to sheet formability. In spite of this early conclusion, taking the CCF into account, it can be inferred that the step size should be deliberately considered as for its negative or positive and also major or minor impact on formability.

Table 3.3 provides more details regarding ANOVA in the case of quadratic RSM and considering CCF as the response factor.

Table 3.3 Outcomes of ANOVA for quadratic RSM and by considering CCF as the response factor

	Sum of Squares	df	Mean Square	F Value	P Value	Significance
Model	17573.25	20	878.6623	12.61552	< 0.0001	significant
A-Tool Tip Diameter	1986.993	1	1986.993	28.52854	< 0.0001	significant
B-Step Size	1049.748	1	1049.748	15.0719	0.0003	significant
C-Feed Rate	5.522757	1	5.522757	0.079294	0.7794	-
D-Spindle Speed	3510.383	1	3510.383	50.40082	< 0.0001	significant
E-Blank Thickness	5542.005	1	5542.005	79.57012	< 0.0001	significant
AB	382.3476	1	382.3476	5.489609	0.0231	significant
AC	14.298	1	14.298	0.205286	0.6524	-
AD	195.7648	1	195.7648	2.810721	0.0998	-
AE	58.85236	1	58.85236	0.844981	0.3623	-
BC	1.674552	1	1.674552	0.024043	0.8774	-
BD	82.40811	1	82.40811	1.183186	0.2818	-
BE	274.4444	1	274.4444	3.940373	0.0525	-
CD	392.4172	1	392.4172	5.634185	0.0214	-
CE	0.195973	1	0.195973	0.002814	0.9579	significant
DE	852.0631	1	852.0631	12.23362	0.0010	significant
A^2	246.3286	1	246.3286	3.536697	0.0657	-
B^2	17.66723	1	17.66723	0.25366	0.6167	-
C^2	29.25939	1	29.25939	0.420096	0.5198	-
D^2	1328.151	1	1328.151	19.06912	< 0.0001	significant
E^2	544.4537	1	544.4537	7.81707	0.0073	significant
Lack of Fit	3349.27	41	81.68951	4.027167	0.0113	significant
Pure Error	202.8461	10	20.28461			-

P value (lower) and F value (higher) can imply the degree of relative effect of each factor. In the case of step size, it can be seen from Table 3.3 that the corresponding F value is in the range of one fifth to half of the values ascribed to the other three significant factors. Consequently, it can be simply interpreted as relatively slight effect of this factor compared to the rest of individual effects. In the same way it is evident from F values in Table 3.3 the strongest effect is related to the sheet thickness and in the

next stage, spindle speed is of high individual effectiveness. The interaction effect between spindle speed and feed rate, and also spindle speed and sheet thickness is in complete agreement with the observations through the screening trials. So that, aforesaid experimental evidence followed by statistical confirmations, emphasize again the need for cautious treatment of spindle speed, especially by consideration of its correlation with feed rate and sheet thickness. Finally the related response model was developed by software as following:

$$\begin{aligned} CCF = 87.83 &- 6.53A - 4.74B - 0.35C + 8.83D + 11.4E + 3.25AB \\ &+ 0.65AC - 2.36AD - 1.32AE + 0.22BC + 1.57BD \\ &+ 2.86BE - 3.51CD + 0.079CE + 5.08DE - 4.67A^2 \\ &- 1.24B^2 + 1.49C^2 - 10.47D^2 - 6.60E^2 \end{aligned} \tag{3.1}$$

Although quadratic model provides physically better interpretable terms and practically it is easier handling; however the moderate value of R^2 and the significant lack of fit reported in Table 3.2, depicts imperfection of this model in the case that prediction or optimization is concerned. Such a defect can be generally diminished by transformation of the model, most commonly into a power function ($y' = (y + k)^{lambda}$, where k and lambda are constant). Nevertheless, transformation is effective in the case that the ratio of maximum to minimum response provides a value of greater than 10, but in this case it is 2.96. Another possibility is application of a model of higher order, yet the cubic model was reported in Table 3.1 to be aliased in terms of individual effects of cubic order. Therefore a modified cubic model was developed after many trials and errors, to address both the problems. By the new model, ANOVA induced to excellent results in terms of LF, R^2 and adequate precision. Outcomes are summarized in Table 3.4.

Table 3.4 ANOVA for modified cubic model

Response Factor	Significant Factors	LF	Chance of LF due to noise	R^2	R^2_{adj}	R^2_{pre}	Adeq Precision[68]
$\boldsymbol{\varepsilon_f}$	A-B-D-E-AB-AC-AD-BD-BE-CD-DE-A^2-E^2-ACE-BCD-AD^2-AE^2-DB^2-CE^2-ED^2-ACDE-BCDE	0.82	58.17%	99 %	95 %	58 %	20.77
$\boldsymbol{\theta_{max}}$	A-D-E-AB-AC-AD-BC-BD-BE-CE-DE-A^2-B^2-D^2-E^2-ABD-ADE-BCE-BDE-CDE-BA^2-CA^2-AD^2-AE^2-CB^2 DB^2-CB^2-DB^2-EB^2-BE^2-CD^2- DE^2-ED^2-ABCD-ABCE-ABDE-ACDE	0.85	62.48%	99 %	97 %	82 %	28.69
$\boldsymbol{\int \theta_{(z)} dz}$	A-D-E-AB-AC-AD-BD-BE-CE-DE-A^2-B^2-D^2-E^2-ABD-ADE-BCE-BDE-CDE-BA^2-CA^2-AD^2-AE^2-CB^2 DB^2-CB^2-DB^2-EB^2-BE^2- CD^2-DE^2-ED^2-ABCD-ABCE-ABDE-ACDE	0.82	64.39%	99 %	96 %	81 %	27.68
$\boldsymbol{h_f - t_0}$	A-D-E-AB-AC-AD-BD-BE-CE-DE-A^2-B^2-D^2-E^2-ABD-ADE-BCE-BDE-CDE-BA^2-CA^2-AD^2-AE^2-CB^2 DB^2-CB^2-DB^2-EB^2-BE^2- CD^2-DE^2-ED^2-ABCD-ABCE-ABDE-ACDE	0.88	60.31%	99 %	96 %	80 %	26.43
$\boldsymbol{CCF}$	A-B-D-E-AB-AD-BD-BE-DE-A^2-B^2-D^2-E^2-BDE-ECD-CA^2-DA^2-AE^2-CB^2-DB^2- AD^2- EB^2- ED^2- DE^2 ABCD-ACDE	0.66	78.72	98 %	95 %	77 %	21.70

A: Tool Tip Diameter | **B**: Step Size | **C**: Feed Rate | **D**: Spindle Speed | **E**: Blank Thickness

To additionally certify the modeled design, some graphic diagnostics are provided by the software, namely normal probability plot of residuals, residuals versus runs and predicted values versus real response. Corresponding graphs to CCF are demonstrated in the following pages.

[68] It is a measure of signal to noise ratio (values greater than 4 are recommended by the software).

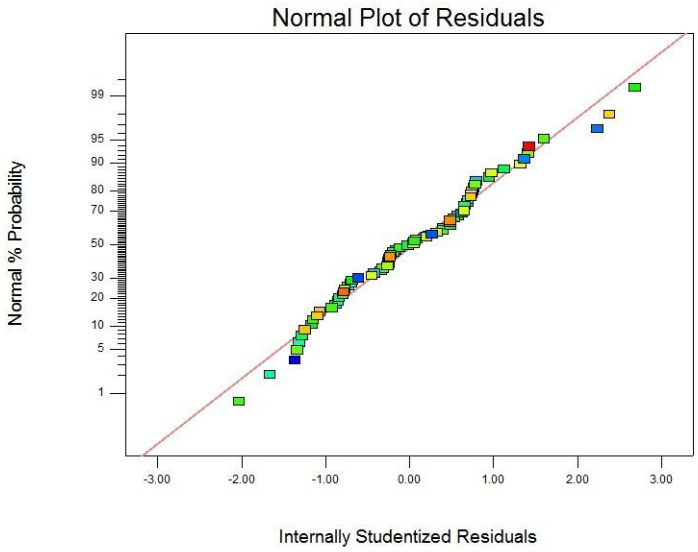

Figure 3.1 The normal probability plot

The normal probability plot (Figure 3.1) exhibits the normal distribution of the residuals (residuals have formed almost a linear distribution) that is the preliminary assumption for ANOVA.

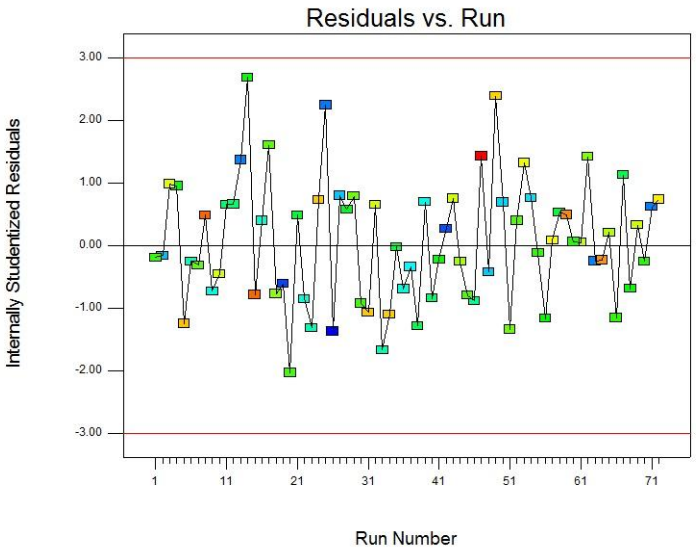

Figure 3.2 Plot of the residuals versus the experimental run order

This plot (Figure 3.2) provides the possibility to discover whether any uncontrolled factor affects the response. To confidently reject this probability, distribution of

residuals against run orders should be randomized that means no particular pattern or trend can be discerned.

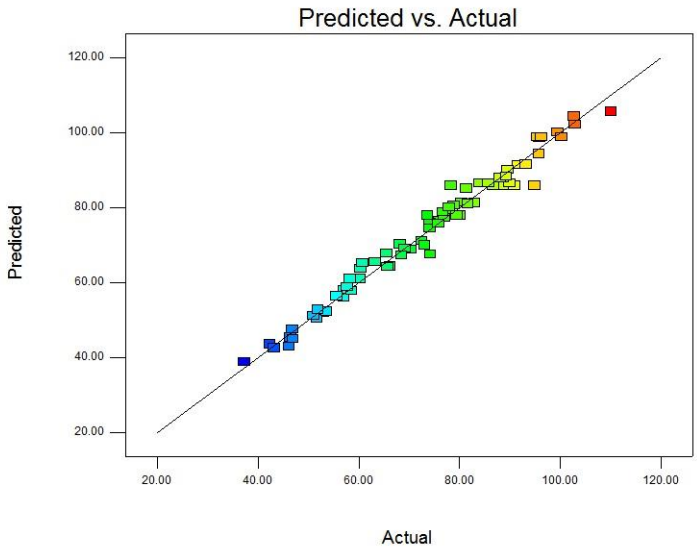

Figure 3.3 The plot of predicted values versus actual response

This graph (Figure 3.3) assists to explore if there is any especial response or bunch of responses that is difficult to be predicted by the assigned model. It is evident by ANOVA outcomes presented in Table 3.4, and also by examination of diagnostic plots that the modified cubic model (Equation 3.2) demonstrates adequate competency to simulate CCF values resulted from experiments.

$$\begin{aligned} CCF = {} & 90.40 - 9.45A - 4.51B + 0.75C + 19.70D + 22.24E + 4.27AB - \\ & 1.38AC - 4.30AD - 1.33AE - 0.04BC + 1.66BD + 1.91BE - \\ & 1.25CD + 0.31CE + 6.59DE - 3.99A^2 - 4B^2 - 9.91D^2 - 7.08E^2 + \\ & 0.47ABC - 0.63ABD + 1.32ABE + 0.50ACD + 0.74ACE + \\ & 1.53ADE + 0.42BCD + 0.92BCE + 3.65BDE - 5.00CDE + \\ & 5.19A^2C - 3.82A^2D + 9.13AD^2 - 5.66AE^2 - 9.16B^2C - 6.17B^2D - \\ & 4.86B^2E + 1.84CD^2 - 8.91D^2E - 4.85DE^2 + 2.51ABCD + \\ & 2.35ABCE - 6.32ACDE \end{aligned} \tag{3.2}$$

3.3. Simulation of individual and interaction effects - Graphs

The principal outcomes of experiments can be succinctly depicted by two dimensional, contour and three dimensional plots provided by Expert Design 8 to portray the individual and interactive effects. For all contributor factors, blank thickness (BT), spindle rotational speed (SRS), feed rate (FR), pitch size (PS) and tool tip diameter (TTD), aforementioned graphs are presented and discussed through the following sections. For the sake of abridgment, lower, mid and upper levels of factors are respectively referred to as -1, 0 and 1.

3.3.1. Blank thickness

Figure 3.4 allows comparison between different curvatures of correlation for CCF and sheet thickness. As it evident from graph (a), by setting all other factors at their midlevel, the increase in blank thickness leads to improved formability (CCF). However, by alteration of other factors, the curvature transforms. Finally, tool tip diameter, feed rate and spindle speed were adjusted to their upper level, and step size was fixed at the lower level. As a result, correlation curvature transformed to a concave shape by which the best formability is achievable about the midlevel of thickness (1.3 mm). Such a behavior definitely will be neglected in the case of using traditional OFAT as the governing method of experimentation. Even, by two-factorial design, it is barely possible discovering such a phenomenon. For this reason, software has provided a caution, warning that this factor participates in some interaction effects; hence the shape of correlation curvature is entirely dependent on the measure of other contributing factors. On the other hand, reasonably wide range of levels is required to realize such an

interactive effect. For instance, by application of blanks with varying thickness in the range of 0.8 to 1.3 mm, aforesaid effects probably will be neglected.

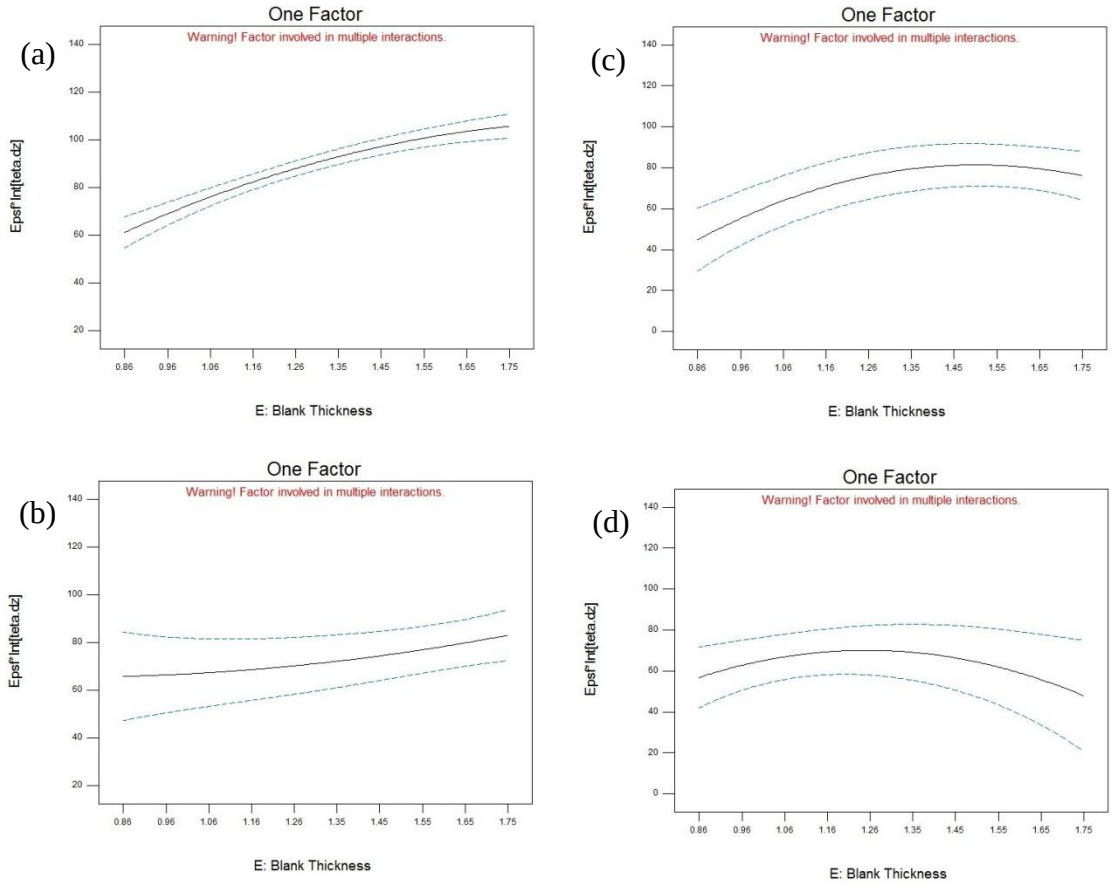

Figure 3.4 CCF versus blank thickness; (a) TTD=0, PS=0, FR=0, SRS=0; (b) TTD=-1, PS=-1, FR=-1, SRS=-1; (c) TTD=1, PS=1, FR=1, SRS=1; (d) TTD=1, PS=-1, FR=1, SRS=1

For better understanding of interaction effect of two factors, contour plots provided by Design Expert can be of great assistance. Figures 3.5 to 3.8 show how interaction effect of sheet thickness by the rest of factors could affect sheet's formability as well as process efficiency.

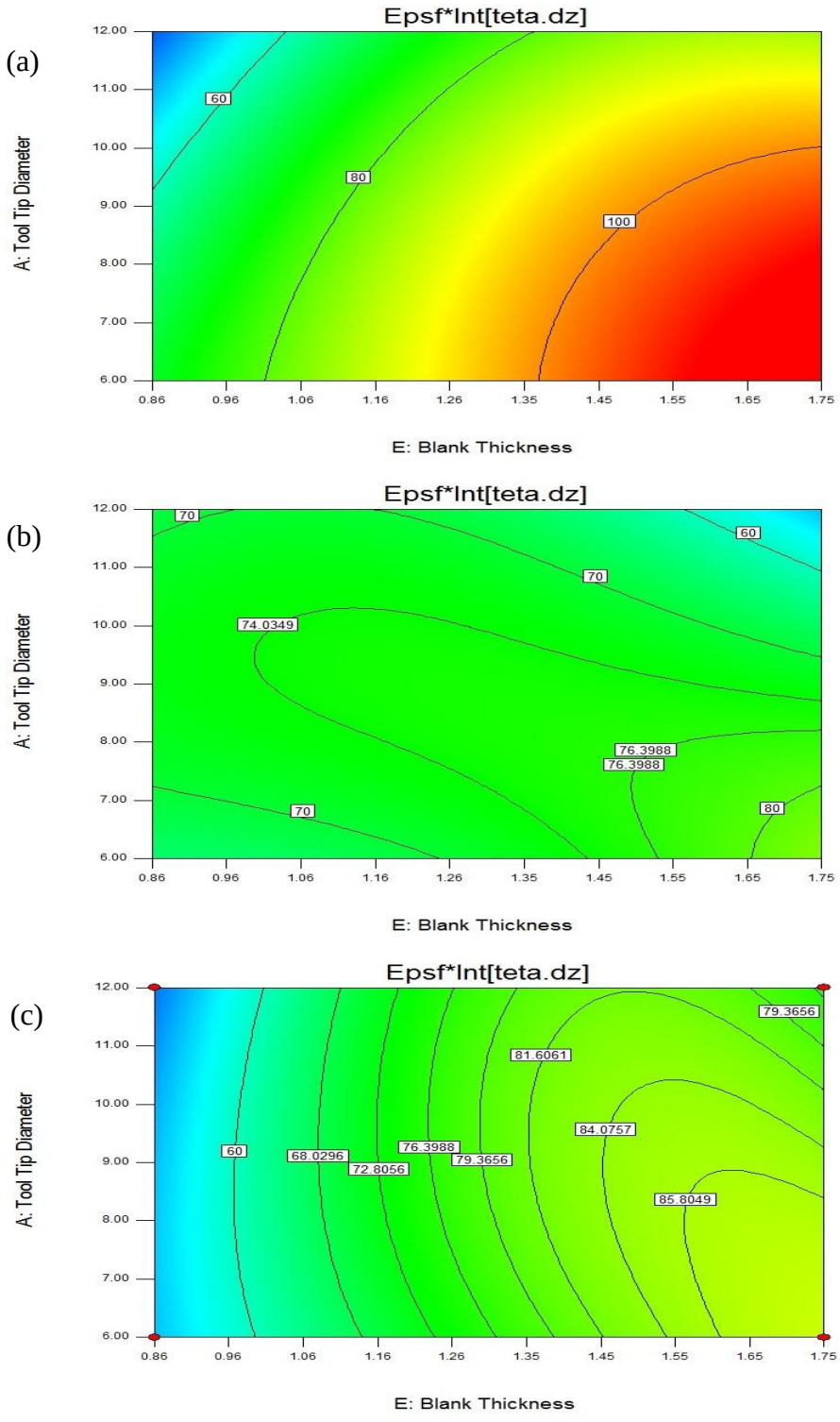

Figure 3.5 Contour plot; Interaction effect of blank thickness and tool tip diameter; (a) PS=0, FR=0, SRS=0; (b) PS=-1, FR=-1, SRS=-1; (c) PS=1, FR=1, SRS=1

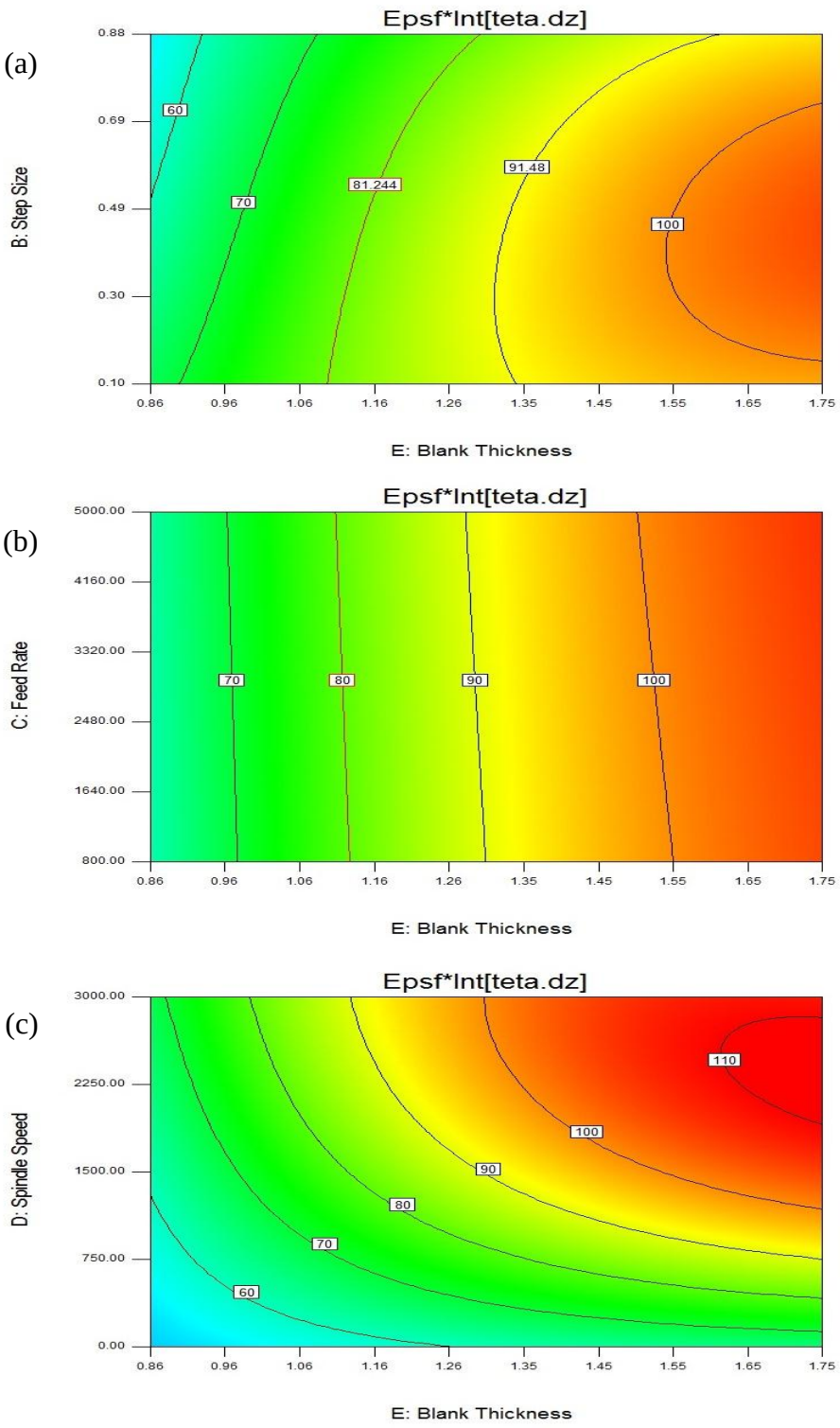

Figure 3.6 Contour plot; Interaction effect of blank thickness and (a) Step size, TTD=0, FR=0, SRS=0; (b) Feed rate, TTD=0, PS=0, SRS=0; (c) Spindle speed, TTD=9, PS=0, FR=0

In Figure 3.5, inconsistency among plots a, b and c, is attributed to the predefined constant values of pitch size, feed rate and spindle speed, while all the three contour plots represent interaction effect of tool size and blank thickness upon CCF. It can be therefore underlined the profound influence of interaction effects and the caution that is needed to be applied for interpretation of experimental results. For example, Figure 3.5 (a), shows that by a small tool size (diameter of 6mm), increase in sheet thickness provides a considerable amount of improvement in formability (more than 80%). However, by Figure 3.5 (b) such an effect can be estimated as to be less than 20%. According to Figure 3.5 (a) by increasing tool size from 6 to 12 mm, while the sheet thickness remains constant at the upper level (1.75 mm), formability decreases by about 30%. Nevertheless, by the same condition for the tool size and the sheet thickness, Figure 3.5 (c) represents a difference of about 14 %. By repetition of the same procedure, considering the increase in tool size from the lower to its upper level, while keeping the sheet thickness constant at 0.86 mm, Figure 3.5 (c) and (a) respectively indicate a reduction of about 12% and 40 %. What is more considerable, the same values of CCF can be attained for the tool size of 6 and 10 mm whilst the blank thickness is respectively set at 0.86 and 1.75 mm. The last example reveals a reduction of 50% in material consumption (so that in parts' weight and the price) that is possible just by cautious appointment of tool size.

Figure 3.6 (a) represents reduction of about 20% in formability by increase in step size from 0.10 to 0.88 mm, while the sheet thickness is kept constant at its lower level (0.86 mm). However the correlation curvature transforms to an elliptical shape by application of the thick sheet (1.75 mm) by which the highest degree of formability can be achieved

using almost the midlevel of step size (0.45 mm). In Figure 3.6 (b), by the straight lines that are nearly parallel to the vertical axis, it is evident that even a great change in feed rate, apart from the measure of sheet thickness, provides negligible influence on formability. Figure 3.6 (c) depicts that the best measure of formability can be obtained by application of the thickest sheet (1.75 mm) along with the spindle speed of about 2500 rpm (not any more). However the least formability can be derived by simultaneously application of the lower levels of spindle speed and sheet thickness.

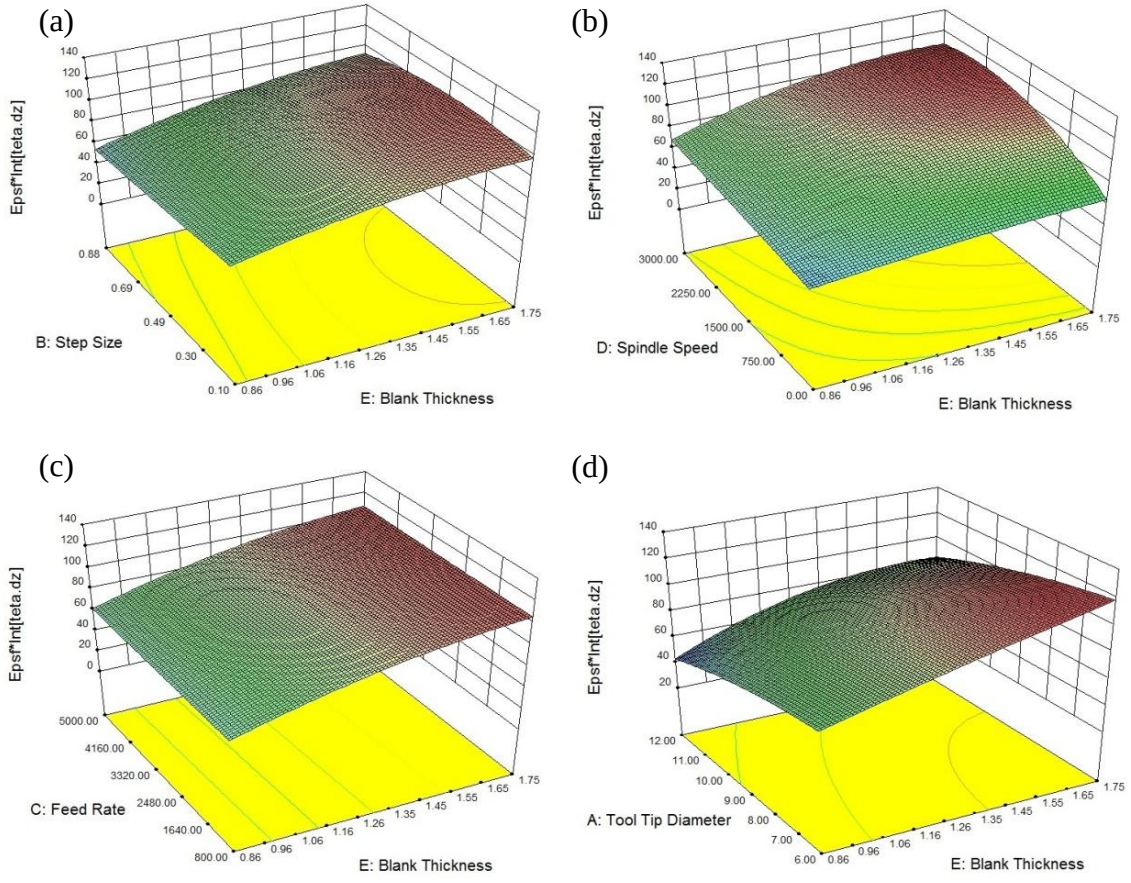

Figure 3.7 3D surface model; Interaction effect of blank thickness and
(a) Step size, TTD=0, FR=0, SRS=0; (b) Spindle speed, TTD=0, PS=0, SRS=0;
(c) Feed rate, TTD=9, PS=0, FR=0; (b) Tool tip diameter, TTD=0, PS=0, SRS=0

Interaction effects of sheet thickness and the rest of factors on CCF are presented with the aid of 3D response surface, in Figure 3.7. According to theses 3D plots, the maximum sheet thickness adapted with the maximum it spindle speed (Figure 3.7. b) or the minimum tool size (Figure 3.7. d) leads to the maximum formability. Nonetheless, feed rate makes no contribution to an interactive effect with blank thickness upon CCF (Figure 3.7. c). Step size, as it is evident from Figure 3.7. a, stimulate the formability at about its midlevel (40 mm) whilst the thickest sheet is utilized. It is notable that all the above made statements are true in the case that the rest of three predictor factors have been already fixed at their midlevel. In order to assess the formability of sheet metal attributed to any especial combination of factors' measures (within the range of these experiments), application of the empirical model (RSM) reported as the Equation 3.2 is recommended.

3.3.2. Spindle speed

Figure 3.8 represents the individual effect of spindle speed upon the sheet formability. Plot (a) reveals almost a steady increase in formability (CCF) from 60 to 100 by raising the spindle speed form 0 to 3000 rpm, while the other factors are set to their midlevel. Plot (b) portraits the situation in which all predictor parameters are fixed at their lower level, so that, by variation of spindle speed from 0 to about 2500 rpm, CCF improves to a maximum level (110) and then show a tendency for slight decrease by further increase in Spindle speed (to 3000 rpm). From Plot (c) it can be seen that, keeping feed rate, blank thickness, step and tool size respectively constant at 5000 mm/min, 1.75 mm, 0.88 mm and 12mm, a linear growth of lower magnitude compared to the former plots happens by amplifying the spindle speed from 0 to 3000 rpm.

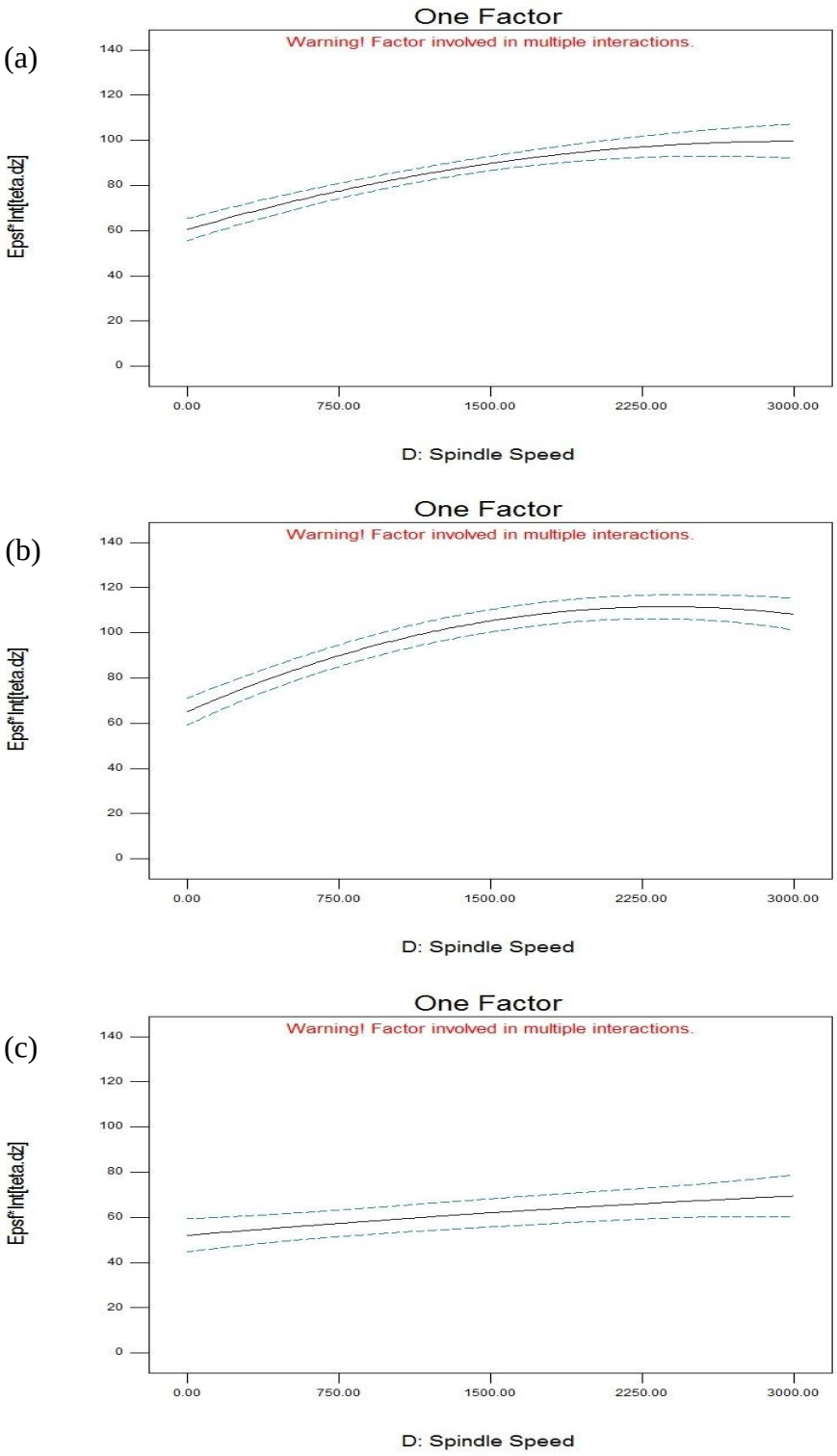

Figure 3.8 CCF versus spindle speed; (a) TTD=0, PS=0, FR=0, BT=0; (b) TTD=-1, PS=-1, FR=-1, BT=-1; (c) TTD=1, PS=1, FR=1, BT=1

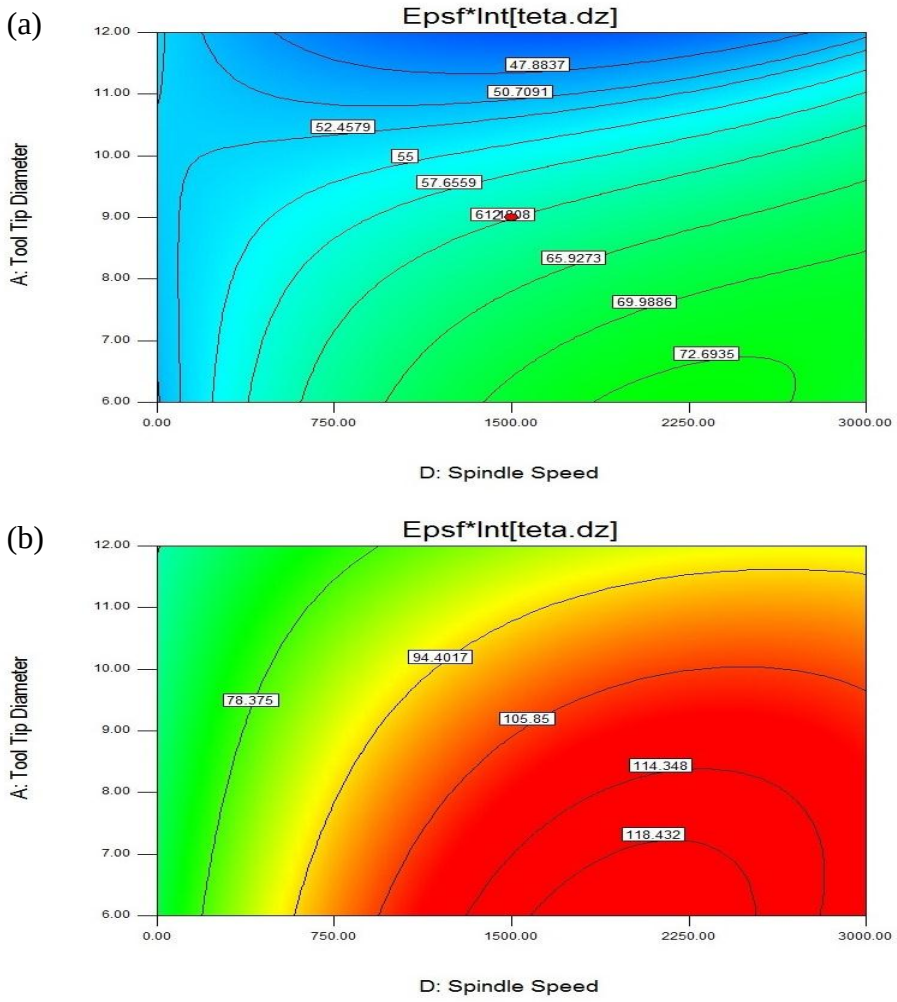

Figure 3.9 Contour plot; Interaction effect of spindle speed and tool tip diameter
(a) PS=0, FR=0, BT=-1; (b) PS=0, FR=0, BT=1

Figure 3.9 allows comparison between two different conditions by which interactive effect of spindle speed and tool size on formability can be differentiated by the effect of minimum (a) and maximum (b) sheet thickness. Both contours illustrate the same concept, but in the case of thicker sheet, overall improvement of about 40% in formability is presented. With the aid of the flags provided at intercepts of interaction plain as well as the center points of elliptical portions, Figure 3.10 provides useful information to examine the interactive effect of spindle speed with feed rate, step and tool size.

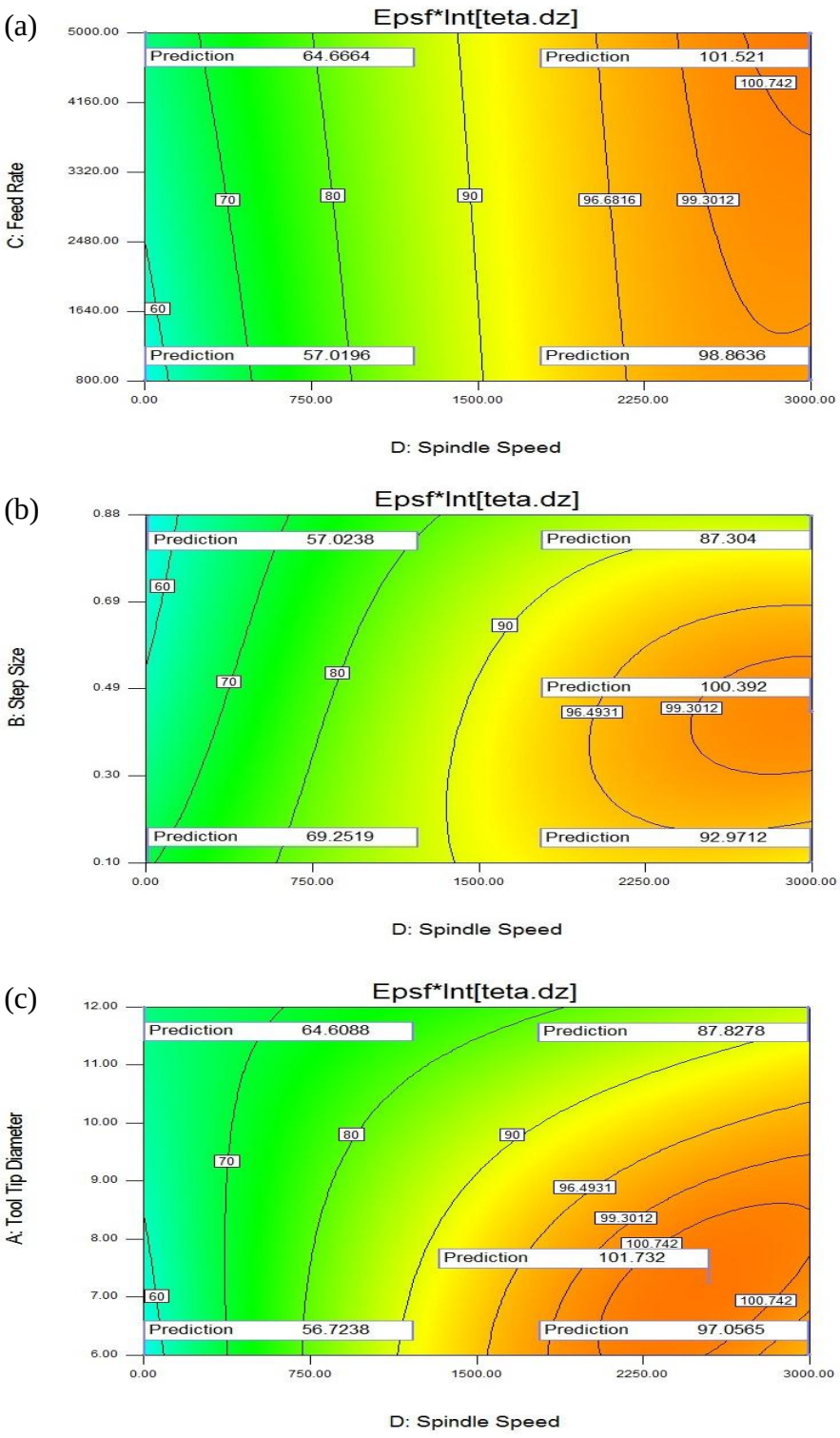

Figure 3.10 Contour plot; Interaction effect of spindle speed and (a), Feed rate TTD=0, PS=0, BT=0; (b) Step size, TTD=0, FD=0, BT=0; (c) Tool tip diameter, BT=0, PS=0, FR=0

(a)

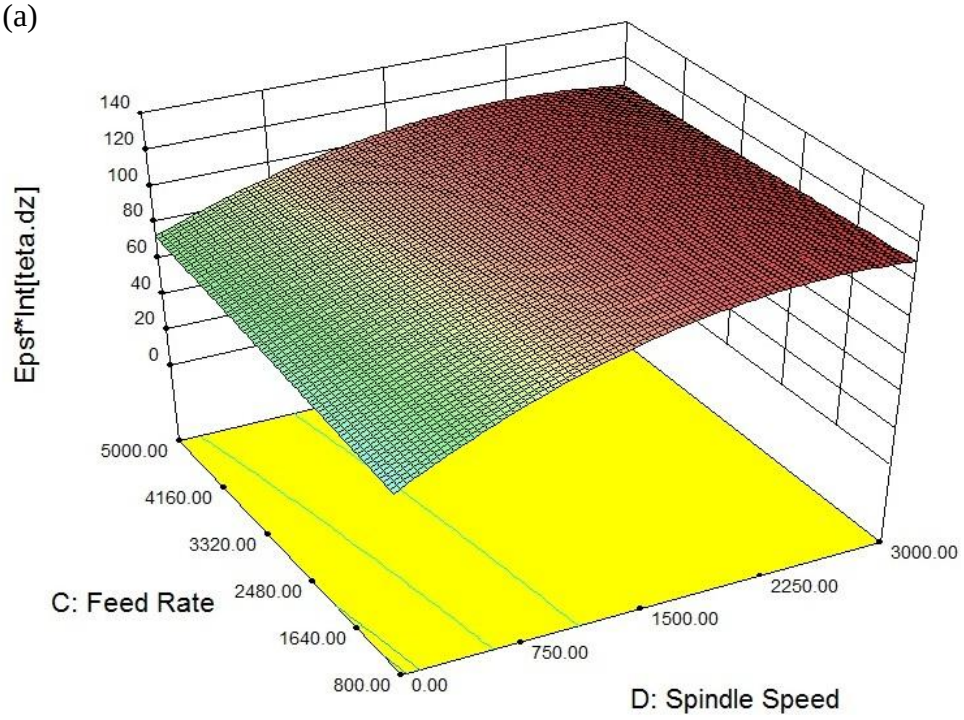

(b)

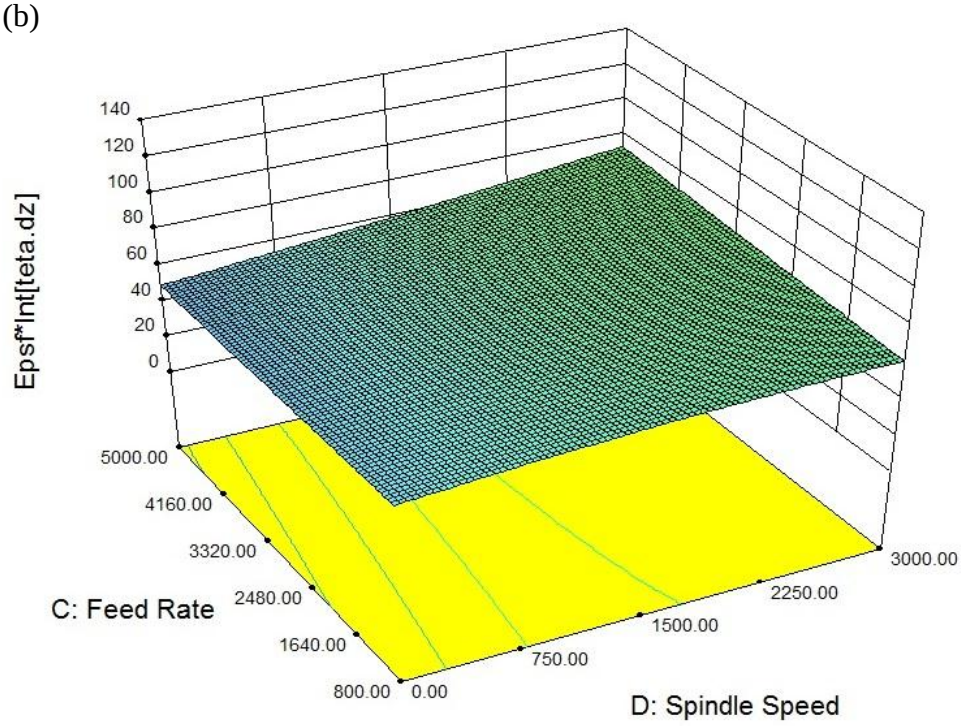

Figure 3.11 3D surface model; Interaction effect of blank spindle speed and feed rate; (a) PS=0, BT=1, TTD=0; (b) PS=0, BT=-1, TTD=0

(a)

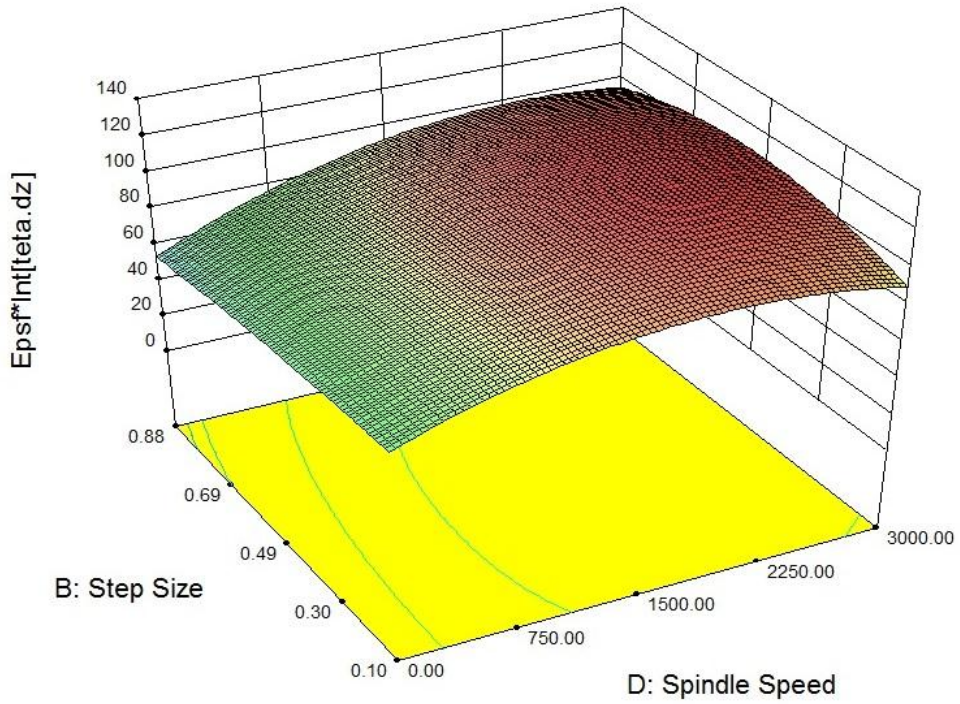

(b)

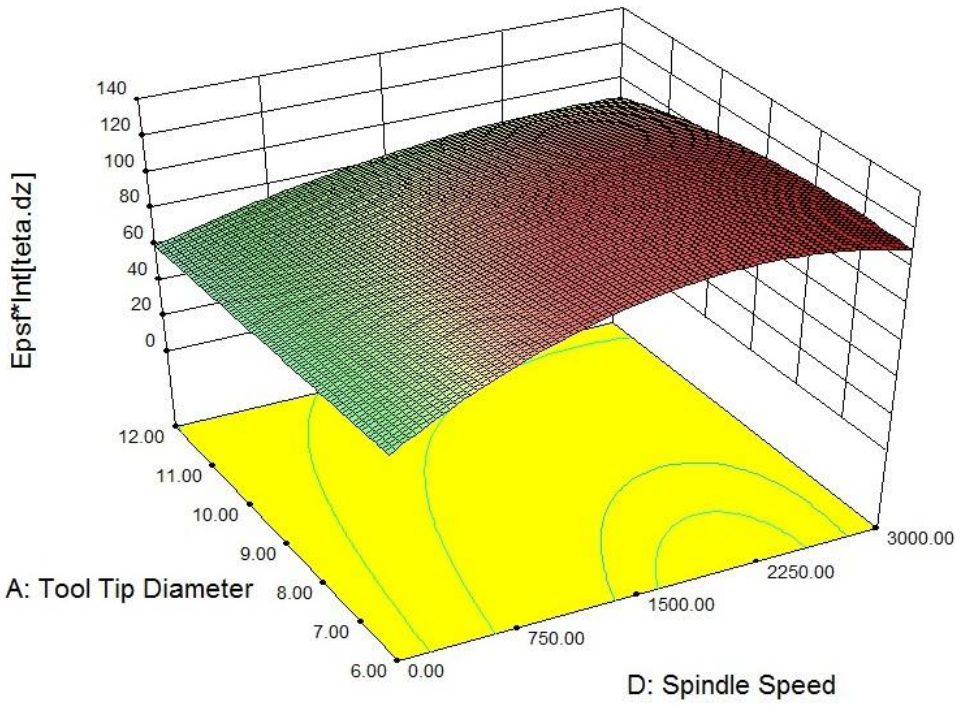

Figure 3.12 3D surface model; Interaction effect of spindle speed and
(a) Step size, TTD=0, FR=0, BT=1; (b) Tool tip diameter, BT=1, PS=0, FR=0

Figure 3.10 (b) depicts the interaction effect of spindle speed and step size upon the formability of sheet material. It can be clearly inferred by this plot that the maximum formability can be achieved by the maximum spindle speed (3000), while step size is about its midlevel (0.45 mm), so that any smaller or bigger pitch size leads to decrease in formability. Similar to the former case, setting all the factors to their midlevel, interaction effect of spindle speed and tool size upon formability is shown by plot (c) in which the highest formability is presented to be attainable by spindle speed of about 2500 rpm and tool of 7.30 mm in radius.

Figure 3.11 allows to see how by the sheet thickness, interaction effect of spindle speed and feed rate upon formability could differ. From plot (a) by which the sheet thickness is preset to its maximum (1.75 mm), it is obviously recognizable the curvature of response surface with respect to the axis of spindle speed. In spite of this, the surface is almost straight (inclination is negligible) along the axis of feed rate, which implies no contribution of feed rate to an interaction effect with spindle speed in this case. On the other hand, blank thickness adjusted to its minimum level (0.86 mm), plot (b) represents a nearly flat response surface for interaction of spindle speed and feed rate. This means, the factor of spindle speed, except at very high levels together with upper level of feed rate, cannot stimulate the formability of sheet material with low thickness (0.86 mm herein).

According to Figure 3.12 (a), formability of sheet material can be boosted to very large degrees, by setting all the parameters including the step size at their midlevel while the sheet thickness and spindle speed are kept constant at the maximum levels. Figure 3.12 (b) suggests that using the sheet of 1.75 mm in thickness accompanied with step size and feed rate of the midlevel, the maximum formability can be acquired through the interaction effect of spindle speed and tool size; if the former adjusted to the maximum level (3000rpm), while the later is specified as its minimum value (6 mm).

By further scrutinizing Figure 3.12 (b) it can be understood that the aforesaid locus of response surface for maximum formability simultaneously plays as the vertex of the laterally extended surface towards the lower (< 6) levels of tool size. More specifically, by further reduction in tool size, reduction in formability is expected. Although such an inference can be drawn here by extension of the RSM besides the experimental space, but it is in complete agreement to what is previously observed through the screening trials. As it was explicitly addressed in the section 2.4, this effect can be explained by excessive contact pressure due to the reduced tool size. It was also emphasized there the aggravation of this effect is deemed to occur by the change in material's mechanical properties, since highly elevated spindle speed generates considerable heat.

3.3.3. Feed rate

Figure 3.13 (a, b and c) presents the curvature of correlation between feed rate and formability as a line that is parallel to the axis of independent variable, feed rate. The only change among theses plots happens by downward shift of aforesaid line towards lower measures of formability, from plot (c) to plot (a). As it is clearly evident from the

foot note of Figure 3.13, such a decrease in formability is associated with the increase in sheet thickness from plot (a) to plot (c). Accordingly, variation of feed rate has no significant effect upon formability; so that it can be cautiously increased to very high levels (5000 mm/min and even more, depending on limitations of ISF machine) in order to considerably improve the time efficiency of the process.

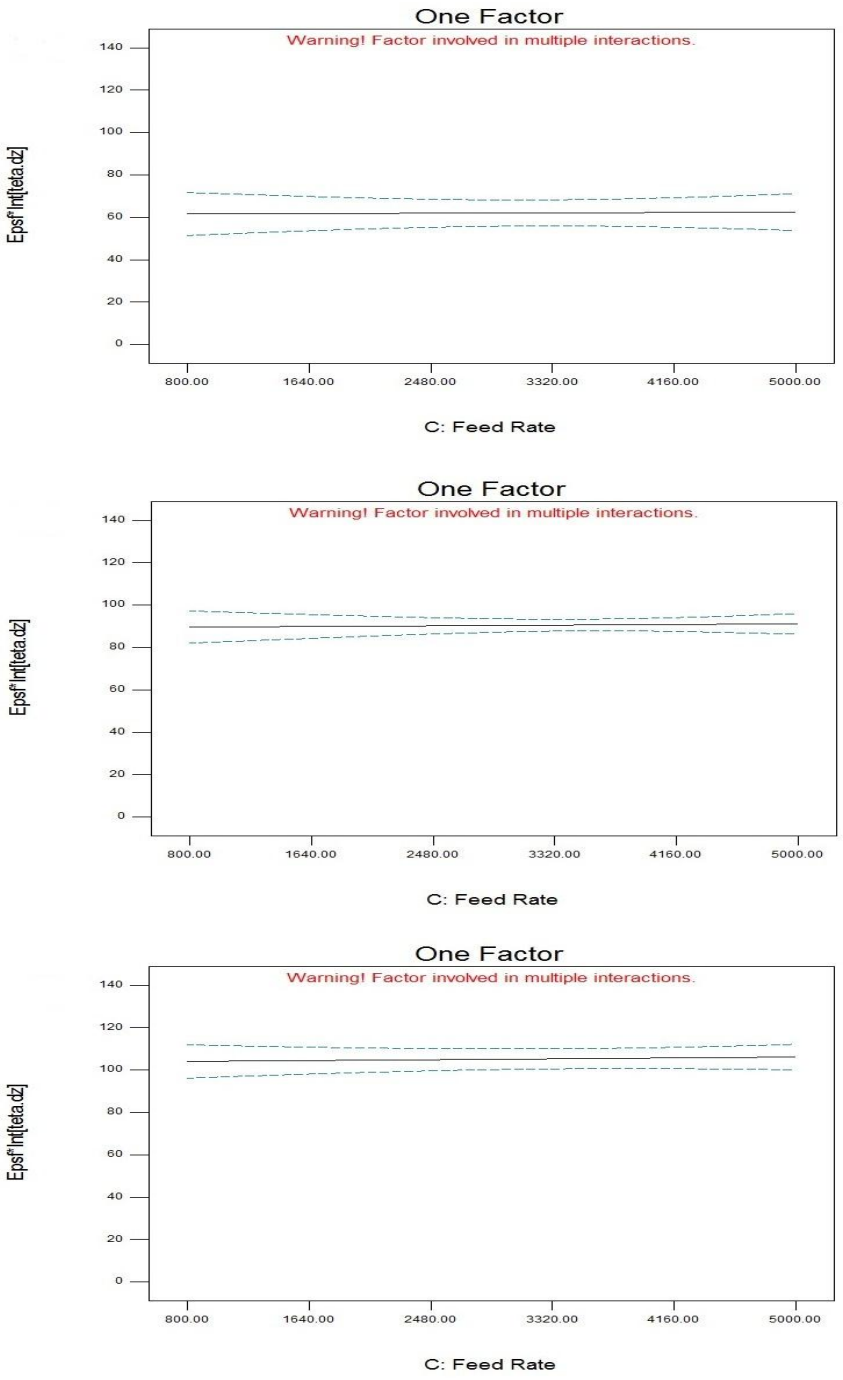

Figure 3.13 CCF versus feed rate; (a) TTD=0, PS=0, BT=-1, SRS=0; (b) TTD=0, PS=0, BT=0, SRS=0; (c) TTD=0, PS=0, BT=1, SRS=0

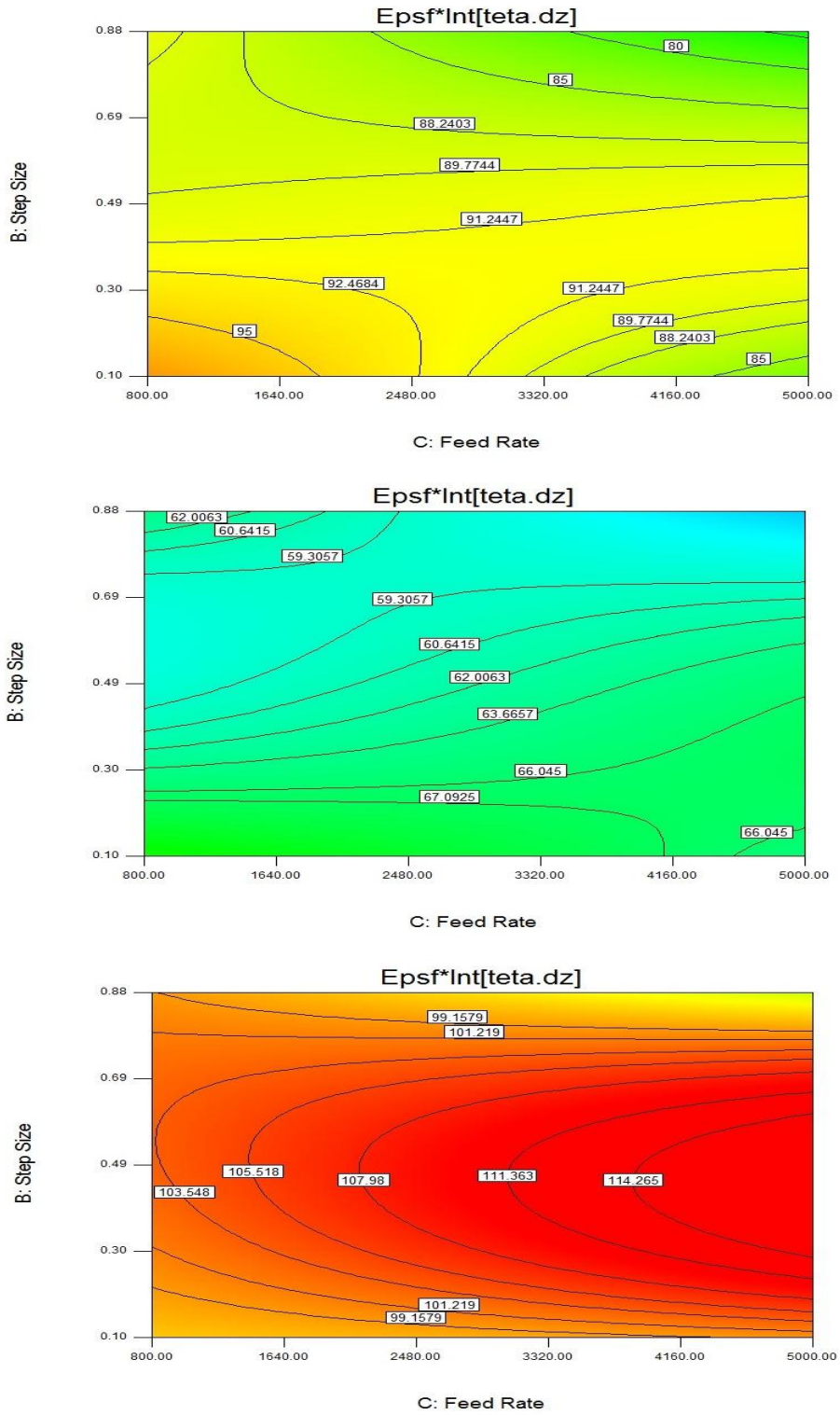

Figure 3.14 Contour plot; Interaction effect of blank thickness and step size;
(a) TTD=0, BT=0, SRS=0; (b) TTD=0, BT=0, SRS=-1; (c) TTD=-1, BT=1, SRS=1

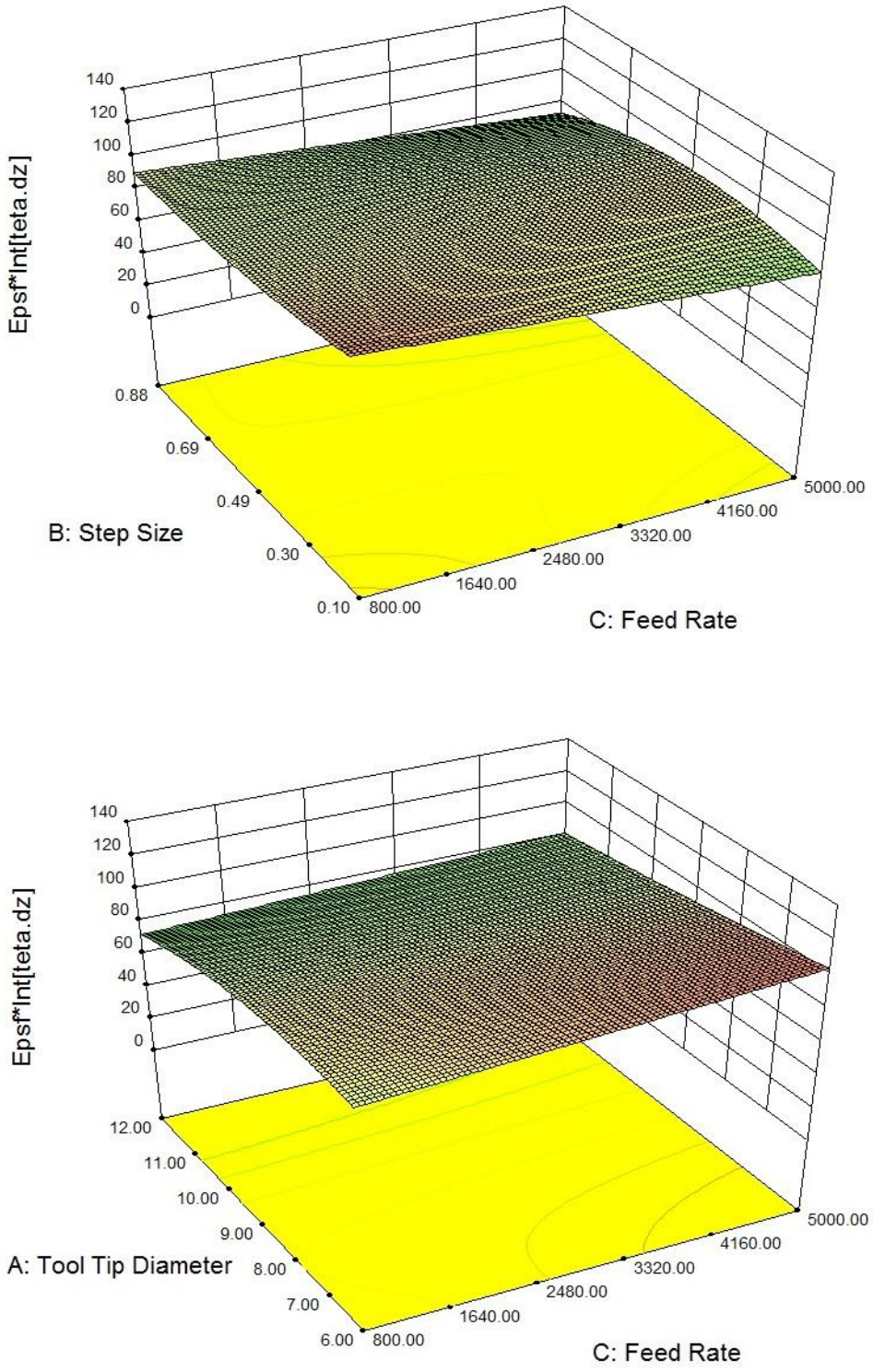

Figure 3.15 3D surface model; Interaction effect of feed rate and
(a) Step size, TTD=0, BT=0, SRS=0; (b) tool tip diameter, BT=0, PS=0, SRS=0

Figure 3.14, represents the interaction effect of feed rate and step size, in which contour plot (a) and (b) differ due to the measure of spindle speed that is 1500 rpm for plot (a) and 0 for plot (b). Plot (a) depicts that the maximum formability can be achieved either by combination of very low step size (0.1 mm) and feed rate (800 mm/min) or by a very high feed rate (5000 mm/min) that is accompanied by step size in the range of 0.30 to 0.50 mm. Making the second choice, formability experiences a reduction of about 7%, however the process time will be improved by about 2500%, which portrays a huge enhancement in terms of time efficiency, in turn, industrial applicability of the process.

Figure 3.14, plot (b) under the same condition as plot (a), except the spindle speed that is set to 0 rpm in this case, illustrates a gradual reduction in formability as step size increases. However, by trend lines drawn at the center area of the plot, it can be derived that a constant measure of formability can be retained either by implementation of very low feed rate and low step size (800 mm/min; 0.3 mm) or very high feed and upper moderate step size (5000 mm/min; 0.6 mm). Similarly, taking the second approach, it can be induced to an improvement of about 1250% in terms of time efficiency, while no compromise in formability. A simple comparison between plot (a) and (b) reveals that the increase in spindle speed can remarkably enhance the formability of sheet material.

Figure 3.14 (c) demonstrate interaction effect of feed rate and step size, under the condition that spindle speed and blank thickness are set to their upper levels (3000 rpm and 1.75 mm) while tool diameter is determined as 6 mm (the lower level). This plot allows optimization of the process to be realized through the most comprehensive view. By the first glance, from the bottom and the top of the contour plot it is clearly evident

that the same value of formability can be achieved by application of a very low level (0.15 mm) or considerably high level of step size (0.70 mm). In the same time, a huge increase in feed rate from 800 mm/min to 5000 mm/min produces insignificant reduction in formability. Moreover, paying careful attention to the middle portion of the plot, the midlevel of step size seems to act such as the transverse diameter for elliptical curvatures of correlation. In the other words, at any fixed measure of feed rate, the same formability can be attained by a pair of symmetrically located points on the circumference of each elliptical curvature. For example, by setting the step size to 0.49 mm, and feed rate to 1500 mm/min the same formability (CCF=105) is achievable as in the case of feed rate is adjusted to 5000 mm/min along with the step size of 0.14 mm or 0.73 mm. Obviously, the last case, maintaining the same formability, provides nearly 500% and 520% improvement in time efficiency, compared to the first and the second situations. What is more, plot (c) depicts that it is practically possible just consideration of the upper half portion of the plot with respect to the midlevel step size in order to improve two response factors, formability and process time. In this case, the higher feed rate along with the lower step size (in addition the midlevel) provides the better formability (at most by 20% of growth in CCF).

Figure 3.15 (a), considering the rest of three factors adjusted at their midlevel, exhibits a slight interactive effect between step size and feed rate upon the measure of CCF. Nonetheless, the most desired formability is presented to be acquired by the maximum feed rate along with a moderate step size (about 0.50 mm). Plot (b) under the same condition as plot (a), translates the similar concept as for the interaction effect of feed

rate and tool tip diameter; nevertheless the higher feed rate accompanied by the lower tool size is suggested to lead to the higher formability.

3.3.4. Step size

Figure 3.16 (a) allows to estimate individual effect of step size upon formability while all the rest of factors are set to their midlevel. It is illustrated by this plot no significant effect duo to the increment of pitch size from 0.1 mm to about 0.49 mm (midlevel), and by further increase in step size to 0.88, a slight decline of about 9% can be realized in formability. By Figure 3.16 (b) the same experimental situation as plot (a) is maintained, except the spindle speed that is fixed to 3000 rpm. In this case, correlation curvature appears as a convex shape in which, associated apex to the maximum formability corresponds to the midlevel of step size (0.49 mm). The spindle speed specified as to be zero, Figure 3.16 (c), represents continuing decline of about 20% in formability by increase in step size from 0.1 to 0.88 mm. It is again emphasized through plots (a) to (b) in Figure 3.16, the positive role that elevated spindle speed can play to magnify the formability.

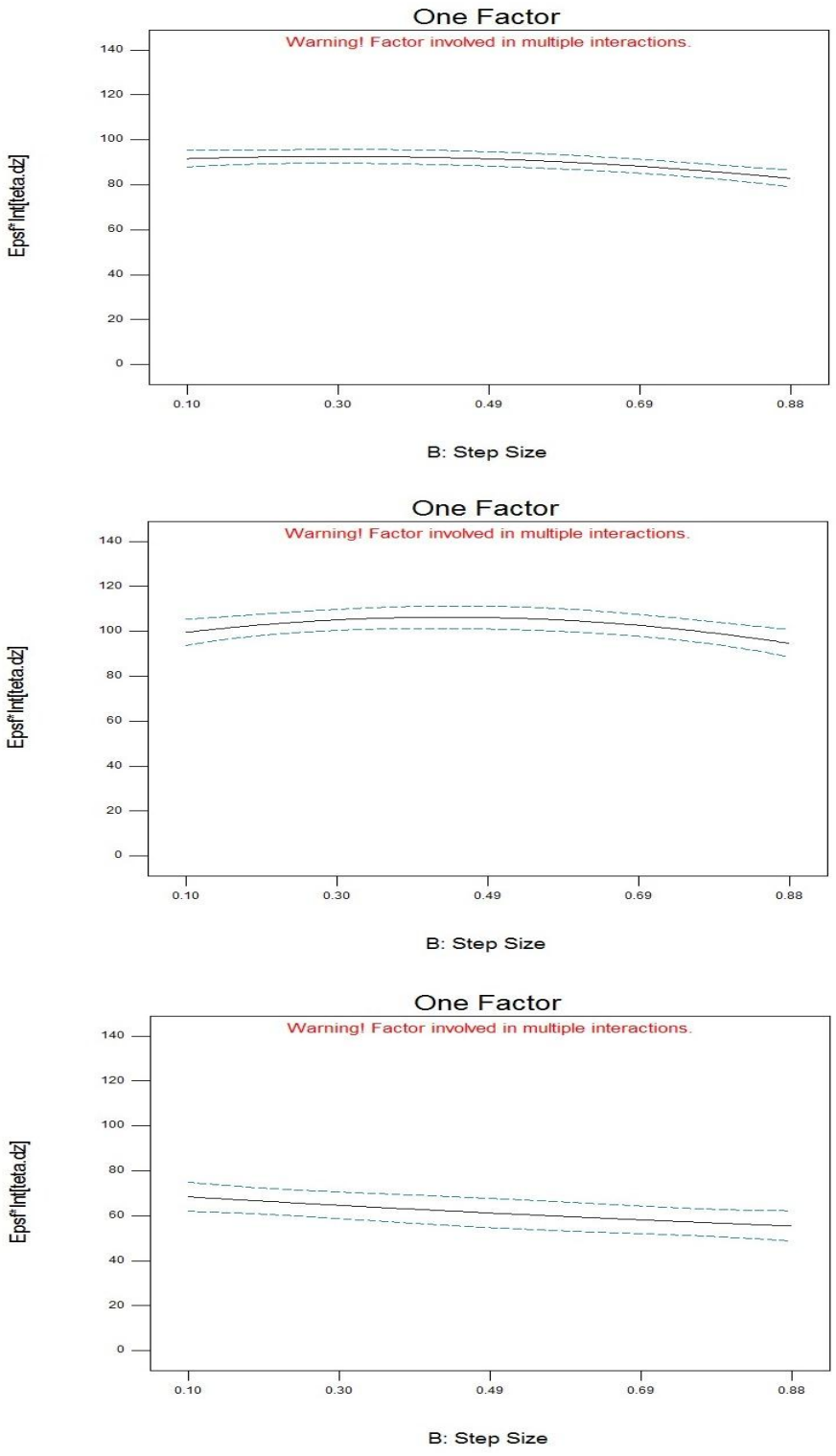

Figure 3.16 CCF versus step size; (a) TTD=0, BT=0, FR=0, SRS=0; (b) TTD=0, BT=0, FR=0, SRS=1; (c) TTD=0, BT=0, FR=0, SRS=-1

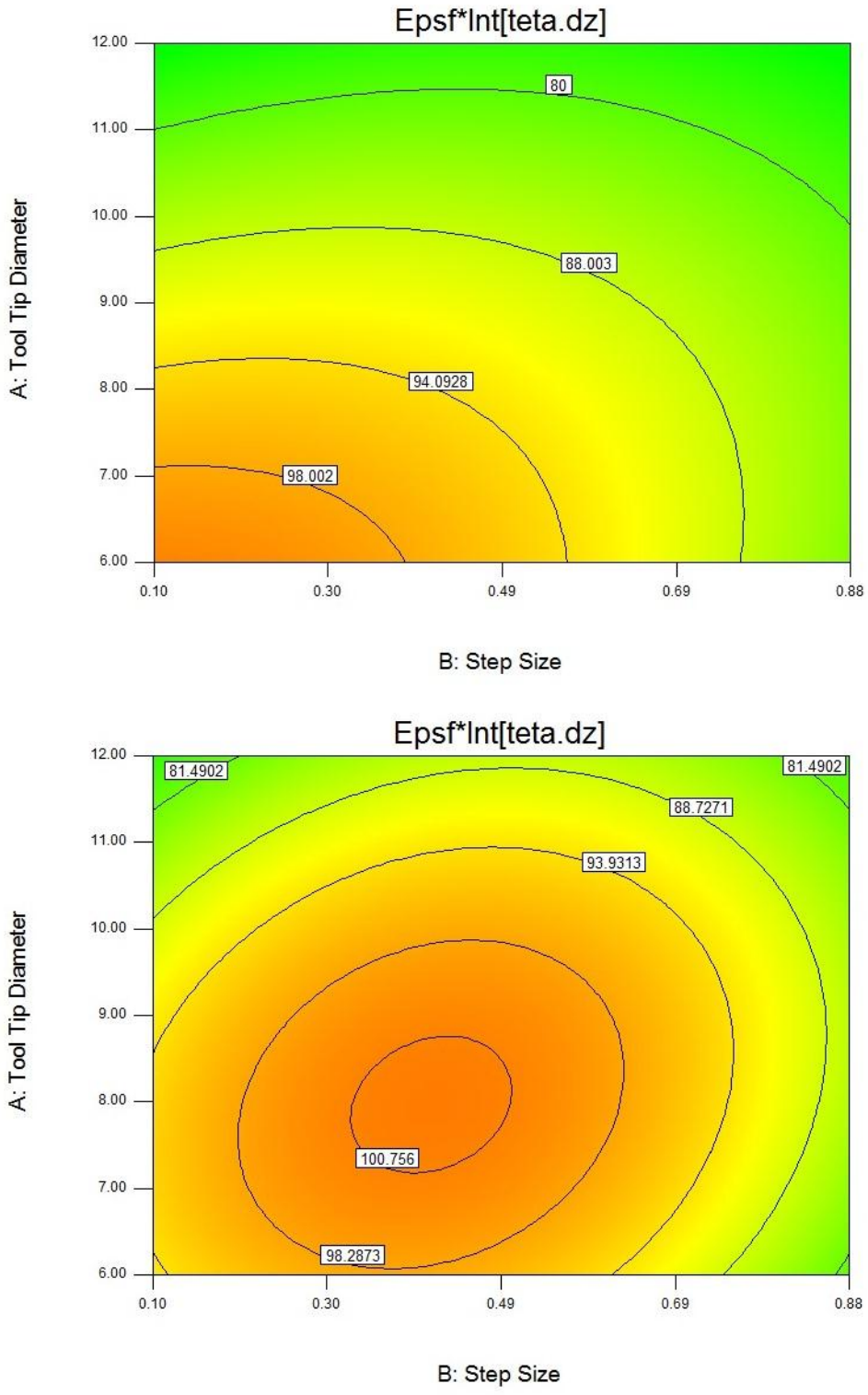

Figure 3.17 Contour plot; Interaction effect of step size and tool tip diameter; (a) BT=0, FR=0, SRS=0; (b) BT=0, FR=0, SRS=1

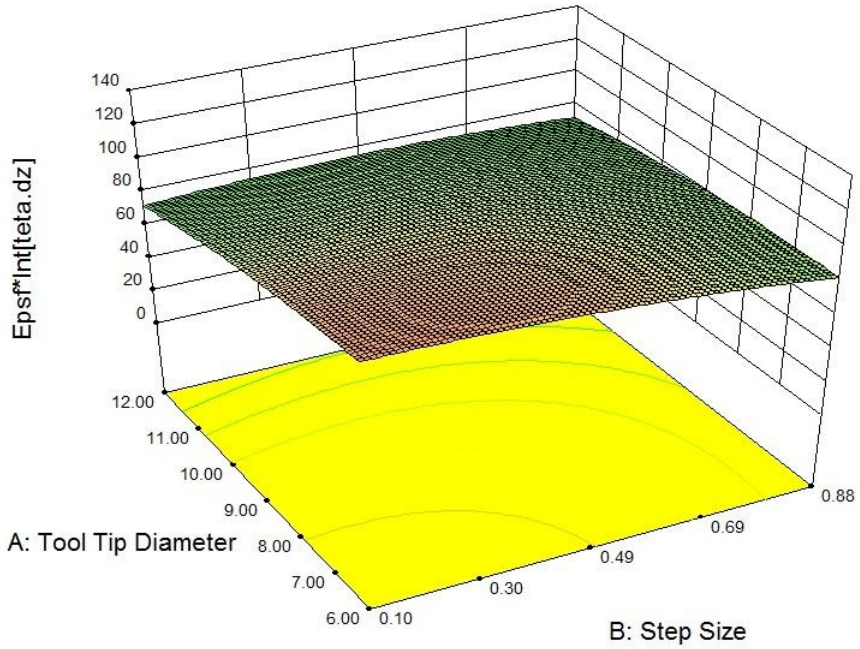

Figure 3.18 3D surface model; Interaction effect of tool tip diameter and Step size, BT=0, FR=0, SRS=0

Figure 3.17 illustrates the interactive effect of step size and tool tip diameter upon the CCF response factor; by which blank thickness, feed rate and spindle speed are set to their midlevel in plot (a) while the last mentioned predictor factor has increased to the level of 3000 rpm for plot (b). As it obviously evident from plot (a), interaction of pitch and tool size at their minimum levels can provide the maximum formability. However, by promotion of spindle speed to its upper level (3000 rpm), the locus of the maximum formability tends to shift to the center of the contour plot. It means that the interaction of these two process parameters, step and tool size, exhibits the most productivity in terms of formability when they are nearly set to their midlevel (under the condition of high spindle speed). In this case, correlation curvatures appear as concentric circles transmitting from closely the plot's middle area to the borders, which means, the same

measure of formability can be attained by a high value of step size and a low level of tool size or invert. Nevertheless, as it also evident from the 3D response surface presented in Figure 3.18, the best formability can be achieved around the midlevel of step size, especially by application of elevated spindle speed.

Figure 3.19 presents individual effect of tool size upon the formability under different experimental conditions as noted under the figure. Other predictor parameters remained constant at different levels, what is in common between plot (a) and (b), the reduction of CCF as tool tip diameter increases. Nevertheless, for a very high sheet thickness and spindle speed accompanied with a very low step size and feed rate, correlation curvature transforms to an arch shape that implies the maximum formability can be achieved by the midlevel of tool tip diameter (9 mm). This phenomenon is in complete agreement with the explanation provided as for Figure 3.12 (b).

3.3.5. Tool tip diameter

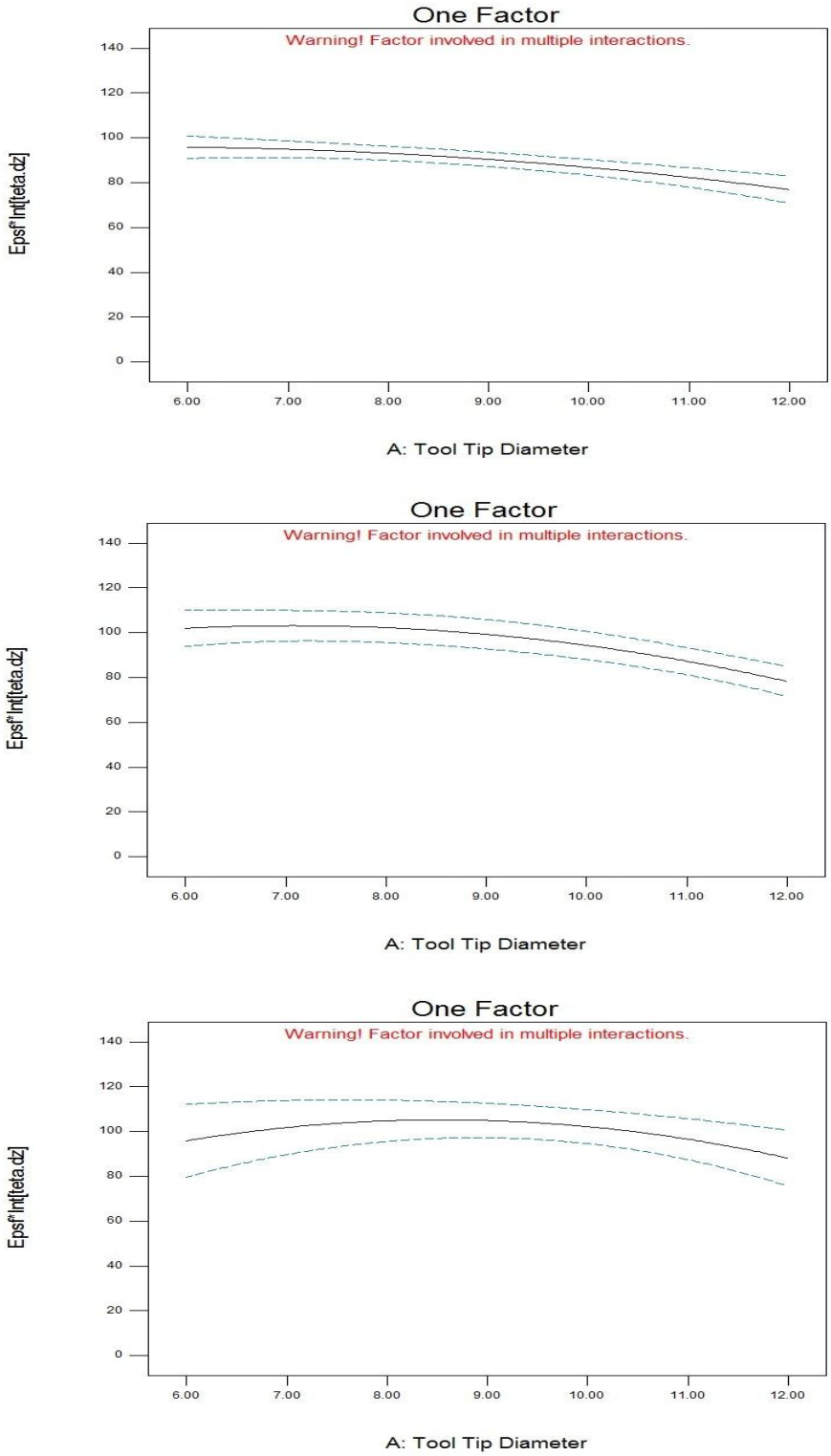

Figure 3.19 CCF versus Tool tip diameter; (a) BT=0, PS=0, FR=0, SRS=0; (b) BT=0, PS=-1, FR=-1, SRS=0; (c) BT=1, PS=-1, FR=-1, SRS=1

3.4. Optimization

Numerical optimization will search the design space, using the response models already created during analysis to find factor settings that meet the defined goals. These goals (criteria) must be set according to one or more responses (or even predictor factors), for example the maximum, minimum or any specific measure of a particular response (or predictor factor) might be desired. The software (Design Expert) will generate a list of potential factor settings meeting the specified criteria. The settings here will affect the hill-climbing algorithm that Design Expert uses to find the most desirable combination of variables. The program combines individual desirabilities into a single number and then searches for the greatest overall desirability. To do so, the software uses an optimization method developed by Derringer and Suich, described by Myers, Montgomery and Anderson-Cook in *Response Surface Methodology*, 3rd edition, John Wiley and Sons, New York, 2009.

Herein, in pursuance of optimization of ISF process, the desired criteria defined as to achieve the maximum formability, the minimum process time. The minimum amount of material (minimum sheet thickness) required to attain the two former objectives, in addition to the minimum propagation of error (POE) were considered among the criteria for optimization. What is more, a relative importance assigned for each criteria (grade five for formability and process time, grade two for blank thickness and grade one for POE). POE depicts how the error is transmitted to the response. Generally, the lower the POE is favorable because less of the error in control factors will be transmitted to the selected response, which results in a more robust optimization.

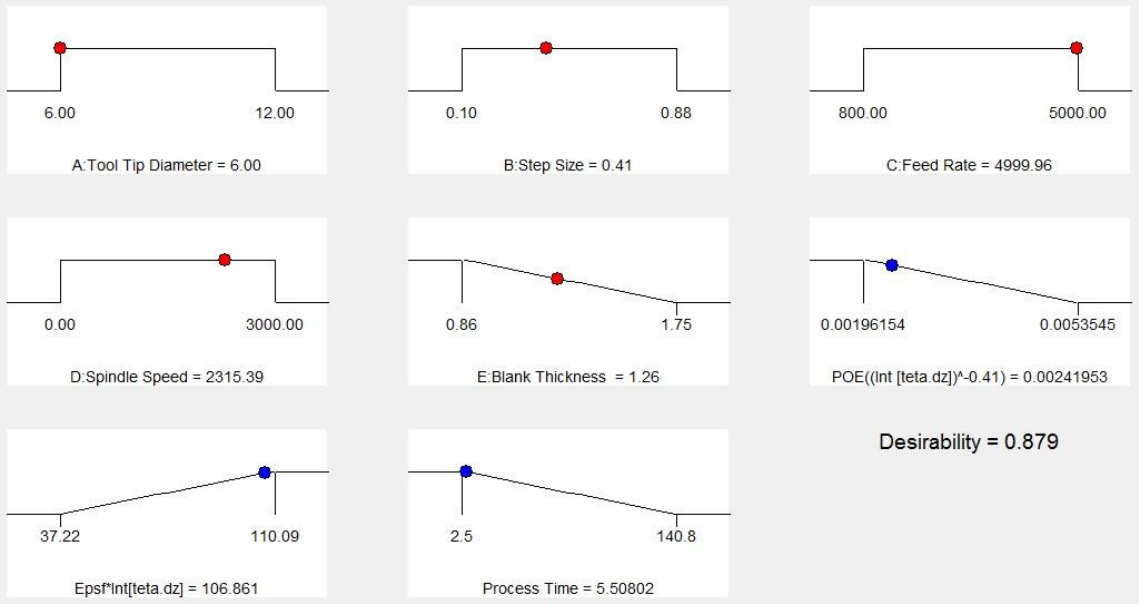

Figure 3.20 Representation of the predictor and response parameters involved in optimized process (optimization criteria are presented with the aid of ramp diagrams)

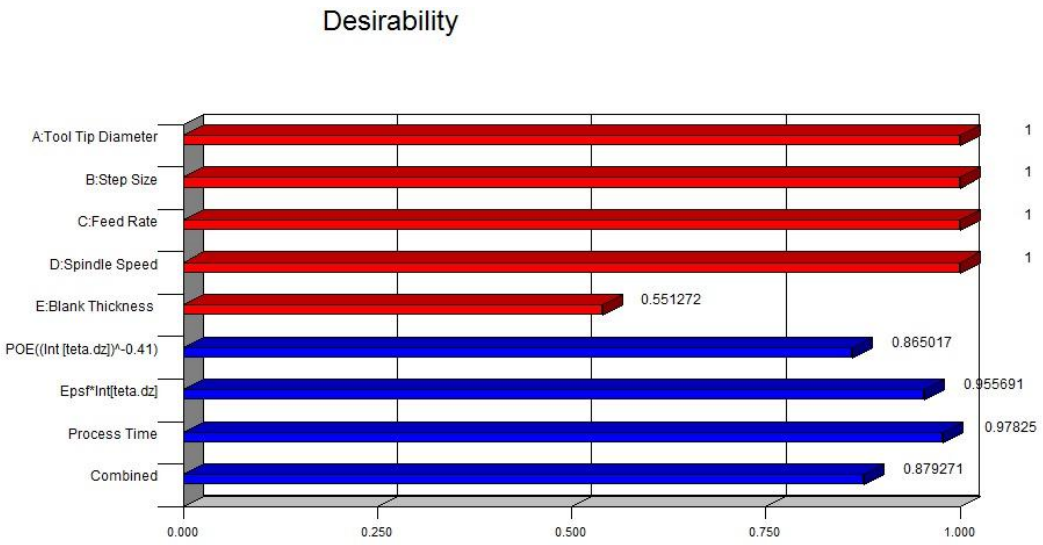

Figure 3.21 Bar graph representing individual percentage of desirability for optimization criteria within optimized process

Figure 3.20 illustrates the optimized values of predictor parameters as well as attained measure of response factors according to aforesaid criteria. Additionally, the overall percentage of desirability as for presented results is provided. Individual percentage of

desirability corresponding to each response-predictor factor is shown by Figure 3.21. The bar graph shows how well each variable satisfies the criteria (values near one are favorable).

In order to further emphasize how profoundly elevated spindle speed could affect the formability of sheet material, in turn the efficiency and productivity of ISF process, optimization process repeated maintaining the same criteria as the previous case but setting the spindle speed at 0 rpm. Outcomes that are presented in Figure 3.22 depict a considerable decline in terms of the best achievable formability and process time, and the overall percentage of desirability. More specifically, the maximum formability (CCF) portrays a decrease of about 29%; the minimum process time depicts increase of about 62% and the overall percentage of desirability declined as about 17%.

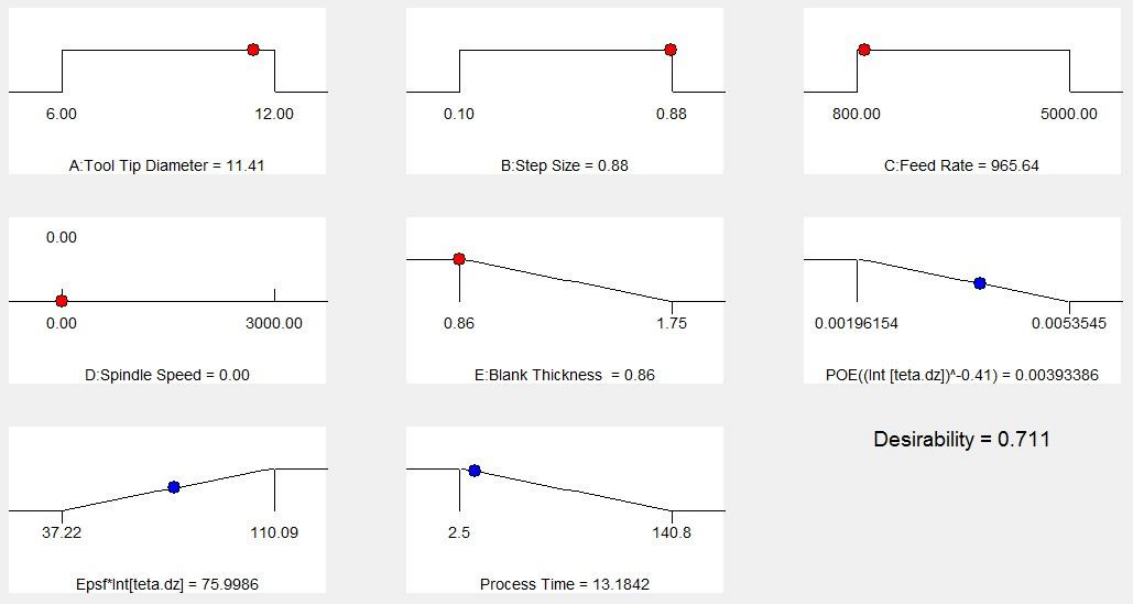

Figure 3.22 Representation of the predictor and response parameters involved in optimized process (optimization criteria are presented with the aid of ramp diagrams); Spindle speed = 0

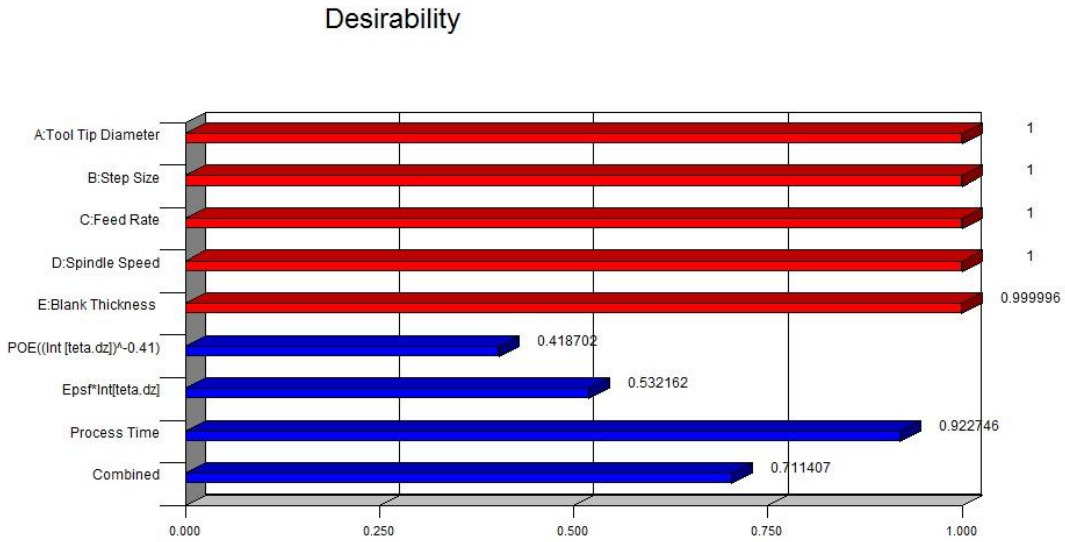

Figure 3.23 Bar graph representing individual percentage of desirability for optimization criteria within optimized process; Spindle speed = 0

Related individual percentage of desirabilities to the condition of zero spindle speed is presented by Figure 3.23. These results further highlight the positive role that spindle speed can play in favor of formability of sheet material in ISF process.

Chapter 4

CONCLUSION

In this thesis, the influence of five predictor parameters, namely tool tip diameter, step size, feed rate, spindle speed and blank thickness, was studied upon the formability in ISF by making use of DOE. Particularly, the interaction effect of associated factors, which was not acknowledged by preceding research, examined by development of quadratic and modified cubic response surface models. In addition, the process was optimized in terms of the maximum formability, the minimum process time and the blank thickness, so that the final price and the weight of finished part, and also by minimization of an error term, POE.

It was clearly observed that the spindle speed does have considerable positive effect on formability, in case of careful consideration of its interaction effects. On the other hand, feed rate provides no significant contribution regarding formability, which means forming speed, can be increased even up to the level of 5000 rpm whilst no harm to formability. As for the individual effect of step size, it provides the least contribution to formability. Particularly, in the case that formability gauge of longitudinal strain to be concerned, it is not even significant, while the higher step size translates to decreased process time. However, interaction effect of tool size and step size realized to be significant by any criterion, and the expected effect was even greater than that of tool

size individually. Mutual action of spindle speed and sheet thickness encountered to provide the strongest interaction effect. In this regard, satisfactory explanation was given by the aid of membrane analysis of a shell element (Silva et al., 2008) at tool-sheet contact zone. These implications suggest that spindle speed should be deliberately adjusted by consideration of sheet thickness.

Roughly speaking, the lower tool size, and to some extent, the smaller step size[69] probably[70] leads to the enhanced formability, while the thicker sheet material and the higher spindle speed are likely induced to better formability. Feed rate, in most of the cases can be easily increased in order to achieve the higher efficiency in terms of process time. For all of aforesaid statements, experienced range of factor's levels in addition to specific mechanical properties of utilized material is presumed.

In fact, the research plan that had been already prepared by author was much more comprehensive compared to what is later performed, and then, hereby presented. This shortening happened due to the limitation of facilities and mostly as a result of time restriction. However, the same approach can be taken for more extensive optimization of the process by simultaneously consideration of other response factors such as dimensional accuracy of final part. Especially, being aware of contradictory (positive-negative) effect of any particular predictor parameter upon different response variables, it highlights the need for such a broaden optimization of ISF process through the future works.

[69] By the most observations it was realized that the midlevel of step size (about 0.5 mm) well serves to maximum formability.
[70] Interaction effect has been frequently observed to produce contradictory results.

REFERENCES

Aerens, R., Eyckens, P., Van Bael, A., & Duflou, J. (2010). Force prediction for single point incremental forming deduced from experimental and FEM observations. *The International Journal of Advanced Manufacturing Technology, 46*(9), 969-982.

Allwood, J., Shouler, D., & Tekkaya, A. E. (2007). The increased forming limits of incremental sheet forming processes. *Key Engineering Materials, 344*, 621-628.

Anderson, M. J., & Whitcomb, P. J. (1974). *Design of experiments* Wiley Online Library.

Anderson, M. J., & Whitcomb, P. J. (2005). *RSM simplified: Optimizing processes using response surface methods for design of experiments* Productivity Pr.

Box, G. E. P., & Behnken, D. (1960). Some new three level designs for the study of quantitative variables. *Technometrics*, , 455-475.

Box, G. E. P., & Draper, N. R. (1987). *Empirical model-building and response surfaces.* John Wiley & Sons.

Box, G. E. P., & Hunter, J. S. (1957). Multi-factor experimental designs for exploring response surfaces. *The Annals of Mathematical Statistics, 28*(1), 195-241.

Box, G. E. P., Hunter, J. S., & Hunter, W. G. (2005). *Statistics for experimenters: Design, innovation, and discovery* Wiley Online Library.

Carrino, L., Di Meo, N., Sorrentino, L., & Strano, M. (2006). The influence of friction in negative dieless incremental forming. *Proceedings of the Ninth International ESAFORM Conference on Materials Forming, Glasgow, UK,* 203-206.

Coleman, D. E., & Montgomery, D. C. (1993). A systematic approach to planning for a designed industrial experiment. *Technometrics*, , 1-12.

Davis, J. R. (1993). *Aluminum and aluminum alloys* Asm Intl.

Dejardin, S., Thibaud, S., Gelin, J. C., & Michel, G. (2010). Experimental investigations and numerical analysis for improving knowledge of incremental sheet forming process for sheet metal parts. *Journal of Materials Processing Technology, 210*(2), 363-369.

Duflou, J. R., & D'hondt, J. (2011). Applying TRIZ for systematic manufacturing process innovation: The single point incremental forming case. *Procedia Engineering, 9,* 528-537.

Duflou, J., Callebaut, B., Verbert, J., & De Baerdemaeker, H. (2008). Improved SPIF performance through dynamic local heating. *International Journal of Machine Tools and Manufacture, 48*(5), 543-549.

Duflou, J., Vanhove, H., Verbert, J., Gu, J., Vasilakos, I., & Eyckens, P. (2010). Twist revisited: Twist phenomena in single point incremental forming. *CIRP Annals-Manufacturing Technology, 59*(1), 307-310.

Filice, L., Fratini, L., & Micari, F. (2002). Analysis of material formability in incremental forming. *CIRP Annals-Manufacturing Technology, 51*(1), 199-202.

Fratini, L., Ambrogio, G., Di Lorenzo, R., Filice, L., & Micari, F. (2004). Influence of mechanical properties of the sheet material on formability in single point incremental forming. *CIRP Annals-Manufacturing Technology*, *53*(1), 207-210.

Ham, M., & Jeswiet, J. (2007). Forming limit curves in single point incremental forming. *CIRP Annals-Manufacturing Technology*, *56*(1), 277-280.

Ham, M., & Jeswiet, J. (2006). Single point incremental forming and the forming criteria for AA3003. *CIRP Annals - Manufacturing Technology*, *55*(1), 241-244. doi: 10.1016/S0007-8506(07)60407-7

Hill, T., & Lewicki, P. (2006). *Statistics: Methods and applications: A comprehensive reference for science, industry, and data mining* StatSoft, Inc.

Hirt, G., Junk, S., Bambach, M., & Chouvalova, I. (2003). Process limits and material behaviour in incremental sheet forming with CNC-tools. *Materials Science Forum, , 426* 3825-3830.

Hirt, G., Junk, S., & Witulski, N. (2002). Incremental sheet forming: Quality evaluation and process simulation. *Proc. of the 7th ICTP Conference, , 1* 925_930.

Hosford, W. F. (2005). *Mechanical behavior of materials* Cambridge Univ Pr.

Hussain, G., & Gao, L. (2007). A novel method to test the thinning limits of sheet metals in negative incremental forming. *International Journal of Machine Tools and Manufacture, 47*(3), 419-435.

Hussain, G., Gao, L., & Dar, N. (2007). An experimental study on some formability evaluation methods in negative incremental forming. *Journal of Materials Processing Technology, 186*(1), 45-53.

Hussain, G., Gao, L., Hayat, N., Cui, Z., Pang, Y., & Dar, N. (2008). Tool and lubrication for negative incremental forming of a commercially pure titanium sheet. *Journal of Materials Processing Technology, 203*(1-3), 193-201.

Hussain, G., Gao, L., Hayat, N., & Dar, N. (2010). The formability of annealed and pre-aged AA-2024 sheets in single-point incremental forming. *The International Journal of Advanced Manufacturing Technology, 46*(5), 543-549.

Hussain, G., Gao, L., Hayat, N., & Ziran, X. (2009). A new formability indicator in single point incremental forming. *Journal of Materials Processing Technology, 209*(9), 4237-4242.

Hussain, G., Lin, G., Hayat, N., Dar, N. U., & Iqbal, A. (2010). New methodologies for the determination of precise forming limit curve in single point incremental forming process. *Advanced Materials Research, 97*, 126-129.

Jackson, K., & Allwood, J. (2009). The mechanics of incremental sheet forming. *Journal of Materials Processing Technology, 209*(3), 1158-1174.

Jeswiet, J., & Hagan, E. (2003). Rapid prototyping non-uniform shapes from sheet metal using CNC single point incremental forming. *TECHNICAL PAPERS-SOCIETY OF MANUFACTURING ENGINEERS-ALL SERIES-*,

Jeswiet, J., Micari, F., Hirt, G., Bramley, A., Duflou, J., & Allwood, J. (2005). Asymmetric single point incremental forming of sheet metal. *CIRP Annals-Manufacturing Technology, 54*(2), 88-114.

Jeswiet, J., & Young, D. (2005). Forming limit diagrams for single-point incremental forming of aluminium sheet. *Proceedings of the Institution of Mechanical Engineers, Part B: Journal of Engineering Manufacture, 219*(4), 359-364.

Kaufman, J. G. (1999). *Properties of aluminum alloys: Tensile, creep, and fatigue data at high and low temperatures* Asm Intl.

Kiefer, J. (1961). Optimum designs in regression problems, II. *The Annals of Mathematical Statistics,* , 298-325.

Leach, D., Green, A., & Bramley, A. (2001). A new incremental sheet forming process for small batch and prototype parts. *9th International Conference on Sheet Metal, Leuven,* 211-218.

Martins, P., Bay, N., Skjoedt, M., & Silva, M. (2008). Theory of single point incremental forming. *CIRP Annals-Manufacturing Technology, 57*(1), 247-252.

Mason, R. L., Gunst, R. F., & Hess, J. L. (1989). Statistical design and analysis of experiments.

Meyers, M. A., & Chawla, K. K. (1999). Mechanical behavior of materials.

Montgomery, D. C. (2008). *Design and analysis of experiments* John Wiley & Sons Inc.

Myers, R. H. (1990). *Classical and modern regression with applications* Duxbury Press Belmont, California.

Piepel, G. F. (1988). Programs for generating extreme vertices and centroids of linearly constrained experimental regions. *Journal of Quality Technology, 20*(2), 125-139. doi: AC06-76RL01830

Ryan, T. P. (2011). *Statistical methods for quality improvement* Wiley.

Shim, M. S., & Park, J. J. (2001). The formability of aluminum sheet in incremental forming. *Journal of Materials Processing Technology, 113*(1), 654-658.

Silva, M. B., Skjødt, M., Martins, P. A. F., & Bay, N. (2008). Revisiting the fundamentals of single point incremental forming by means of membrane analysis. *International Journal of Machine Tools and Manufacture, 48*(1), 73-83.

Silva, M., Alves, L., & Martins, P. (2010). Single point incremental forming of PVC: Experimental findings and theoretical interpretation. *European Journal of Mechanics-A/Solids, 29*(4), 557-566.

Skjødt, M., Silva, B., Bay, N., Martins, P., & Lenaul, T. (2007). Single point incremental forming using a dummy sheet. *2nd International Conference on New Forming Technology, Bremen,*

Stat-Ease, I. (2011). *Design-expert 8 User's guide* (8.0.7.1 ed.). 2021 East Hennepin Ave., Suite 480, Minneapolis, MN 55413:

StatSoft, Inc. Electronic Statistics Textbook. Tulsa, OK: StatSoft. (2012). Retrieved 2012, 7/20, 2012, from http://www.statsoft.com/textbook/experimental-design/?button=1

Taguchi, G., Tung, L. W., & Clausing, D. (1987). *System of experimental design: Engineering methods to optimize quality and minimize costs* Unipub New York, NY,, USA.

Takano, H., Kitazawa, K., & Goto, T. (2008). Incremental forming of nonuniform sheet metal: Possibility of cold recycling process of sheet metal waste. *International Journal of Machine Tools and Manufacture, 48*(3-4), 477-482.

Ziran, X., Gao, L., Hussain, G., & Cui, Z. (2010). The performance of flat end and hemispherical end tools in single-point incremental forming. *The International Journal of Advanced Manufacturing Technology, 46*(9), 1113-1118.